2016

Data Acquisition Systems design for Quality Assurance in advanced radiation dosimetry

Iolanda Fuduli
University of Wollongong

UNIVERSITY OF WOLLONGONG

Department of

Engineering and Information Sciences

Data Acquisition Systems design for Quality Assurance in advanced radiation dosimetry

Iolanda Fuduli

"This thesis is presented as part of the requirements for the Award of the Degree of Doctor of Philosophy the University of Wollongong"

August 2016

ABSTRACT

During the past years, radiotherapy has become a widely used technique for treatment of tumors on different areas of the human body. The evolution of the technology has led to the necessity to assure the safety of the patient at any time during any kind of treatment. A wide range of instrumentation has been developed to perform a state of art dosimetry for the Quality Assurance (QA) of the irradiating beam. Tumors can be treated using different methodologies, depending on their position and dimension. The radiation techniques have been classified in three major groups: Microbeam Radiation Therapy (MRT), Brachytherapy and External Beam Radiation Therapy (EBRT). Each of them presents different characteristics in terms of intensity of delivered dose, timing and speed of the irradiation. The aim of this research project is to study and design a unified Data Acquisition system (DAQ) able to monitor and measure the irradiating beam of any of the three clinical scenarios. A DAQ is a very complex system comprising multiple aspects. It can be divided in four main sections: detectors, the sensitive part; electronic and analogue front end; digital core and Graphical User Interface. The goal to create a unified dosimetry platform has been achieved by the design of a modular read out electronic section and a modular digital core, which can be easily adapted to the different detectors and analogue front ends. The project started with the development of a single channel DAQ to read out a single microstrip diode for MRT application. The goal of the DAQ was to have high spatial resolution, to resolve a 50 μm wide microbeam, and a large sensitivity range. In fact, for this application, the beam instead of being flat has very narrow peaks where high radiation dose is delivered, spaced by areas where radiation is very low or none (named valley). Then the system has been upgraded into a multi-channel DAQ able to acquire a 128 diodes array for Brachytherapy treatments. In this scenario, the source moves during the treatment and can be placed far away from the detector. By using an array of diodes, the system has been able to reconstruct the movement of the source at any time during the treatment. A new high sensitivity front end has been introduced to perform dosimetry up to 12 cm distance from the irradiating source. The same DAQ has been used in multi-channel configuration for EBRT treatments and its modular design allowed the introduction of larger detectors, up to 512 channels, to best suit each different application. Moreover, the flexible timing constraints of the front-end used

to read out the detector, allowed the setup of a triggered acquisition which can be synchronized with the LINAC beam to have a highly efficient dosimetry measure. Lately, a new standalone section has been introduced: it comprises a rotatable phantom and its movement control. It features an inclinometer, which detects the position of the LINAC gantry, and a control system made by an encoder and a stepper motor to align the detector to the gantry. This setup is particularly useful for application like VMAT and IMRT, where the treatment is delivered by rotating the LINAC around the patient and it is also compatible with all the previously developed DAQ.

Overall this research project has given a relevant contribution to the development of a unified platform for advanced radiation dosimetry. The outcome is a modular DAQ whose setup can be chosen to best suit each particular application. Even if the DAQ can be improved and upgrades are already undergoing feasibility studies, this research study has contributed to the publication of many peer reviewed papers internationally recognized.

ACKNOWLEDGEMENTS

First of all, I would like to thank my supervisors, Prof. Anatoly Rozenfeld, A. Prof. Michael Lerch and Prof. Peter Metcalfe their support during my PhD studies.

My gratitude goes to the many other PhD students who, during the past years, contribute to the realization of this research project by sharing their work, results and skills.

And then, my biggest “thank you” goes to my partner-supervisor-boss-friend Marco who gave me the possibility to reach the end of this journey. He believed I could use my skills to do something different and rewording and he was right.

TABLE OF CONTENTS

LIST OF PUBBLICATIONS

- Porumb, C., Aldosari, A. H., **Fuduli, I.,** Cutajar, D. L., Newall, M., Metcalfe, P. E., Carolan, M., Lerch, M. L. F., Perevertaylo, V., Rosenfeld, A. B. & Petasecca, M. (2016). "Characterisation of silicon diode arrays for dosimetry in external beam radiation therapy." *IEEE Transactions on Nuclear Science, 63 (3), 1808-1817.*

  Author has entirely designed the firmware, which is one of the main sections of the DAQ, and has given major contribution to the design and testing of the electronics used by Mr Porumb to carry out its measurements.

- Petasecca, M., Newall, M. K., Booth, J. T., Duncan, M., Aldosari, A. H., **Fuduli, I.,** Espinoza, A. A., Porumb, C. S., Guatelli, S., Metcalfe, P., Colvill, E., Cammarano, D., Carolan, M., Oborn, B., Lerch, M. L. F., Perevertaylo, V., Keall, P. J. & Rosenfeld, A. B. (2015). "MagicPlate-512: a 2D silicon detector array for quality assurance of stereotactic motion adaptive radiotherapy". *Medical Physics, 42 (6), 2992-3004.*

  Author has entirely designed the firmware, which is one of the main sections of the DAQ, and has given major contribution to the design and testing of the electronics used by Dr Petasecca to carry out its measurements.

- Alrowaili, Z. A., Lerch, M. L. F., Carolan, M., **Fuduli, I.,** Porumb, C., Petasecca, M., Metcalfe, P. & Rosenfeld, A. B. (2015). "2D mapping of the MV photon fluence and 3D dose reconstruction in real time for quality assurance during radiotherapy treatment". *Journal of Instrumentation, 10 (9), 1-14.*

  Author has entirely designed the firmware, which is one of the main sections of the DAQ, and has given major contribution to the design and testing of the electronics used by Dr Alrowaili to carry out its measurements.

- Petasecca, M., Alhujaili, S., Aldosari, A. H., **Fuduli, I.,** Newall, M., Porumb, C. S., Carolan, M., Nitschke, K., Lerch, M. L. F., Kalliopuska, J., Perevertaylo,

V. & Rosenfeld, A. B. (2015). “Angular independent silicon detector for dosimetry in external beam radiotherapy”. *Medical Physics, 42 (8), 4708-4718.*

Author has entirely designed the firmware, which is one of the main sections of the DAQ, and has given major contribution to the design and testing of the electronics used by Dr Petasecca to carry out its measurements.

- Espinoza, A., Petasecca, M., **Fuduli, I.,** Howie, A., Bucci, J., Corde, S., Jackson, M., Lerch, M. L. F. & Rosenfeld, A. B. (2015). “The evaluation of a 2D diode array in “magic phantom” for use in high dose rate brachytherapy pretreatment quality assurance”. *Medical Physics, 42 (2), 663-673.*

  Author has entirely designed the firmware, which is one of the main sections of the DAQ, and has given major contribution to the design and testing of the electronics used by Dr Espinoza to carry out its measurements.

- **Fuduli, I.,** Porumb, C., Espinoza, A., Aldosari, A., Carolan, M., Lerch, M. LF., Metcalfe, P. E., Rosenfeld, A. & Petasecca, M. (2014). “A comparative analysis of multichannel data acquisition systems for quality assurance in external beam radiation therapy”. *Journal of Instrumentation, 9 (6), 1-12.*
- Aldosari, A. H., Petasecca, M., Espinoza, A., Newall, M., **Fuduli, I.,** Porumb, C., Alshaikh, S., Alrowaili, Z. A., Weaver, M., Metcalfe, P., Carolan, M., Lerch, M. L. F., Perevertaylo, V. & Rosenfeld, A. B. (2014). “A two dimensional silicon detectors array for quality assurance in stereotactic radiotherapy: MagicPlate-512.” *Medical Physics, 41 (9), 091707-1-091707-10.*

  Author has entirely designed the firmware, which is one of the main sections of the DAQ, and has given major contribution to the design and testing of the electronics used by Dr Aldosari to carry out its measurements.

- **Fuduli, I.,** Newall, M. K., Espinoza, A. A., Porumb, C. S., Carolan, M., Lerch, M. L. F., Metcalfe, P., Rosenfeld, A. B. & Petasecca, M. (2014). “Multichannel

Data Acquisition System comparison for Quality Assurance in external beam radiation therapy". *Radiation Measurements, 71 338-341.*

- Gambarini, G., Carrara, M., Tenconi, C., Mantaut, N., Borroni, M., Cutajar, D., Petasecca, M., **Fuduli, I.,** Lerch, M., Pignoli, E. & Rosenfeld, A. (2014). "Online in vivo dosimetry in high dose rate prostate brachytherapy with MOSkin detectors: In phantom feasibility study". *Applied Radiation and Isotopes, 83 222-226.*

  Author has provided Prof. Gambarini with detectors and support for her experiments.

- Aldosari, A. H., Espinoza, A., Robinson, D., **Fuduli, I.,** Porumb, C., Alshaikh, S., Carolan, M., Lerch, M. L. F., Perevertaylo, V., Rosenfeld, A. B. & Petasecca, M. (2013). "Characterization of an innovative p-type epitaxial diode for dosimetry in modern external beam radiotherapy". *IEEE Transactions on Nuclear Science, 60 (6), 4705-4712.*

  Author has entirely designed the firmware, which is one of the main sections of the DAQ, and has given major contribution to the design and testing of the electronics used by Dr Aldosari to carry out its measurements.

- Metcalfe, P., Quinn, A., Loo, K., Lerch, M., Petasecca, M., Wong, J. Hsiu Ding., Hardcastle, N., Carolan, M., McNamara, J., Cutajar, D., **Fuduli, I.,** Espinoza, A., Porumb, C. & Rosenfeld, A. (2013). "Review of four novel dosimeters developed for use in radiotherapy". *Journal of Physics, 444 012008-1-012008-7.*

  Author has entirely designed the firmware, which is one of the main sections of the DAQ, and has given major contribution to the design and testing of the electronic, object of the paper.

- Espinoza, A., Beeksma, B., Petasecca, M., **Fuduli, I.,** Porumb, C., Cutajar, D. L., Corde, S., Jackson, M., Lerch, M. L. F. & Rozenfeld, A. B. (2013). "The feasibility study and characterization of a two-dimensional diode array in

"magic phantom" for high dose rate brachytherapy quality assurance". *Medical Physics, 40 (11), 111702-1-111702-10.*

Author has entirely designed the firmware, which is one of the main sections of the DAQ, and has given major contribution to the design and testing of the electronics used by Dr Espinoza to carry out its measurements.

- Wong, J. Hsiu Ding., **Fuduli, I.,** Carolan, M. G., Petasecca, M., Lerch, M. L. F., Perevertaylo, V. L., Metcalfe, P. E. & Rozenfeld, A. (2012). "Characterization of a novel two dimensional diode array the "magic plate" as a radiation detector for radiation therapy treatment". *Medical Physics, 39 (5), 2544-2558.*

  Author has entirely designed the firmware, which is one of the main sections of the DAQ, and has given major contribution to the design and testing of the electronics used by Dr Wong. She also helped and assisted Dr. Wong during the last year of experiments.

- Petasecca, M., Cullen, A., **Fuduli, I.,** Espinoza, A., Porumb, C., Stanton, C., Aldosari, A. H., Brauer-Krisch, E., Requardt, H., Bravin, A., Perevertaylo, V., Rozenfeld, A. & Lerch, M. L. F. (2012). "X-Tream: a novel dosimetry system for Synchrotron Microbeam Radiation Therapy." *Journal of Instrumentation, 7 (16), 1-15.*

  Author has entirely designed the firmware, which is one of the main sections of the DAQ, and has given major contribution to the design and testing of the electronics used by Dr Petasecca to carry out its measurements.

- Chuamsaamarkkee, K., **Fuduli, I.,** Cutajar, D. L., Lian, C., Harvey, S. & Rozenfeld, A. (2011). "Skin dosimetry of thyroid radioiodine with MOSkin detector: a phantom study". *IEEE Nuclear Science Symposium Conference Record, 258-260.*

  Author has provided Mr Chuamsaamarkkee with the electronic necessary for his experiments.

- Morganti, E., **Fuduli, I.,** Montefusco, A., Petasecca, M. & Pignatel, G. U. (2005). "SPICE modelling and design optimization of micropumps". *International Journal of Environmental Analytical Chemistry, 85 (9-11), 687-698.*

  Dr. Morganti article followed the Thesis published by the Author for the Master Degree in Electronic Engineering

LIST OF FIGURES

LIST OF TABLES

1 INTRODUCTION

1.1 Role of Radiotherapy in Cancer Treatment

There were about 14 million new cases and 8 million related deaths in 2012 where cancer is a major cause of morbidity and mortality worldwide [1]. With optimum referral patterns of cancer patients to radiotherapy as part of their treatment being 50% then enhancements in radiotherapy delivery can have a positive impact on millions of patients worldwide [2].

In the pursuit of sparing more normal tissue and reducing side effects, radiotherapy delivery has steadily increased in complexity. Standard of care external beam radiotherapy now includes complex radiotherapy techniques such as Intensity Modulated Radiation Therapy (IMRT), Volumetric Modulated Arc Therapy (VMAT) and Tomotherapy. All the named techniques use modulated radiation beamlets to target the affected volume within the body of the patient. As the technology evolves, treatments have changed over the time and higher levels of image guidance have also ensued, these include cone beam CT and frameless stereoscopic x-ray targeting systems such as those used in Stereotactic procedures (e.g. stereotactic ablative body radiotherapy (SABR), frameless stereotactic radio surgery).

1.2 Developing new generation dosimeters for QA

To ensure a proper treatment is planned and to guarantee the safety of the patients, the machines used to deliver the treatment need to be constantly checked and maintained. An important part of these checks is the Quality Assurance (QA) of delivered dose and treatment plans. Thus involves the use of an electronic measuring device which stands instead of the patient. Being irradiated as a patient would be, the device ensures the dose planned to be delivered during each treatment is equal to the actual delivered dose. The electronic device used for this purpose is a dosimeter, defined as an instrument that measures the amount of radiation absorbed in a given period [3]. That could be a very complex system made by a detector, which physically detects the delivered dose, and a readout system or procedure to translate the information acquired from the detector in value which can be handled and understood by physicists and operators. Dosimetric devices and readout electronic have been following the evolution of the treatments allowing planar 2D, 3D and 4D dose reconstructions, including features such as angle and speed detection. The system, comprising detector, readout electronic and software, is then called Data Acquisition system (DAQ). A DAQ is, per definition, a process by which physical phenomena from the real world are transformed into electrical signals. Those signals are then measured and converted into a digital format allowing processing, analysis and storage by a computer [4]. The “physical phenomena” taken into account is the radiation, whether X-Rays or photons (i.e. usually megavoltage photons which interact to create electrons and sometimes positrons). Referring to a DAQ means that the

system does not only acquire data but is capable to add some control over them. In the case of a dosimeter, it will not just read the amount of dose delivered but can act as safety device. In the event of an unexpected reading, for example, it can issue a warning to the user or ultimately shut down the machine and then can be used for QA purposes.

1.3 Modular Approach to a new generation QA system

In the following work, a modular approach to designing a DAQ suitable for use in three different kinds of radiotherapy scenarios have been taken into account: experimental Microbeam Radiation Therapy (MRT), Brachytherapy and External Beam Radiation Therapy (EBRT). The named treatments use different techniques to deliver the radiation and then the DAQ is required to be adaptable to the various specifications (e.g. beam energy, dose rate). The experimental MRT treatment uses a high intensity X-ray beam shaped into microplanes of few tens of microns. DAQs need to have high spatial resolution and high range of sensitivity to be able to detect each microplane. The Brachytherapy technique instead uses one or more radiation sources inside or next to the target area to deliver the treatment. Thus brings the advantage to deliver more precise and shorter treatment but, as the dose rate of the source can be high (more the 12 Gy/h for High-Dose Rate (HDR) therapies [5]), the accuracy of the placement of the source plays a key role. QA is then focused on 2D and 3D reconstruction in order to be able to accurately verify the source dwell positioning and timing patterns. In the third type of treatment, the EBRT, the radiation beam is pointed to the target area. The radiation is pulsed and the delivery can be modulated over the time. A specific treatment plan is required and the QA focuses on 2D, 3D and eventually 4D dose reconstructions either during the planning phase then during the delivery phase. As there are multiple clinical scenarios, the choice of the appropriate radiation detectors which can be placed in different phantoms or applicators for in vivo dosimetry and operating in different modes coupled with the requirements of the particular application, directly influences the design of the readout front end or procedure.

Centre for Medical Radiation Physics has designed a wide range of radiation semiconductor detectors to address quality assurance for three mentioned radiation oncology modalities and all of them are required sophisticated DAQ system. They vary from a single channel to multi-channel radiation detectors and have different range of sensitivity. In all three radiation oncology modalities associated with radiation source motion (HDR brachytherapy), direction and intensity change of external radiation beam (IMRT and SBRT) or fast motion of the detector across the highly modulated radiation field (MRT), the DAQ should provide a fast sampling rate of the radiation detector(s) and gantry angle in the case of EBRT on the LINAC for a real time dose monitoring. Thus a DAQ becomes a very complex system design of which requires expertise in various disciplines.

Commercial DAQs are expensive, which prompted developing of a cost-effective multichannel unified platform flexible enough to be used in multiple applications.

1.4 Project Aim

The aim of this research is to design a unique system which can be used with different radiation detectors in a wide range of clinical scenarios with minor changes; in particular, this work is focusing on the project and design of the electronic front end of the DAQ with a major effort on the digital design. The final design of the DAQ has been done by steps; gradually building up the complexity of the systems and adjusting its specifications in order improve its performances. As the various systems designed have been used in multiple projects, the aim of this thesis is to walk through the steps the author followed to reach the final product. More than the experimental results and the description of each single application, the idea is to emphasize the design flow behind the development of a multichannel DAQ starting from a single channel DAQ for a particular application. The project started with the design of the digital section of a single channel DAQ for MRT, project called X-Tream [6]. The system was upgraded to realize a multichannel DAQ able to acquire a 128 channels radiation detector using a research grade front end. Then a new front end based on commercial multichannel ASIC has been introduced in order to reduce the cost of the DAQ, and allowing to use radiation detectors with a larger number of channels and add flexibility to the system. The new DAQ was designed with a modular approach and it can be used to read out up to 512 channels by stacking 128 channels front end modules. The next level complexity of the DAQ system was associated with introduction of a rotatable phantom containing 2D array of radiation detectors which is rotated synchronously with a LINAC gantry. This setup has the advantage to have radiation beam always orthogonal to the detector plane, avoiding taking into account the angular dependence of the detectors. A new module has been introduced the control of the rotation angle of both gantry and phantom. It includes an inclinometer for the real time information of the gantry angle, a step motor for the alignment of the detector and an optical encoder for the feedback of the position of the phantom. A similar design is going to be used in a dynamic movable phantom with array of radiation detectors for the verification of dose delivery on movable targets as lungs, prostate and breast.

Figure 3 schematizes the main modules of the unified platform developed during this research project. The three applications taken into account have different characteristics in terms of timings, intensity and modality of dose delivery. To satisfy the electrical specifications of each of them, some elements of the DAQ need to be adapted, others will be constant and they will create the common platform which unifies the different DAQs. In particular, detectors are designed to fit the requirements of each application. They can be roughly classified in single channel and multi channels. The first one is manly designed for

MRT application but can be used for Brachytherapy application too. The multi channels instead are equally used in both Brachytherapy and EBRT applications. There are three different read out front ends to interface the detectors with the ancillary electronics, which will be explained in detail in the following chapters. They must adapt to accommodate the growing number of channels of the detectors and their electrical characteristics. Ancillary electronic and logic core provide a common hardware and software element shared by all the projects, along with the main structure of the GUI. Ultimately, the rotatable cylindrical phantom is a standalone module and can be incorporated to any configuration of the DAQ.

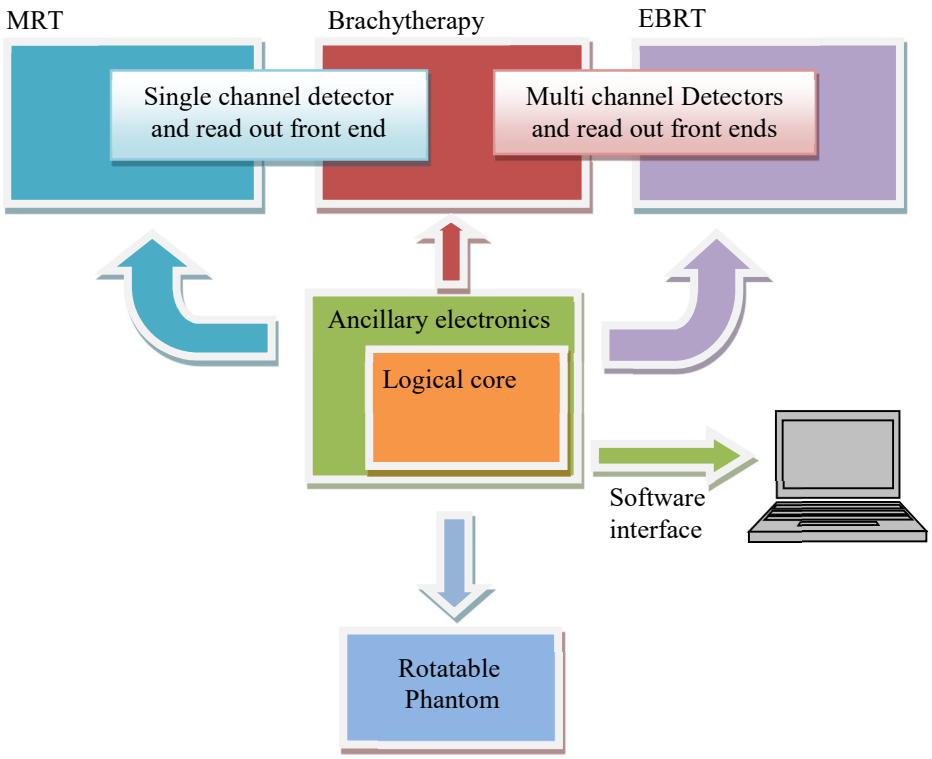

Figure 1: Functional schematic of unified platform design of DAQ system.

1.5 Summary of chapters' content

The thesis is organized into chapters describing in detail the design flow of the DAQ system and the solutions used to adapt the system to the various applications. A brief literature review in the first chapter gives the general contest of the radiotherapy techniques and the evolution of the DAQs for QA purposes in radiation therapy. An overview of the different detectors used for clinical applications and the commercially available systems will be presented in a second chapter and compared in order to justify the choices made at the design stage.

The third chapter describes a general introduction about the DAQ. The system will be comprised of modules and the ones which are the specific object of this work will be

highlighted and explained in the contest of the related project. Components used to develop the final design of some of the modules of the DAQ are software and hardware resources which will be described in detail in materials and method chapters of the thesis.

The fourth chapter describes the first clinical radiation oncology modality, which will be the MRT, and the single channel DAQ system developed for that specific project. The requirements of the application will be pointed out in order to justify the specific constraints, the design flow and results obtained.

The fifth chapter describes the second radiation oncology modality, which will be the Brachytherapy, and the DAQ developed for QA for the specific application. As the single channel DAQ is no longer a suitable solution, two different electronic front ends will be introduced with the aim of design a multichannel system. The project will be explained in detail and different stages of the design flow will be identified. A preliminary characterization of the front ends will be presented and their performances will be compared. Then the results obtained both in the test bench and in a clinical environment will be summarized pointing out the outcome of the research.

The sixth chapter describes the third radiation oncology modality, which will be the EBRT on LINAC. Both systems described in chapter five are suitable for this application but few modifications will be added. The nature of the application requires to slightly changing the dynamic of the acquisition and the modular approach used on the previous design becomes a key point to upgrade the existing DAQ. A section of the chapter will be dedicated to the rotatable phantom, which has been fully designed and realized during the research project as major upgrade to improve the systems and the QA for this specific application.

The seventh chapter presents conclusion and future works. A summary of the performances of the DAQs and their application will be proposed. They will be compared in terms of accuracy, spatial and temporary resolution, reliability showing the outcome obtained from each of them in terms of QA in clinical settings and publications. New solutions will be proposed as possible front ends to be developed either for future application or to upgrade the existing DAQs.

2 LITERATURE REVIEW

Radiotherapy is a widely used clinical technique for the treatment of many tumors. During the past years, as the technology evolved, treatments have been improved becoming shorter, the target areas smaller and the total dose has been increased whilst containing the side effects at an acceptable level [7]. To ensure a proper treatment is planned and to guarantee the safety of the patients, the machines used to deliver the treatment need to be constantly checked and maintained. Geometry, intensity and duration of the treatment can be verified by the use of a dosimeter, which ideally would be flexible enough to be used in various clinical scenarios and with the newest technologies. Dosimetric devices and readout electronic have been upgraded, following the evolution of the treatments, and are able to perform multidimensional dose reconstructions. A dosimeter could be a very complex system made by a detector, which physically detects the delivered dose and a readout system or procedure to translate the information acquired from the detector in value which can be handled and understood by physicists and operators. Dosimetric devices and readout electronic have been following the evolution of the treatments allowing planar 2D, 3D and 4D dose reconstructions. The design of a DAQ is driven by several aspects: first of all by the clinical application. There are multiple types of treatments and each one with peculiar characteristics. In the following work three of them are taken into account: Microbeam Radiation Therapy, Brachytherapy and External Beam Radiation Therapy for development of DAQ for QA. The MRT treatment uses a high intensity X-ray beam shaped into parallel planes of few tens of microns width. The optimal DAQ is then required to have high spatial resolution and wide dynamic range of sensitivity. In the Brachytherapy treatment, in contrast to LINAC applications, dose is delivered in continuous mode by the placement of one or more radiation source inside or next to the target area. Thus brings the advantage to deliver more precise and shorter treatment but, as the dose rate of the source can be high (1 Gy/min for HDR brachytherapy [5]) the accuracy of the placement of the source plays a key role. QA is then focused on accurate verification the source dwell positioning and timing patterns. In the third type of treatment, the EBRT on linac, radiation beam is pointed to the target area. The radiation is pulsed and the beam intensity can be modulated over the time. A specific treatment plan is required and the QA focuses on 2D, 3D and eventually 4D dose reconstructions either in a phantom and then during the real time treatment delivery to the patient.

The most common dosimeters are radiochromic films, Electronic Portable Imaging Devices (EPID), ion chambers and silicon diodes. Films have the advantage of having a high spatial resolution but the outcome of the measure is dependent on the processing conditions. In addition, films are sensitive to light and heat; the measure involves two steps, irradiation

and off-line scanning and analysis, thus preventing the use of this dosimeter in real-time application [8].

Ion chambers are energy independent but with a large active area they lack of spatial resolution [8]. They can be used for a single point dose measurement or arranged in matrix for planar dose mapping and still represent the standard reference for system commissioning [9].

Silicon detectors are an interesting alternative due to their small size and well defined sensitive volume. The diodes are energy dependent but almost independent from the irradiated dose when pre-irradiated without compromising the mechanical endurance [10]. Also, they can provide a real time output, which is a peculiar characteristic if related to a QA system, and can be used to produce 2D and 3D arrays of mini-sensors for high spatial resolution dosimetric imaging [11].

The literature review is focussing on the design of a DAQ. An overview of the most advanced multi channels DAQ is followed by a comparison between the solution available in the market and the DAQ developed by the Centre for Medical Radiation Physics, known as CMRP DAQ systems.

Currently there are multiple commercially available instruments which have been designed for 2D, 3D and 4D dose mapping. Sun Nuclear developed a 2D array of diodes called MapCheck2 and PTW-Freiburg developed an ionization chamber array called seven29. They have a typical spatial resolution of about 1 cm. MapCheck2 is designed to be used in a single plan of the phantom and orthogonal to the radiation beam. It is a quite large in dimension and the radiation field is significantly perturbated when the beam is not normally incident. Also, sampling rate is fixed to 50 ms. Same issue occurs with the seven29 device, which is an array of 729 ionising chambers. In addition, the ionising chambers are 5x5x5 mm^3 which is a large size and causes a poor spatial resolution. MatriXX from IBA is a matrix of 1020 ionising chambers in an active area of 24 x 24 cm^2 which can be used in fluence mode directly attached to the gantry. It can reach sampling rates of 20ms without dead time.

With the overcoming of new treatments as VMAT and IMRT which involve the rotation of the gantry during the delivery of the treatment, new QA systems have been introduced, and the old ones have been up gradated. MapPHAN, from Sun Nuclear, is a water equivalent phantom which holds MapCHECk2 at isocenter for arc delivery dosimetry. The detector can be used for coronal or sagittal measures. The same approach has been used for MatriXX introducing MULTIcube, a cubical phantom which allows positioning MatriXX at various depths on the couch either coronal or sagittal to the beam. Furthermore, ArcCHECK, form Sun Nuclear also, has a helical grid of SunPoint diode detectors built in a cylindrical phantom. The system has been designed for QA in rotational delivery. Although the phantom is static, the position of the diodes avoids any angular dependence of the global measure up to a 10x10

cm^2 field size. The angle of the gantry is measured by a virtual inclinometer and embedded in the calculations performed by the software. Data are logged and stored every 50 ms [12] [13]. PTW introduced Octavius 4D. The system consists in a rotating phantom which can house different detector plates, including the seven29, all based on an array of ionising chambers but with different dimensions and spatial resolution to cover radiation beam of different filed size [14] [15]. It has been designed for QA in Rapid Arc deliveries, were the directional dependence of the detectors can dramatically affect the measure. The system has the capability to keep the detector always perpendicular to the beam using an inclinometer placed onto the LINAC gantry. The inclinometer gives an independent position monitoring of the head and the phantom rotates in agreement with the estimated position. The dose is estimated by software reconstruction. The system has no dead time and it communicates with the PC via RS232 or Ethernet protocol. The minimum acquisition time frame of the sensor array is limited to 200 ms.

Delta4 represents another example of QA equipment for IMRT and VMAT deliveries based on silicon diodes. Sensors are arranged in two 2D arrays of 1069 elements distributed across 20x20 cm^2 of sensitive area placed orthogonal to each other in an X-shape. The orientation of the phantom can be adjusted by the user and the 3D dose measure is calculated by the software interpolation [16]. The acquisition frame is synchronised with the LINAC and integration of the current is performed only during the beam pulse (i.e. 360 Hz for a Varian 2100 EX linear accelerator). The system communicates to the PC via a proprietary protocol through a Cat-5 cable.

Table 1 summarizes the DAQ commercially available. Although the existing read-out systems are performing, they are expensive, usually designed for a specific application or to suit a set of similar ones and they lack in flexibility. The study has focussed this field of research on the development of a unified platform which can be used as DAQ for QA in different clinical scenarios with minimal modification. The final design is a cooperation of multiple expertises covering all the aspects of the DAQ: the design of the detector; the analog front end and read-out electronic; the digital design and the programming of the GUI. The main aspect of this work is the design of the read-out electronic and the digital interface. The aim is to deliver a full custom designed DAQ which in a modular approach suits all the three types of treatments previously described.

Table 1: Summary of commercial DAQ

	Phantom	**System**	**Advantages**	**Disadvantages**
PTW Octavius seven29 2D detector array	Octavius 4D	729 Ionisation Chambers	-No dead time -houses different detectors	-Volume averaging effects: data degradation in steep dose gradients -10mm pitch - estimated position of the phantom
MatriXX 2D detector array	MULTIcube	1020 Ionisation Chambers	-20ms response time -Parallel read out -No dead time	-Volume averaging effects: data degradation in steep dose gradients -7.5mm pitch
MapCHECK & MapCHECK 2	MapPHAN	445 & 1527 n-type diodes	-0.64mm^3 active volume	-Intrinsic angular dependence, physical size -7-14mm pitch
ArcCHECK		1386 n-type diodes	-0.64mm^3 active volume -Large amount of detectors	-Physical size preventative for use in-vivo, during treatment -50ms response time -virtual inclinometer
Scandidos Delta 4		1069 p-type diodes	-5mm pitch in centre -synchronized with LINAC pulses	-Complexity of integration of angular results with measured dose
QUASAR Verification Phantom		Ion Chamber and Film Cassette	Dual modality	Intrinsic limitations of IC and film, designed for head and neck treatments

Although the listed DAQs have high-performance and are readily available, they also have some limitations for clinical research environment. First of all they are expensive, meaning that it is necessary to choose the one which is best suitable for the application; then they lack flexibility: each front-end is to be used with its own detector; the parameters of the acquisition such as sampling rate, acquisition time, are fixed by the manufacturer's GUI. That justified developing a unified platform for real time data acquisition system which would allow using the same system with different detectors and the same detector with different configurations of the front-end. It would give all the flexibility needed to choose the best DAQ, comprising detector and front-end, for the QA in each of the clinical applications.

3 UNIFIED PLATFORM DATA ACQUISITION SYSTEM DESIGN

Definition of DAQ has been given in the introduction to this work as “the process by which physical phenomena from the real world are transformed into electrical signals that are measured and converted into a digital format for processing, analysis and storage by a computer” [4]. For the purposes of this research the “physical phenomena” is radiation, whether particles, X-Rays or photons and the detector is the component designed to transform the effect of the radiation into electrical signal, which typically is an analog electric current. Front end converts the current into a digital signal which will be the “digital format” that can be handled by software and stored by a computer. If the front end used generates an analog signal, then an ADC is needed as further stage in order to obtain the final format. Generally, a DAQ is composed of the following main blocks: sensors or transducers, field wiring, signal conditioning, data acquisition hardware, host PC and data acquisition software. A brief description of the DAQ sections will help explain the design flow for each project.

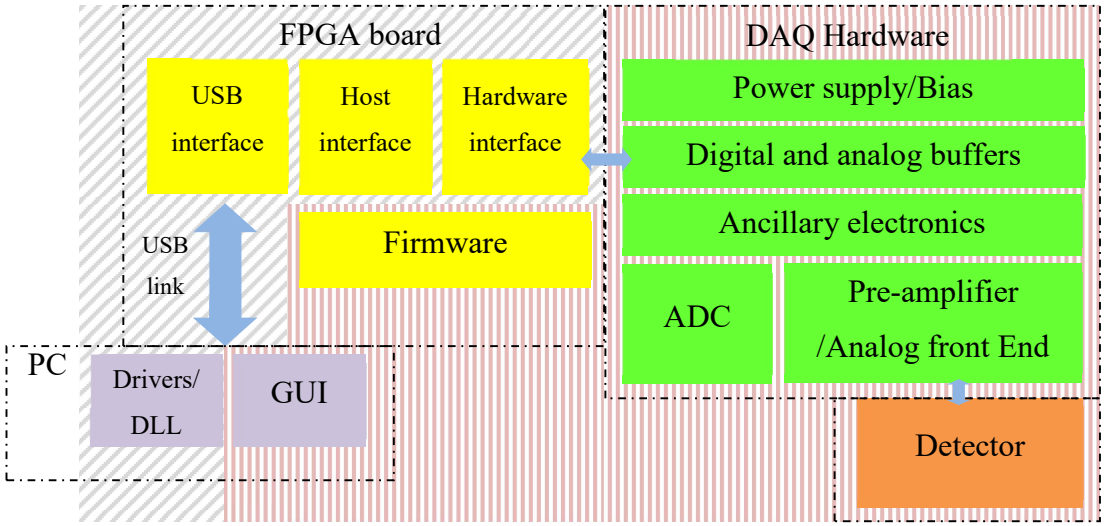

Figure 2: DAQ block diagram

Figure 2 shows a simplified block diagram of the main modules which constitute the DAQ. The four dashed blocks identify the main sections as: detector; DAQ hardware, FPGA board and PC. Inside each block there are several sub-modules which are interlaced and allow the communication within the main blocks. In particular, the detector is physically connected to the analog front end. All the sub-modules of the DAQ hardware work together to provided power supply, signal conditioning and everything else needed for the electrical functioning of the DAQ. A number of buffers are normally needed to regenerate the signals to and from the FPGA, and that is the physical interface to the FPGA board. The FPGA board hosts a physical connection to

the PC, given by the USB link, and is the logical core of the system where the firmware is loaded, that contains all the instructions to drive the signals according to the DAQ specifications. On the PC side, few DLL and drivers need to be installed to allow the data transfer through the USB protocol to the custom GUI. Whilst drivers and DLL, USB interface, Host interface and Hardware interface of the FPGA board are given by the manufacturer of the FPGA board itself and cannot be edited, Firmware, GUI, DAQ hardware and detector are the sections object of research and development.

Detectors

A detector is the first element of the DAQ and it is very complex. The ones taken in account for this research project are typically silicon diodes, either single or array. Their shape, number of channels, spatial resolution and electrical characteristics vary to suite a specific application. Although the detector plays the main role in the design of the DAQ, it requires an extensive and detailed description which is not the focus of this work. A brief description of the ones used will be given for each application in order to justify the solution adopted for the design of the DAQ.

Field wiring

Field wiring usually refers to the physical connection between the detector and the hardware. It is a passive component which can badly affect the performances of the DAQ adding unwanted noise. The systems developed have either a detector directly plugged into the data acquisition hardware or connected through high density flat cables. Length of the cables depends on the setup and it can vary from few centimetres up to couple of meters leading to the need for a proper ground shielding of the whole system to keep the signal from the detector as clean as possible from external noise. Noise, which causes measurement uncertainty and overall sensitivity degradation, will be then investigated for each DAQ.

Signal conditioning

Signal conditioning is the post-processing of the analog signal before it can be converted into digital form by the data acquisition hardware. It includes filtering, amplification, linearization, ADCs and eventually a buffering stage which adapts the

output of the front end to the inputs of the digital interface. Some front end devices available on the market have signal conditioning features embedded.

Data acquisition hardware

Data acquisition hardware is the main hardware section of a DAQ. It generates all the power supplies required by the single elements on the design; provides polarization and bias for the detector, and physically houses the analog front end and the digital sections. It is the logic core of the DAQ and the main part of this work. It controls the analog front end and maintains a communications protocol with the Host PC. In this project the logic core is based on a commercial integration module with an embedded Field Programmable Gate Array (FPGA). The FPGA is a very powerful element which gives flexibility to the DAQ by way of programming with a custom firmware, which will be the focus of this research project and it will be described in detail. The FPGA module also provides the connection to the Host PC.

Host PC

The Host PC is the computer physically connected to the data acquisition hardware. It can be either a laptop or a desktop PC. They typically communicate through a well-known protocol like RS-232, RS-485, I2C, serial, USB. For this DAQ, USB link has been chosen.

Data acquisition software

The Data Acquisition Software, also called Graphical User Interface (GUI) is the software for communication between the Host PC, the Data Acquisition Hardware and the user. The GUI uses dedicated drivers/DLL to establish the communication and enables the user to send commands, set up parameters and have a real-time feedback about the acquisition. All the information set on the software is sent to the hardware allowing the system to run on demand. The GUIs are specifically written for this project. Once the firmware is developed, a document explaining the instructions and functions to be implemented and their signal allocation is filled to start programming the GUI. Although the software interface is strictly linked to the logic core of the DAQ and to the application, it requires an extensive description and its development is not part of this work.

The aim of the project is the design of a unified platform for data acquisition and real time quality assurance of dose delivery for multiple radiation treatments. Since different applications require different specification from a DAQ, the strategy of the design is to build a modular and flexible system to be adapted with minimal modifications. Each of the clinical scenarios taken into account during this research project has particular characteristics in terms of dose delivery method, intensity and timing, which determine the specifications for the DAQ. The detectors designed by the CMRP span from single to multichannel in order to achieve planar 2D, 3D and eventually 4D dose reconstruction. The signal conditioning section, preamplifier and analog front-end, need to match its electric characteristics and properly read the current generated by the exposure. The data acquisition hardware instead, is the section which can be mainly designed to be modular and used in different contexts. In fact, the FPGA Board, which allocates the FPGA and the chip for the USB connection, is an invariable element of each of the system described and it is used in all the applications with different suitable firmwares loaded into the FPGA. As the firmware design is the main focus of this thesis, a more detailed description of the hardware and the tool used for the digital design will be given prior to introducing the design of the DAQ itself.

3.1 Digital design tools

The tools used to develop the digital interface are two: the hardware FPGA Board and the software to design the firmware. Both of them are readily available cost-effective easy accessible commercial tools, allowing upgrading or modifying without costly rework.

The hardware section is a XEM3001 board from Opal Kelly equipped with a Xilinx Spartan-3 XC3S400 FPGA (Figure 3) [17], which is the smallest and cheapest of the FPGA integration modules available from its manufacturer.

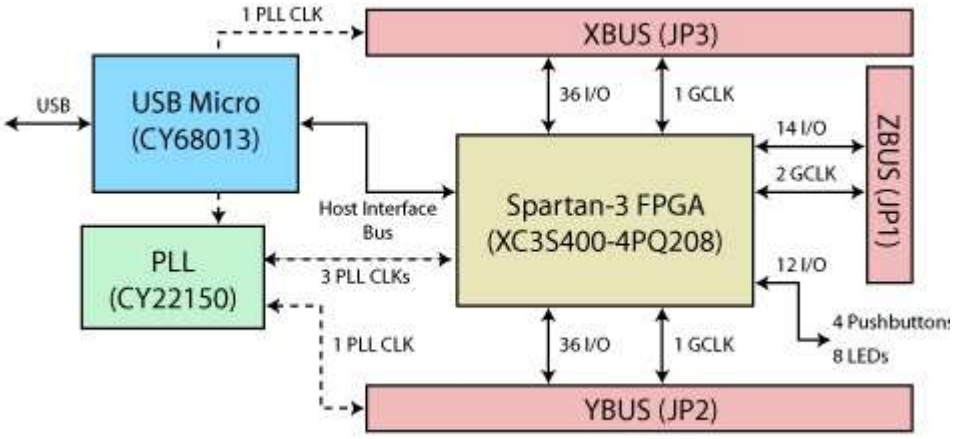

Figure 3: Opal Kelly XEM3001

Table 2 reports a shortlist of the devices which have been taken into account at the stage of the selection of the FPGA Board, all of them made by the same manufacturer. The XEM5010 is the top performing one in terms of memory, both as RAM blocks into the FPGA and as on board memory, and for the number of I/O available; but is also the most expensive. Although the FPGA of the XEM3001 has the smallest memory on board and fewer resources available, it also has minor constraints on the design and routing of the clocks. The XEM3001 has been chosen during the feasibility study of the DAQ as trade-off between cost and flexibility. Moreover, XEM3001 is pin-out compatible with the XEM6001, allowing to upgrade to a bigger device without any hardware rework. If fact, the XEM3001 and the XEM6001 can be interchanged with only minor changes to the firmware and the software interface to communicate to the different FPGA.

Table 2: FPGA Boards

	XEM3001 Spartan3 XC3S400	XEM6001 Spartan6 XC6SLX16	XEM5010 Virtex5 XC5VLX50
Clock speed	150MHz	150MHz	150MHz
Internal RAM	18KB	36KB	2MB
Interface	USB 2.0	USB 2.0	USB 2.0
I/O	88	88	Up to 200
Flash memory	No	32Mbit SPI	32Mbit SPI
External memory	No	32Mbit SPI	256MB+36Mbi
Transfer rate	36MByte/s	36MByte/s	36MByte/s

The XEM3001 incorporates the Cypress CY68013, which allows communication though the USB, and a Phase Lock Loop (PLL) CY22150, which provides three independent clocks for the FPGA and two extra output directly available at the output of the board. The frequency of the clock of the PLL can be set through the GUI or the FrontPanel, software provided by the manufacturer, and the configuration is stored into the on-board EEprom. Figure 4 shows the interface provided by the FrontPanel software to set up the frequency of the PLL. The reference clock at 48MHz is driven by the USB. An internal Voltage Controlled Oscillator (VCO) increases the frequency up to 400MHz. Although there are five available output points, only two secondary frequencies, other than the reference and the VCO, can be adjusted using “Divider #1” and “Divider #2” and fed into the FPGA.

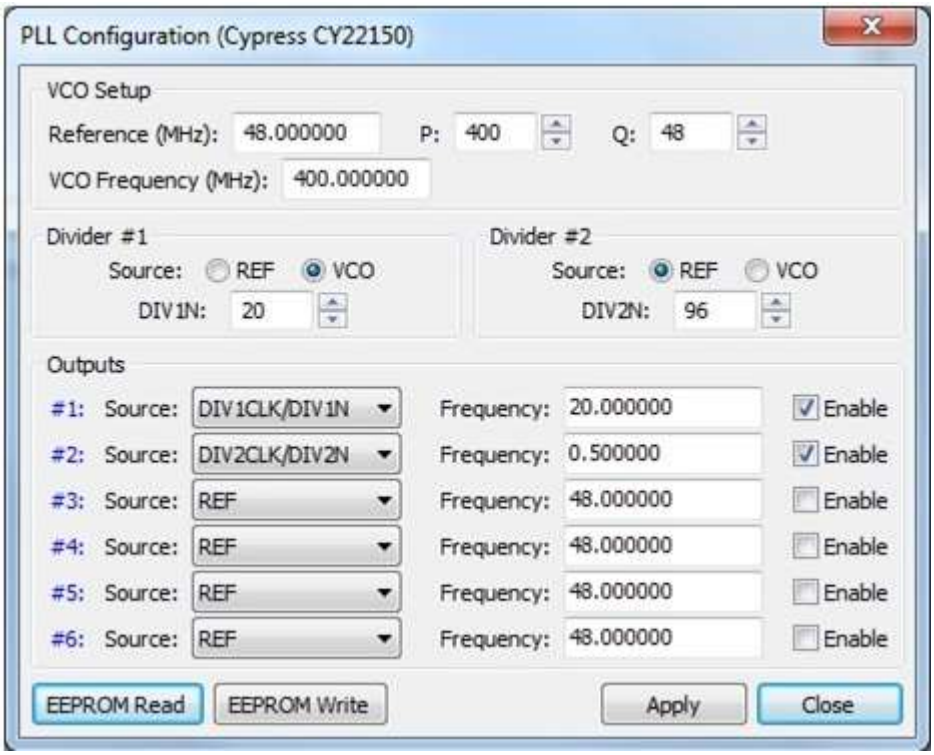

Figure 4: PLL configuration interface via FrontPanel

The FPGA has 88 I/O connected to the output of three standard connectors JP1-JP3 ready to be used for a user application. The board can be powered from the USB cable in standalone mode or from an external power supply through the sockets JP1-JP3, which are standard Dual-In-Line (DIL) with 2.54 mm pitch.

The XEM3001 interfaces FPGA and PC through “endpoints” (Figure 5). These endpoints are allocated on the FGPA side by including the VHDL (Very High Level Description Language) or Verilog libraries into the firmware as long with the User Constraint File (.ucf) which defines the physical connection to Host Interface Bus. From the PC side, there are DLLs (Dynamic Link Library) to be included to the GUI to share the same endpoints with the FPGA; and drivers to be installed on the PC. The pre-compiled VHDL files are black boxes for the user but they set up all the different range of endpoints. Endpoints are classified in WireIn (input signals), WireOut (output signals), TriggerIn (input trigger signals), TriggerOut (output trigger signals), PipeIn (input data for memory), PipeOut (output data from memory). Each of them defines a connection between FPGA and GUI, based on a 16-bit word, which is updated on

demand by the PC. By addressing the right endpoint, FPGA and GUI are able to exchange commands and data in real time.

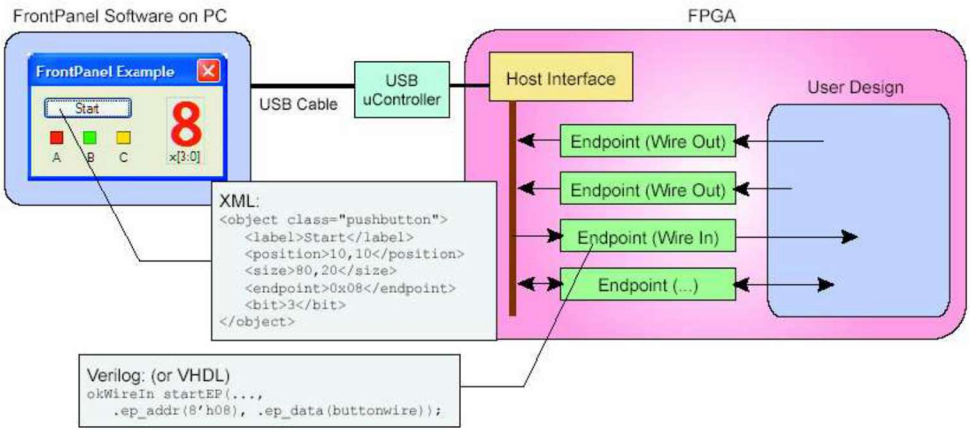

Figure 5: Endpoint description from Opal Kelly manual.

The firmware is loaded into the FPGA through the USB so that the same device can be used in different application, simply changing the bitstream (.bit) file. The choice of the FPGA offers many advantages:

- the USB connection is embedded and components and libraries needed to set up the communication are provided by the manufacturer, so ideally it can be plugged in directly into a PC;
- is extremely versatile and reprogrammable: a bitstream file can be loaded into the FPGA through the USB, which means no need for expensive programming tools, and the same device can be shared by different DAQ;
- is reliable: same module can be programmed thousands of times with different firmware and so it can be used in any application;
- IO pins are easily accessible through standard DIP connectors: no needs of outsourcing soldering facility.

The programming tool used for all the design is ISE Design Suite 14.3 and following releases. The software, in its lite version, is a free tool which can be downloaded from the Xilinx website. It allows writing the firmware using a mixed coding of descriptive languages (Verilog and VHDL), schematics and pre-designed IP cores. Within the IP cores available, two of them are the most useful: the Clocking function and the FIFO (First In First Out). The clocking function is used to generate the DCM (Digital Clock Manager). This component allows deriving, from the main clock signal, all the

secondary clocks minimizing phase jitter and skewing in between them. The FIFO core allocates a number of RAM block into the FPGA which will be used as memory stack. The memory follows the rule of first in is the first out. Data is stored during the acquisition and once the GUI calls a PipeOut endpoint, blocks of 16 bit words are transferred through the USB in the same order in which they were loaded into the memory.

The software provides an additional tool which simulates the logical behaviour of the synthesized code. Although the number of elements which can be simulated is limited by the lite version, it is still enough for preliminary debugging of the design. Libraries and User Constraint File are added to the firmware at this stage and, once the project has been built, the bitstream (.bit) is generated and can be loaded into any FPGA.

4 MICROBEAM RADIATION THERAPY PROJECT: SINGLE CHANNEL DATA ACQUISITION SYSTEM

Methodologies and results discussed in this chapter have been published by *Petasecca et al.* [6]. The author has entirely developed the firmware for a proper functioning of the DAQ; had a relevant contribution to the electronic design, debug and test of the front-end and has actively participate to one test session at the ESFR.

The pilot project for the development of a custom DAQ was the design of a new system for Microbeam Radiation Therapy application. The MRT technique uses a synchrotron X-ray beam physically collimated into an array of microbeam, few tens of microns wide with a pitch of few hundred microns, to target tumours. The photon energy ranges between 50 and 350 keV [6] thus making the dose in correspondence of the beam very high (called microbeam peak) whilst the area in between the peaks, identified as valley, would get very low dose. This clinical scenario has the following main requirements: wide sensitivity range of the front end (10^4 as minimum order of magnitude according to Monte Carlo simulation [18]) to detect the dose rate both in the peak and in the valley; high spatial resolution, on the micron range, to resolve each single microbeam. Currently, dosimetry for such treatment is carried out using a combination of Gafchromic films and ionisation chambers. However, both techniques have some limitations: films are not a real-time dosimetry system and their dynamic range is not enough to cover the amplitude of a peak-to-valley signal; whilst ionisation chambers have a real-time output but their spatial resolution cannot resolve the X-ray beams. The idea is to design a new system which can combine the accuracy of the films, in term of spatial resolution, and the real-time response of the ionisation chamber. CMRP had already available a microstrip single diode able to perform the measure. the diode will move, scanning the beam during the treatment. The idea is to design a readout system with a fast readout rate to have high spatial resolution; a wide gain range and an output which can be displayed in real time. A detailed representation of the experimental setup is shown in

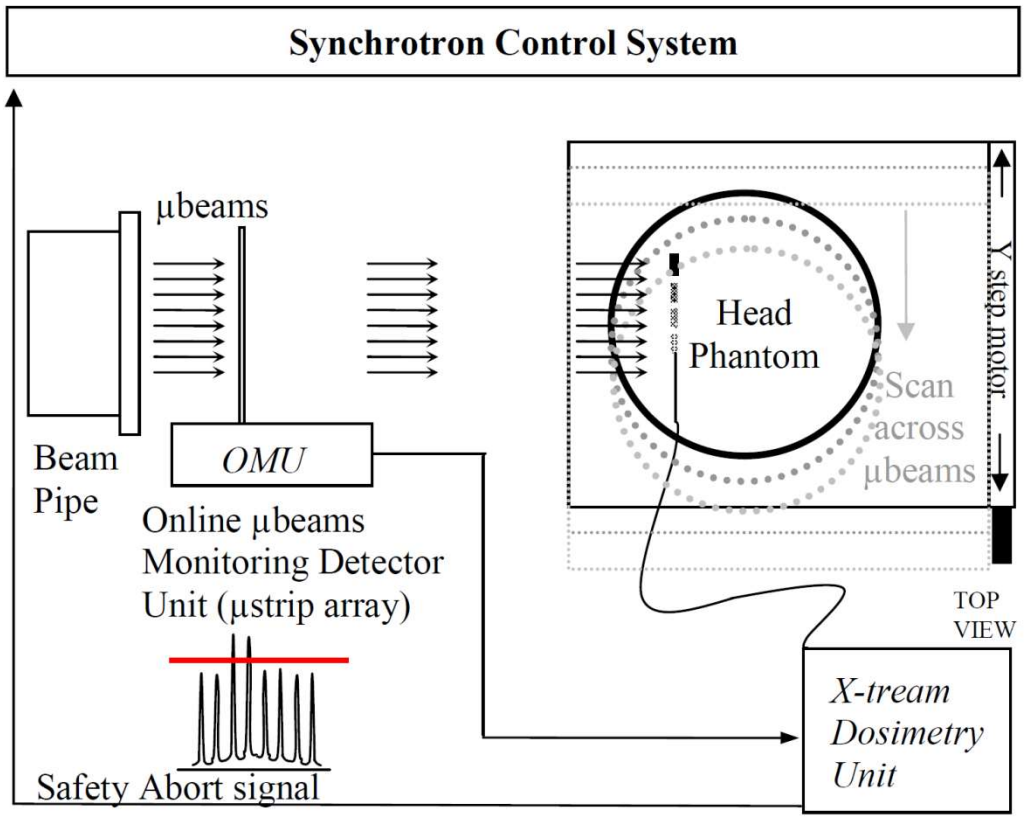

Figure 10.

4.1 Hardware description

The first step of the design of the new DAQ is the selection of the detector. The detector chosen was a single microstrip silicon diode. The microstrip is 10 µm wide and it is surrounded by an n^+ guard ring which allows reducing the sensitive area of the detector. It has been designed by CMRP using a patented technique, called "drop in" technology, which minimizes the dose enhancement due to the material surrounding the chip by encapsulating the sensitive area into a Kapton probe. It can be used either in passive mode with bias up to 200V. To be able to read the detector, the electronic hardware of the DAQ needs a single channel front-end with an optional High Voltage bias. The main parameters driving the design of the electronic are: the wide dynamic range, in which the sensitivity of the preamplifier must remain linear; and the equivalent capacitance at the front end input. By the mean of Monte Carlo radiation transport simulation, a Peak to Valley Dose Ration (PVDR) of a 51 microbeams array has been estimated to be about few thousand. This information translates on a minimum sensitivity range of 10^4 at the dosimeter front end. The

photocurrent generated by the sensitive volume of the detector is directly proportional to the dose rate of the MRT beam and then the expected variation range of the input signal will be of the same order of magnitude of the expected dose rate. In addition, the detector and its Kapton probe have a capacitance of 7pF at 50V that has to be matched by the input impedance of the preamplifier. The logarithmic option, for the preamplifier module, has been discarded due to its strong dependence on temperature; the solution chosen was a transimpedence amplifier, based on commercial JFET input stage operational amplifier (AD795) from Analog Devices, with a gain of 10^5. In this configuration the detector is directly plugged into the signal conditioning preamplifier module which is located close to the beam. A long cable is needed to connect the pre-amplifier module enclosure to the data acquisition hardware. In order to reduce noise in field wiring and to preserve the integrity of the signal, a differential driver/receiver pair has been added at both ends of the twin-axial cable based on EL5172 and EL5072 from Intersil as driver and receiver. As the output of the differential stage is still an analog signal, an ADC is included in the data acquisition hardware to convert the output into digital numbers.

Other than having a large sensitivity range, the front-end has to be fast enough not to cause alteration on the signal read from the detector while scanning the beam. The output of the detector in fact will have a steep gradient between a peak and a valley. A fundamental parameter of an electric circuit is the slew rate (SR). It represents the maximum voltage change per unit time that can be applied at the input of the circuit and it is usually measured is voltage per microseconds (V/μs). An analysis of the SR of the system will show how the front-end is capable to follow the quick variation of the input signal.

A single micro beam has been simulated by the mean of Monte Carlo to help with the selection of the ADC.

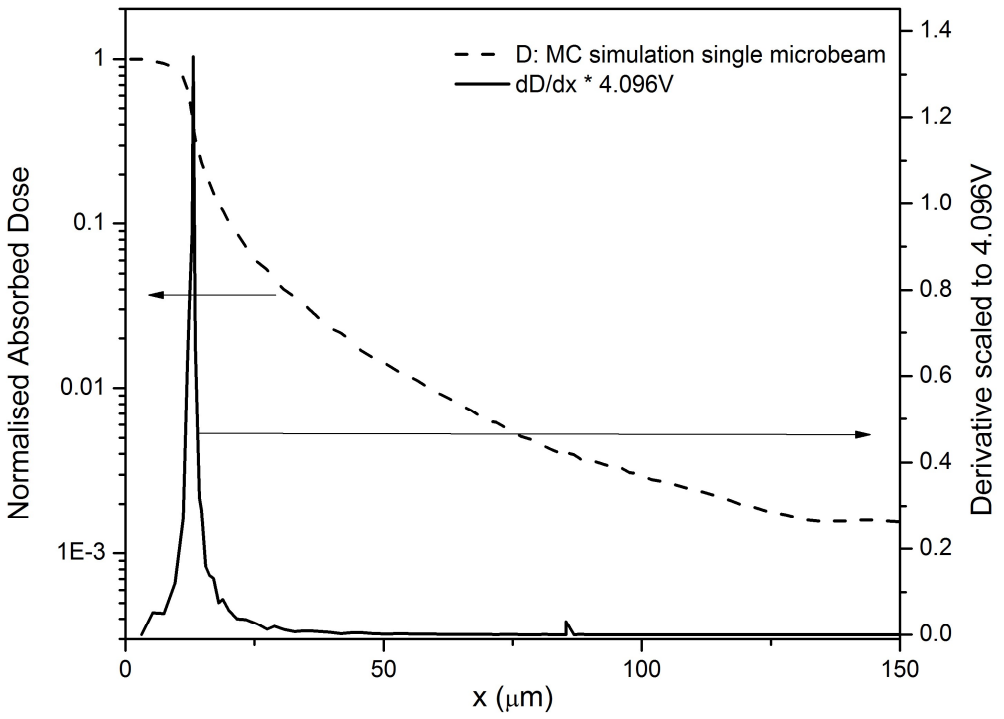

Figure 6: Dose profile across half microbeam and its derivative.

Figure 6 shows a normalized profile of half microbeam, as per Monte Carlo simulation, scaled against the voltage reference of the ADC; a value of 4.096V has been chosen as typical ADC reference. The microbeam is 52μm wide and the dose is calculated at 10mm depth in a water equivalent material. This is the worst case scenario when the peak of the microbeam corresponds to the ADC full scale, which is 4.096V, and the following point will be a valley at zero amplitude. Theoretical maximum derivative value, normalized to the ADC full scale, is calculated as 1.4V/μm. Given the detector is moving at a constant speed of 1mm/s it translates into 1.4mV/μs slew rate. In order for the ADC to be able to measure amplitude of 1.4mV, a resolution of 14 bit is an optimal requirement, in fact the typical reference of 4.096V divided by 16383 steps of the 14-bits digital resolution gives 0.25mV per step. The ADC will be directly connected to the FGPA and its output is stored into memory blocks which normally allocate 16 bit per word. A 16-bit ADC is then the best solution to increase the sensitivity of the DAQ and optimize the communication with the FPGA. The chosen device is the ADS8405 from Texas Instruments [19]: it has a 16-bit digital parallel output which can be feed directly into the next section with no delay; it runs at 1MHz conversion rate and uses an external reference of 4.096V which gives a sensitivity of 0.0625mV/bit. The goal of the high spatial resolution is reached thank both to the

physical dimension of the detector and to the fast sampling rate of the ADC. The ADC is connected directly to the FPGA to be read in real time. The FPGA also controls the High Voltage bias supply source and the communication with the PC Host through a USB link and temporarily buffers data from the ADC. The FPGA module is the XEM3001 from Opal Kelly described in the previous paragraph.

The bias for the detector is realized using two commercial chips from EMCO. They allow generating a high voltage output of ±100V with a ripple of ±2.5mV at 100V. The output is tuned by adjusting the voltage at the programming voltage input. To avoid the need of physically access the board to set the bias, a digital trimmer has been used allowing the high voltage to be selected and applied through the GUI. As that could potentially be a critical procedure, a second ADC dedicated to the high voltage section has been added to provide feedback. The chip will be giving a feedback about the voltage at the programming input before the bias is applied to the detector; both the digital trimmer and the ADC are controlled by the same FPGA.

4.2 Firmware description

Figure 7 shows a block diagram of the firmware used on the MRT project. The design of the firmware is entirely author's original work.

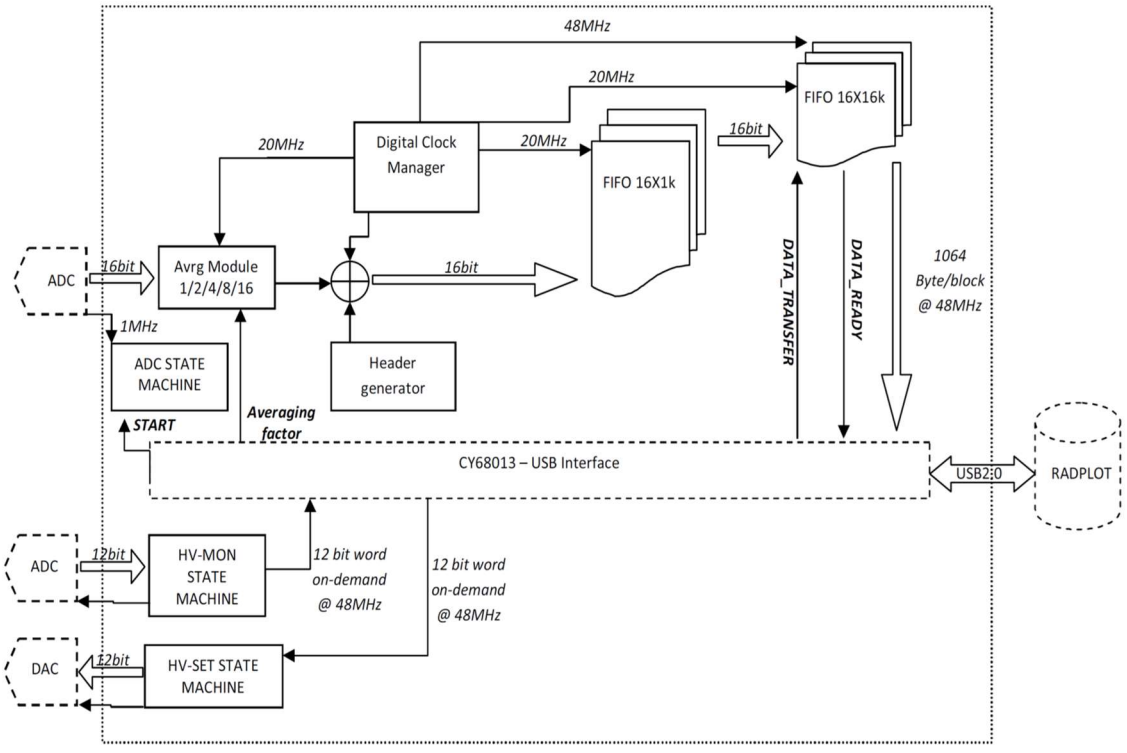

Figure 7: MRT firmware block diagram.

There are five major blocks: Digital Clock Manager (DCM); ADC state machine; Average Module; HV set module and monitoring; Data store.

- Digital Clock Manager uses an IP-core (Intellectual Property core) DCM component to generate all the clock frequencies used by the FPGA. As the minimum input frequency of the DCM is 18MHz, the time base has been set to 20MHz, which can be easily divided into submultiples by the DCM itself and used by different sections of the firmware. The 20MHz clock gives the time base for the internal counters that set the duration of the acquisition according to the user's settings. Once a START command is assessed by the operator, the timer starts and makes the acquisition running for the length set on the GUI (Appendix B Figure 57).
- High Voltage set and monitoring allows the user to set up the value of the bias to be applied to the detector through the GUI. The value is loaded into the FPGA and sent to a DAC. The analog output of the DAC drives the reference input of the EMCO which sets the HV. Before applying the HV to the detector, the voltage is read by an ADC, fed back into the FGPA and displayed by the GUI. The user can then confirm the value and apply the setting to the detector enabling a safety relay on board, thus to avoid accidental high voltages which can damage detector and electronics. All the High Voltage set and monitoring section runs on demand by the user (appendix B Figure 58).
- ADC state machine is designed to control the conversion cycle of the ADC, connected to the preamplifier output. The chosen ADC has a relatively simple interface with just three basic signals: the chip select (CS) to activate the chip; the read enable (RD) to enable the output and the CONVST which starts the conversion. The ADC replies with a BUSY, meaning that the chip is working and the conversion is in progress, then all the sixteen pin of the output are updated at once with the converted value. As the DAQ is a single channel system, having an ADC with a 16-bits parallel output is acceptable in terms of I/O occupancy, and reduces the complexity of the firmware as the output can be directly transferred to the following section of the firmware without any post-processing. The maximum conversion speed by datasheet is 1.25MHz which has been downscaled to 1MHz to be compatible to the main clock of the firmware and yet fast enough to guarantee

a high oversampling rate. The ADC state machine runs automatically every time the acquisition starts (Appendix B page 89 ADC state machine).

- Average Module: as the detector moves at 1mm/s speed across the radiation field, the 1 MHz sampling rate gives a huge and in most cases excessive amount of data to be stored and analysed. Thus, the averaging module helps downscaling throughput to the FIFO by a factor of 2, 4, 8, or 16 without reducing the conversion sampling rate of the ADC. The averaging also reduces the noise to some extent acting as filter. The choice of using power of 2 as averaging factors does not increase the use of the logical resources into the FPGA, as it translates in a simple shift of the digital numbers. Dividing by numbers whose do not fall in that range in fact must be done by a dedicated IP-core and the division itself takes about one clock cycle per bit to be completed. The Average Module is an optional function which can be selected by the user.
- Data Store memory block. Data is temporary stored in the IP-core based FIFOs, which are implemented by the digital design tool. The FPGA XC3S400 has 16 blocks RAM available to be organized as FIFO. In order to maximize the use of the on board RAM, the memory stage comprises two FIFOs: the first one, contains 1024 words at 16 bits and uses one block of RAM and a second one, cascaded to the first one, contains 16384 words at 16 bits and uses 15 blocks of RAM. Although this choice requires a synchronization of data transfer between the two FIFOs, it guarantees no data losses during the handshaking of the USB link. In fact, when the second FIFO starts to be filled up, a flag rises and a DATA_READY signal is sent to the GUI. The software then replies with a DATA_TRANSFER command which enables the download of the FIFO. The latency of the first communication between the DATA_READY and the DATA_TRANSFER has been measured to be about 3ms, due to the processes already running on the PC and the performance of the USB as well. Once the transmission starts, data is transferred in bursts of 1KB until the completion of the selected buffer size. The dimension of the buffer size, which is defined through the GUI, plays a key role on the integrity of the data: in fact if the buffer size is too small, the transmission rate slows down, the FIFOs will overflow and there will be data losses as the download rate will be slower than the ADC data rate; in the other hand, if the buffer size is too big compare to the real amount of data, the GUI will

keep accessing the FIFO in order to fill up its memory burst and spurious values might occur. Before being loaded into the FIFO, the data is multiplexed with a 16-bit header internally generated. The header acts as error detection tool: it is in fact necessary for the GUI to identify the real data and discard the spurious value. However, in the negative side, it doubles the number of words to be stored. For the designed DAQ a 3ms delay corresponds to a maximum of 3000 words at full speed and without any averaging; by adding the header, the maximum number of word transferred during the latency time can reach 6000 words, which is still well under the memory size (Appendix B Figure 59 and Figure 60).

The redundancy added by using a header for each value transmitted as been evaluated against standard algorithms used for error detection. The most common are parity check, Cyclic Redundancy Check (CRC) and checksum. All of them imply the need of extra code to be appended to the original binary data to be able to detect if the value has been corrupted. The mentioned algorithms are very well defined, widely used and are effective for errors occur during the transmission [20] [21]. In regard to the system designed, the USB link will be handled by the black boxes and DLL provided by Opal Kelly and the USB protocol already includes CRC error detection [22]. The use of the header then remains an effective way to identify data and discard spurious values without using an extra error control tool.

The firmware has an additional operating mode called “Multi-trigger”. All the functionalities previously described do not change but the system uses an external signal from the beam to trigger the acquisition. Instead of being read continuously, the detector is acquired only when the trigger happens, thus allowing the optimal alignment of the detector with the beam (Appendix B Figure 61).

The custom designed GUI for the project is called RadPlot. It allows setting up the parameters of the acquisition; visualize the output from the detector in real time; download the data into a binary file which can be converted as text file and easily handled for post process analysis.

4.3 Preliminary characterization

A preliminary characterization of the front-end has been carried out on a test bench. Figure 8 shows the response of the real transimpedence amplifier to a current step signal of about 50µA. The output voltage shows a transimpedance gain of 2V/50µA (40kOhm), which is the order of magnitude expected by design. The total slew rate is

calculated as 1.56V/µs, value which is much greater than the theoretical slew rate. The bandwidth of the analog front end is estimated to be about 520Hz with an equivalent noise of 0.83 pA/√Hz.

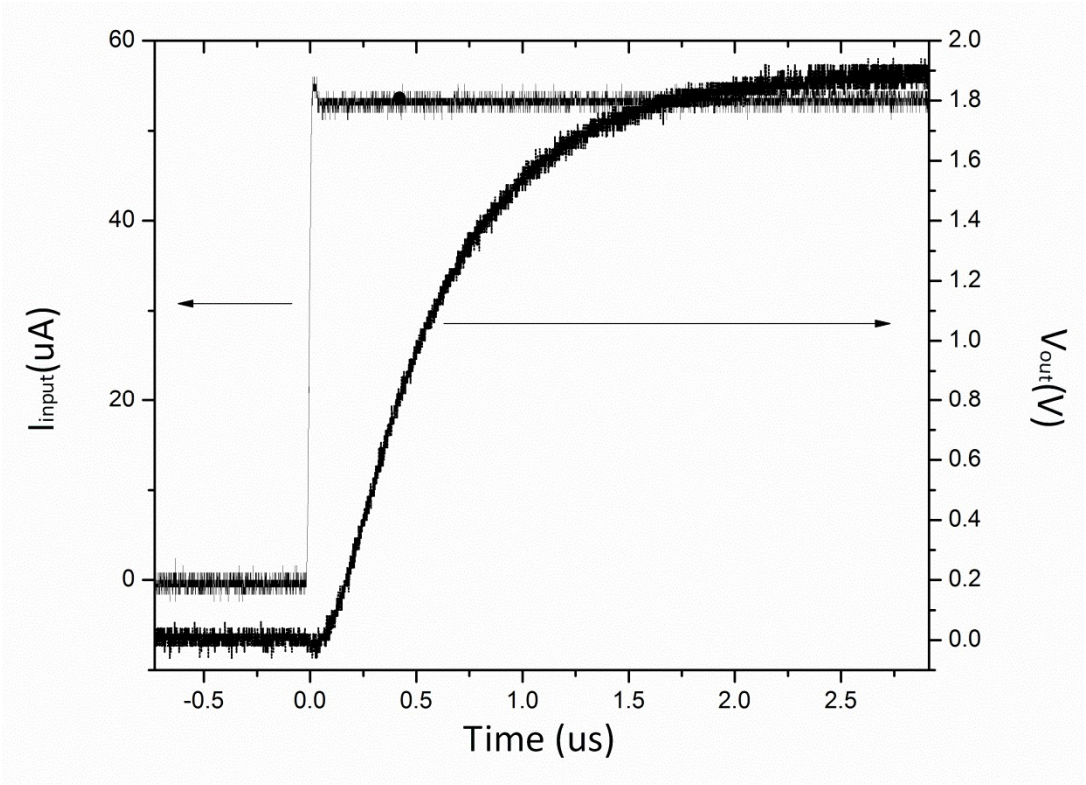

Figure 8: Transient response of the transimpedance amplifier

Linearity of the system was tested to by feeding a constant current from 4nA up to 20µA at the input of the preamplifier. Figure 9 plots the output of the ADC in counts against the current. The conversion factor was calculated as 2.51counts/nA.

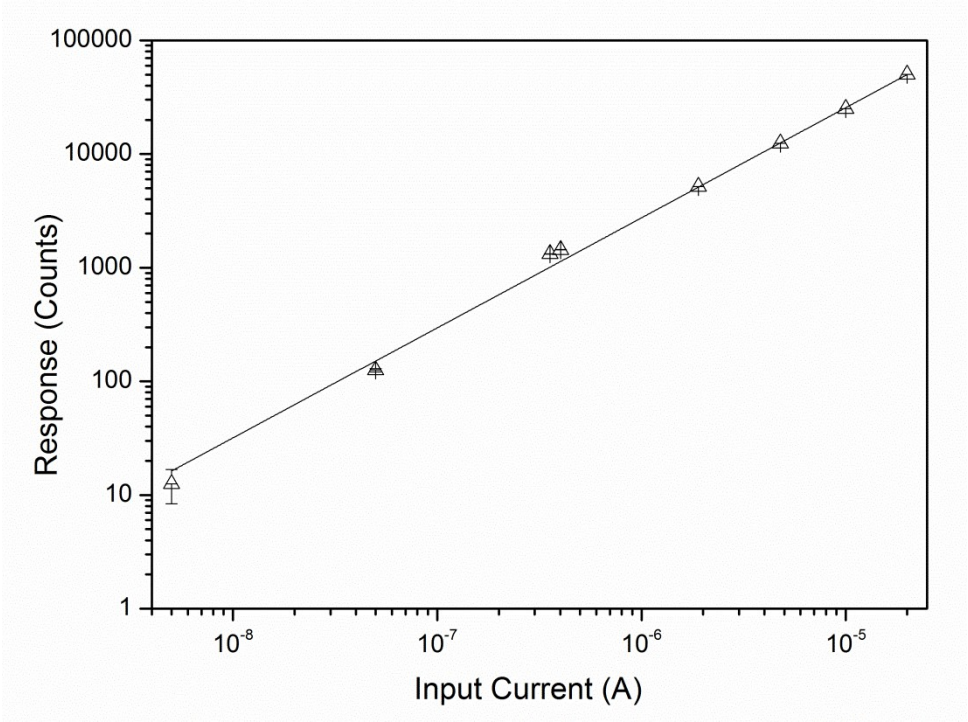

Figure 9: X-Tream linearity.

Noise performances have been evaluated in the worst case scenario: sampling a valley in between two peaks. As this condition lead to nearly no dose seen by the detector, it has been simulated by sampling the dark current of the detector diode, and the noise manifests in the fluctuation of the baseline. The standard deviation of the Gaussian fit of the baseline gives a value of the noise of approximately ±0.43nA (±1.1 counts of the ADC).

4.4 Experimental results

The X-Tream DAQ has been fully tested at the biomedical beamline ID17 of the European Synchrotron Research Facility in Grenoble. The detector was mounted on a central axis of a cubic phantom (15 x 15 x 15 cm^3) made of Perpex. Initially, the detector has been aligned by using the "Multi-trigger" operating mode, and then all the measures were taken by scanning through the radiation beam; a -30V bias has been applied to the diode (set up shown in

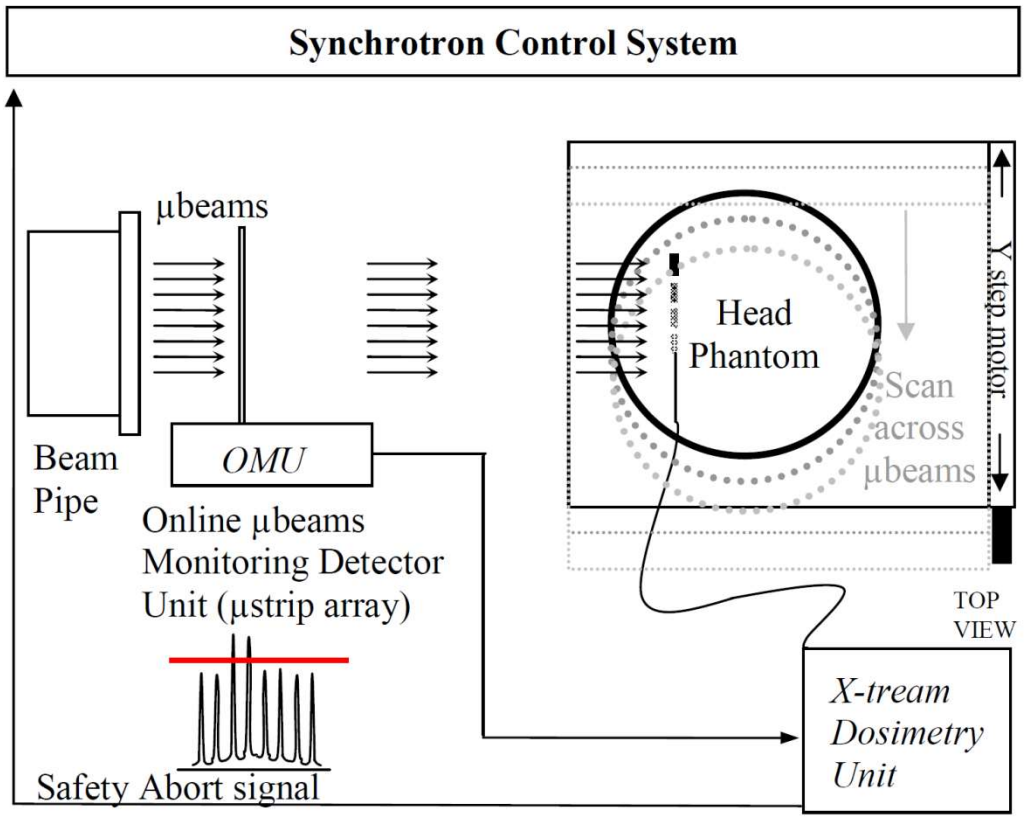
Synchrotron Control System
µbeams
Beam
Pipe
OMU
Online µbeams
Monitoring Detector
Unit (µstrip array)
Safety Abort signal
Head
Phantom
Scan
across
µbeams
Y step motor
TOP
VIEW
X-tream
Dosimetry
Unit

Figure 10).

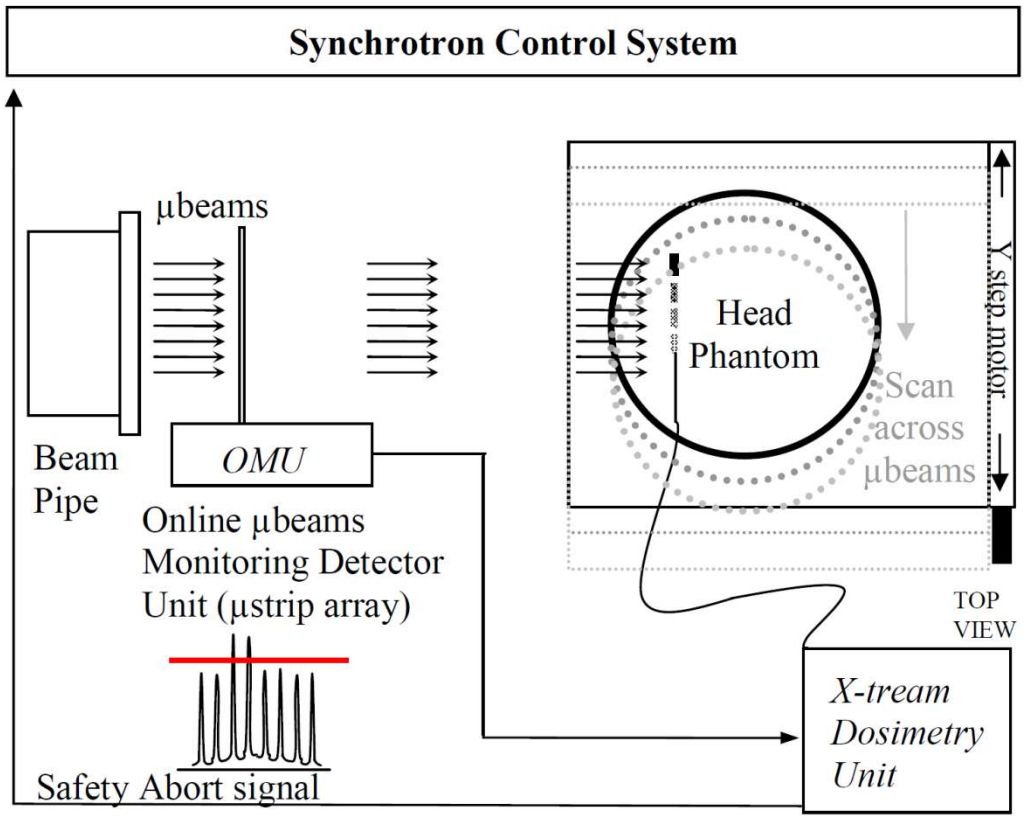

Figure 10: MRT test set up at the ID17 at ERSF.

Two different sets of measures have been analysed: radiation field profile and the profile of the microbeam array. A typical radiation beam profile before multi slit collimator (MLC) is shown in Figure 11 (left side), and a magnified view of the uniformity of the peak response is highlighted on the right side. The height of the single microbeam was 50 µm, which is approximately the dimension of the sensitive volume of the detector. The results show a profile uniformity in agreement with what expected and conform with the Gafchromic films measures found in literature [23]. The width of the beam is conforming to the setup used.

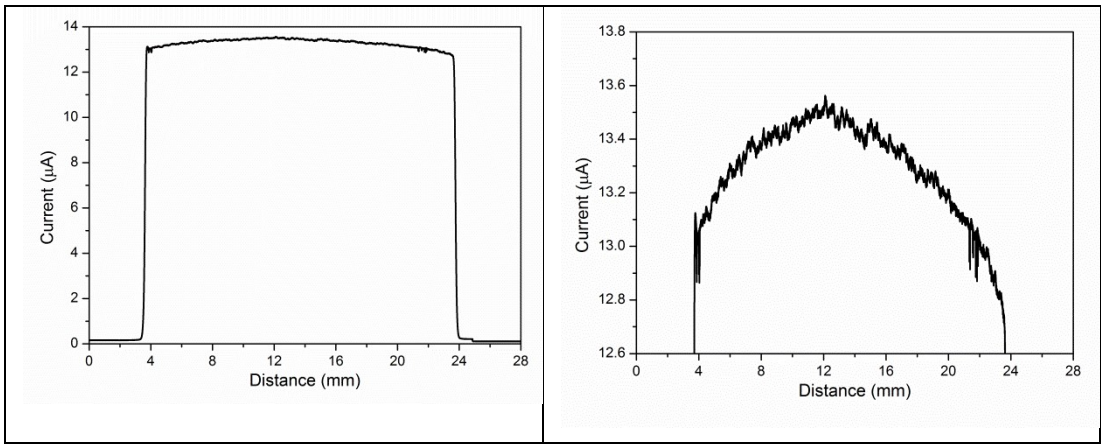

Figure 11: MRT beam profile before MLC (left side); magnified view of the fluctuation (right side).

A second set of measures is shown in Figure 12 where a microbeam array after multi slit collimator has been measured. The beam is 500 μm heights, which gives a much higher response, and all the 49 peaks can be clearly identified. A magnified view of the peaks (Figure 12 right side) shows a higher fluctuation of the intensity of the microbeams. This effect is likely due to the mechanical shaping of the beam with the Multi Slit Collimator. All the statistics of the measure as FWHM, PVDR and peak to valley response, have been analyzed using the RadPlot GUI, custom designed for the project.

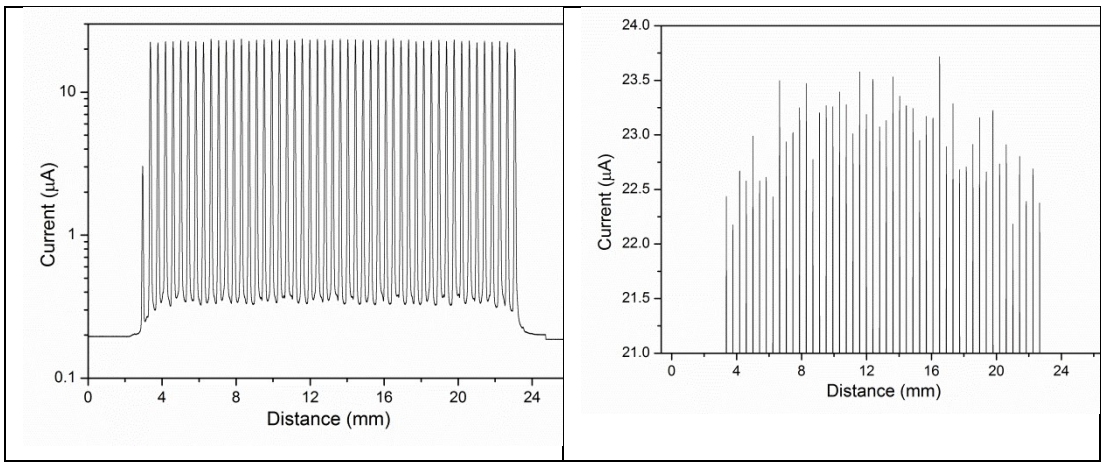

Figure 12: MRT microbeam array profile (left side); magnified view of the peaks (right side)

The FWHM of a single microbeam measured by the system was 62 ± 2 μm with a confidence of 99%, which indicates that the effective spatial resolution of the DAQ is

10-12 μm if compared with the physical dimension of the slots of the Multi Slit Collimator of 50 ± 1 μm. The distance in between the peaks is 400 μm and it has been measured as 410 ± 3 μm, in agreement with the expected centre-to-centre distance of 412 μm which comprises the X-ray beam divergence. For an extended discussion about materials and methods and results of the experimental tests refer to *Petasecca et al.* [6].

Overall, the developed system shows the ability of measure the instantaneous peak-to-valley ratio of the MRT and analyses the data in real time. This can enable generating a safety abort signal, if the measured dose differs from the expected one. The performance of the DAQ appears to satisfy the requirements of the application. A major improvement can be obtained by allowing the communication between the DAQ and the MRT control system. The Beamline Control Unit has his own software for data acquisition and control of the beam, called SPEC [23]. SPEC is coded in a proprietary language which is a mix of Python and C++, and appears to the user as a command line interface. It allows accessing any information about the beamline, like intensity of the beam, timestamps and any other setting. SPEC communicates via Ethernet protocol and allowing the DAQ to load its dataset into SPEC means modifying its communication interface. The implementation of the Ethernet protocol instead of the USB has a huge impact on the design of the system: in fact every section of X-Tream should undergo some modification. At the hardware level, the Opal Kelly board cannot be used anymore and a similar solution hosting the Ethernet connection must be found or it has to be designed. Thus implies a rework of the electronics and a new design of the firmware as the endpoint protocol cannot be implemented. The software interface as well has to handle the Ethernet communication protocol and be able to share its datasets and acquisition settings with SPEC. The upgrade will be part of future works.

5 BRACHYTHERAPY: DATA ACQUISITION SYSTEM FOR QUALITY ASSURANCE

Methodologies and results discussed in this chapter have been published by *Espinoza et al.* [24] [25], *Fuduli et al.* [26], *Wong et al.* [27]. The development of the firmware, digital core of the DAQ used for all the named publication, is entirely original work of the author of this thesis. She has also actively collaborated to the electronic design as long as the debug and testing of the hardware.

A data acquisition system for QA during brachytherapy treatments is the second project explored during this research work. This technique can be subdivided into two categories: permanent implant or temporary brachytherapy. For the first one, a small radioactive source is placed into the body of the patient, to the area to be treated, and permanently left in place; for the second kind of treatment instead the source is inserted into or placed nearby the tumour for a certain amount of time and then retracted. Temporary brachytherapy can use Low Dose Rate (LDR) or High Dose Rate (HDR). The difference depends on the activity of the source used which determines the duration of the treatment. The HDR is widely used to treat tumours in different areas of the human body such breast, prostate and skin. It takes the advantage of delivering high dose rates in a short treatment time with minimal fractionations by placing a radiation source in contact with the target tissue or in a space or cavity next to it [28]. As the radiation source moves during the treatment (e.g. prostate treatment) to reach its dwell position, a QA system should ideally be able to measure speed, dwelling position and timing of the source; measure the dwell and the transit times; provide a 3D reconstruction of the dwell position and reconstruct the absorbed dose distribution as well. All these parameters should be compared in real time with the treatment plan. Few solutions are already available for verification of dwelling which use radiochromic film, ion chambers array or high spatial resolution video camera, but they require an extensive imaging processing and do not provide real time results. Once again the system must have high spatial resolution, fast real time response and adequate sensitivity.

The X-Tream System, as designed on the MRT project, has been tested for the HDR brachytherapy using single epitaxial diode. Its fast sampling rate at 1

Megasample/second fulfils the goal of measuring the instantaneous dose rate and the DAQ is able to track the source while it moves from the first dwell position into the second one then back into the afterloader (Figure 13). Figure 13 shows a profile of the source moving versus time. The Ir-192 source used has a 7.052Ci activity, the dwell positions last for 5 seconds each and the step size is 2.5mm. As the sampling rate is 1Msample/s, the DAQ gives an excessive amount of data which can be easily averaged by a factor 100 without losing resolution. The system shows good agreement with the results from the literature, but it shows as well its limitation of having a single detector because the source speed measure is just an average measurement, calculated by taking in account the step size. The measure of the speed of the source is a key parameter to accurately calculate the transient dose [29]. For this reason, an average measure is not accurate enough for the purposes of the QA.

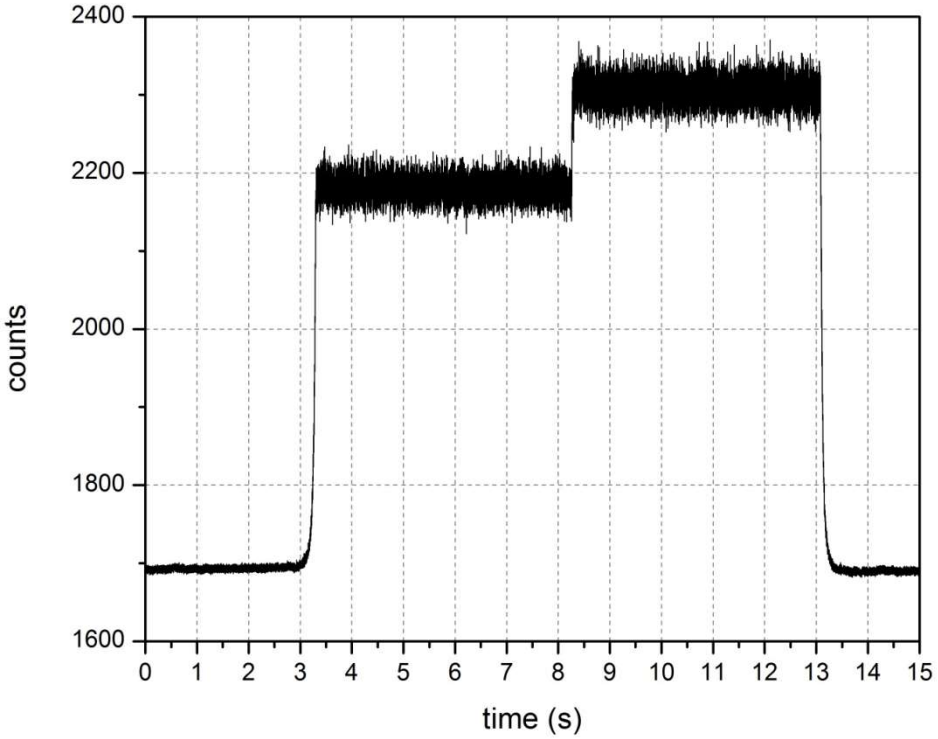

Figure 13: MRT speed test, 5s dwell 2.5mm step size

Although the single channel DAQ has been successfully designed and characterized for the MRT application, the same approach is unfortunately no longer valid for QA in HDR brachytherapy, when the system is to be used for dose reconstruction.

5.1 Hardware description

A different detector has then been chosen as sensor section of a new DAQ. It is a 2D detector array populated by silicon diodes named Magic Plate (MP). The epitaxial

diodes are placed in a matrix shape of 11x11 elements with a pitch of 10mm. Each of them has a sensitive volume of 0.5x0.5x0.05 mm^3 (Figure 14). The detector has already been fully described and characterized by Wong et al [10] and it demonstrated promising results in terms of agreement with the ion chambers (within 0.7%) and good dose linearity and reproducibility. In order to use MagicPlate for QA in brachytherapy, a new DAQ needs to be designed as it has to acquire up to 121 parallel channels. As first attempt, a research grade analog front end, Tera06, has been selected and adapted to read the detector. Prior to this research project, Tera06 has been used in conjunction with a Labview script and National Instruments (NI) hardware. Labview is a graphical programming platform distributed by NI which, like ISE, allows the design of logic networks. A Labview script was used to drive digital I/O through a NI hardware slot installed into a tower personal computer. The setup had few disadvantages: firstly, the NI hardware is a quite expensive tool and so the system could not have been easily replicated. In order to run the DAQ, students and users were required to use the dedicated PC and even carry the PC to the hospital to perform experimental measures. Secondly, the NI hardware had a limited set of I/O and it did require a very long wiring section (two by 34ways flat cables 15m long) to connect the PC to hardware and detector when used for LINAC applications. With the introduction of the FPGA and the development of the new electronics to read the front-end, the setup has been significantly simplified: any laptop can be used to run the system; a single USB cable was necessary to connect the laptop to the DAQ; the increased number of I/O allowed the use of plug-in modules to add flexibility and features to the DAQ; hardware, software and firmware can be easily modified and adapted for ongoing applications.

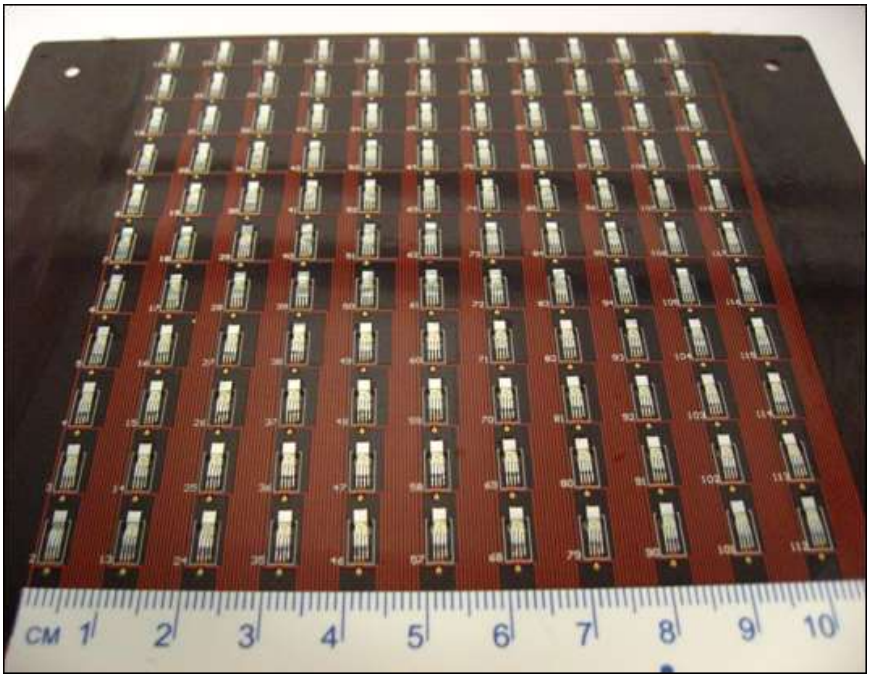

Figure 14: Magic Plate detector [10]

5.1.1 TERA06 front end

Tera06 is a charge-to-frequency converter followed by a 16-bit digital counter. The ASIC has been developed by the INFN of Torino for the monitoring and control of hadrontherapy beams [30] [31]. The chip has 64 parallel input and each board of the TERA06 comes with two chip already fitted for reading of 128 channels in total. The two chips are directly connected to the detector through a small adapter which interfaces the connectors of the detector to the ones on the TERA06 board. Operation principal is as follow: input current from the detector (I_{in}) is integrated by an operational amplifier configured as an integrator with the feedback capacitance C_{int} = 600fF. When the output of the integrator exceeds a given threshold V_{th}, a fixed amount of charge Qc (reset charge) is subtracted from the capacitor C_{int} and a pulse is sent to the counter. Minimum value of Qc is 100fC set by design by the resolution of the comparator performing the subtraction, although all the preliminary test performed on the ASIC report 200fF as typical value [31]. Pulse frequency follows the relation $f=I_{in}/Qc$. As important feature, subtraction of Qc reduces the output of the amplifier and resets the comparator without affecting the acquisition. The values of V_{th} and Qc can be set by the user by external potentiometers. The output of the TERA06 is a 16 bit digital number. As the output of the ASIC is already a digital signal, data acquisition hardware provides power supply voltages and a digital buffer section to

translate the voltage level of the digital signals from TTL 5V (I/O of the TERA06) to 3.3V (I/O of the FPGA) and vice-versa [26]. The FPGA module used to drive Tera06 is the same XEM3001 module previously described.

5.1.1.1 Firmware description

Figure 15 shows a block diagram of the firmware designed to control TERA06 front end.

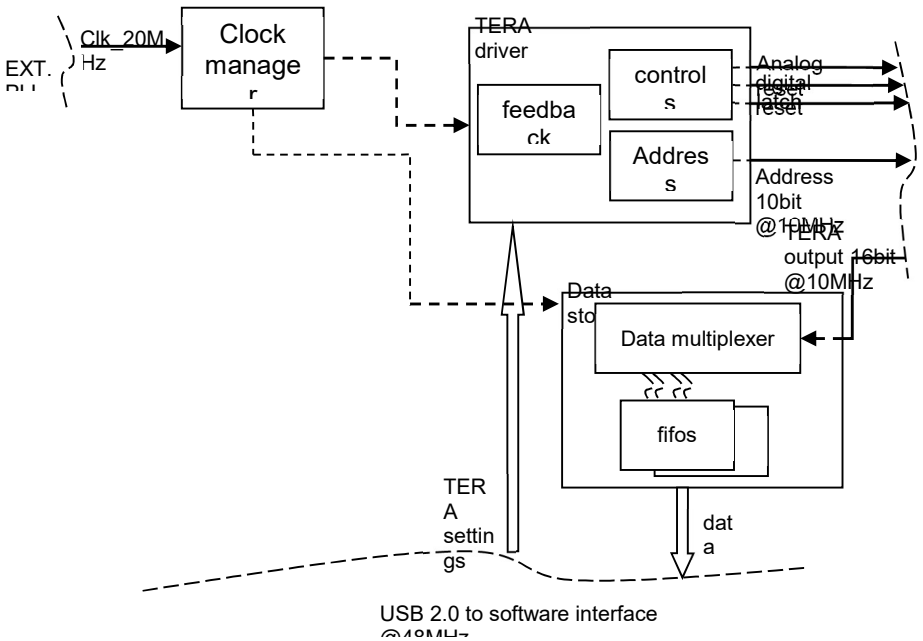

Figure 15: Tera06 firmware - block diagram

- DCM section is an update of the one implemented for the MRT firmware. The main clock signal runs at 20MHz, so the setting of the external PLL (Figure 4) remains the same, plus there is an extra 10MHz clock, generated from the main one, which is used as time base for the commands of the TERA06 (Appendix B Figure 57).
- Tera drive is the logic core designed to drive the TERA06. The chip requires four commands: analog reset, digital reset, latch and address. The first one, analog reset, is sent only after power up of the hardware and resets all the components of the board; then the digital reset clears the digital counters; the latch stores the value of the counters in a shift register and enables the output of the shift register available to be read; the address is the request for data from any channel. TERA06 can be read in two modes: Single Sampling (SS) and Double Sampling (DS). In SS, counters are reset after each read-out cycle, thus means the

number of events counted meanwhile the addresses are requested will be cleared at the beginning of each reading. Therefore, during data transmission the system will not register any information, thus introducing a dead time of approximately 14 μs for 128 channels. In DS mode instead, as the digital reset will not be sent prior each acquisition, the counters continuously accumulate the number of events without any dead time. The value read must be subtracted from the current reading to obtain the number of events read on each frame. As the measure adds up, counters eventually will overflow and restart without notice. Although the dead time is predictable, for the use of the DAQ under a continuous irradiation the DS technique appears interesting. The two modes have been investigated to estimate their effect on measure.

In SS once the acquisition starts, a digital reset is sent from the FPGA followed by a latch, the delay between the two commands is determined by the selected Integration Time (IT). If the acquisition runs in DS mode, the digital reset is omitted and the IT determines the delay between two following latches. The latch command stores the number of events read by each channels into its 16-bit shift register. Then the FPGA queries each channel by sending the address and the TERA06 replies with the value. The rate of the transmission is driven by the FPGA at 10MHz, which is the maximum speed for the front end (Appendix B Figure 62).

- As for the firmware of the MRT project, Data Store is the memory stage allocated to temporarily store the data coming from the TERA06. In terms of setting up the FIFOs, the configuration remains the same, with the two FIFOs cascaded to maximize the usage of the RAM. Multiplexing of data needs to be modified. The header length must be increased for the GUI to be able to identify the first channel of each acquisition. The redundancy of bits also avoids any false decoding; as spurious values can occur with the single 16-bit header. However, the multiplexing header-data is not one to one, as it was for the single channel DAQ, but is one header followed by 128 channels. The write command to the first FIFO must be synchronized with the output of the TERA, which runs at 10 MHz; the read command is synchronous with the write command of the second FIFO and they must share the same clock frequency; the read command, which enables the communication through the USB link, must be clocked by the 48MHz clock. Once the FIFO starts to fill in, a flag rises, thus to request to the GUI to start the download

of the data and empties the FIFO into a binary file; the process goes on until more data comes from the TERA06 (Appendix B Figure 60 and pages 93-94).

The dissertation provided on chapter 4.2 about the latency during the USB transmission still applies to the Data Store section of the TERA06 firmware and following releases. In this case, each acquisition is not a single value anymore but a frame containing up to 128 values plus a double-word header. However, data rate is much slower than the one achieved with X-Tream, and even stretching the timing of the front end, the expected incoming data during the 3ms latency will not exceed 390 words, number which is well enough contained into the memory stack.

5.1.1.2 Preliminary characterization

In order to understand the performances of the front end, the DAQ has been bench-tested using a fixed current of 2.65±0.01 nA generated by applying a fixed voltage across a set of 128 resistors, each 1 GΩ. The two modes of acquisition have been compared. In particular Figure 16 left side shows the charge measured in a single frame as function of integration time. The chip has a good linearity and there is an excellent agreement between SS and DS mode. Figure 16 right side shows the total charge, obtained as the sum of all the frames, for different integration times. At high sampling rates (integration time (IT) below 1ms) there is a strong discrepancy between the measured and the expected total charge which is even more pronounced when the DS modality is used.

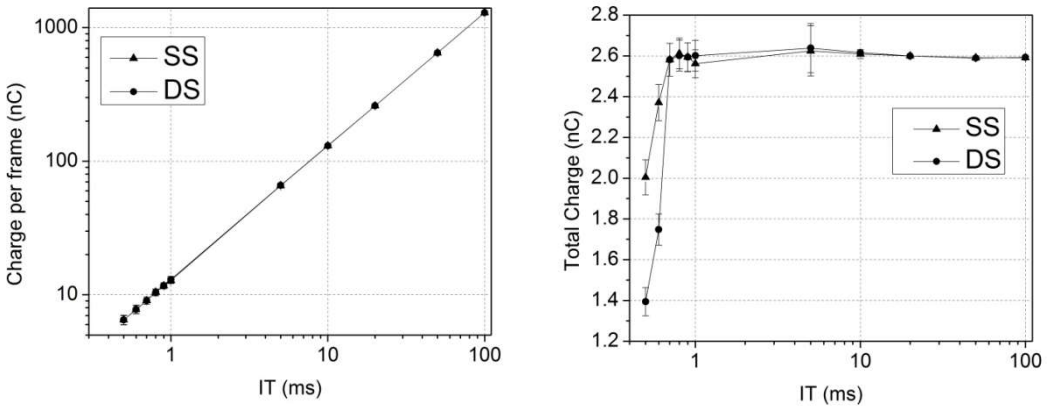

Figure 16. (left-side) Charge measured in a single frame as a function of the IT (logarithmic scale); (right-side) Total charge as a function of IT in one second total acquisition time. Error bars have been calculated considering two standard deviations of the distribution of the response around the expected value.

The sampling frequency of 1 kHz, corresponding to 1 ms of IT seems to be the higher limit for a reliable operation of the TERA06. The chip seems to be unresponsive for higher sampling frequencies with the digital output occasionally frozen. This effect is much more evident when the DS mode is adopted. In DS mode, the response for the n-frame is calculated by the subtraction of the counts of the (n-1) frame. If the system is in stall, the digital output will not change and there will be occasionally frames which are identical and will be read as null response. Cumulating the response across the total acquisition time produces deficiency of total charge measured. Overall the two sampling modalities show comparable performances resulting on the selection of the SS mode as standard setup in order to decrease the computational load of the GUI. Comparative tests of TERA06 versus X-Tream indicate that TERA06 is better suited for tracking of the source movement. X-Tream outperforms TERA06 in terms of time domain resolution but TERA06 DAQ allows reading all the matrix of 121 diodes of the MP detector and is able to perform the dose reconstruction and identify the position of the source as well. The new described TERA06 based front end presents many advantages:

- ✓ Simple digital design required due to the relaxed timing and fewer commands
- ✓ Multichannel and daisy-chain configuration embedded
- ✓ Simple data acquisition hardware required
- ✓ No dead time in DS modality

It also has some disadvantages:

- TERA06 board is expensive
- 1 ms limitation on the minimum integration time
- Low sensitivity

In order to address the disadvantages of the TERA06, a new front-end has been introduced based on a commercial ASIC named AFE0064 which allows designing a new system with better performances in terms of time resolution and sensitivity. AFE0064 front end has many advantages: is capable of a faster sampling rate; it is multichannel and can be used to read the same matrix of detectors; it has a wide user selectable range of sensitivity; and ultimately it is a cheap solution. On the negative side, it requires full redesign of the ancillary electronics.

5.1.2 AFE0064 front end

AFE0064 is a commercial electrometer from Texas Instrument (TI) [32], originally developed to readout Thin-Film-Transistor panels (TFT) for portable imaging device. It has been selected for its electrical characteristics:

- charge integrator with hardware selectable integration polarity;
- analog input charge range is selectable between 0.13pC and 9.6pC;
- low noise referred to integrator input of 700 electrons at 14us integration time;
- short integration times with a minimum value of 14us;
- 64 parallel inputs simultaneously.

The chip is very promising and it is a low cost solution for a new front end. The low noise input is achieved due to Correlated Double Sampling (CDS) mode of the device, which resets the integrators, zeroes-out common mode noise and then integrates the signals. As opposed to TERA06, the AFE0064 has to receive several commands in order to activate the CDS as shown in Figure 17. The IRST command resets the integrators of each channel, while the EOC output indicates the data are ready to be read. The STI command enables the retrieving of the data from the previous conversion, which can occur during the reset time. After all the channels are clocked at the output and the EOC becomes inactive, a SHR command allows the sampling of the noise/offset. Then the integrators integrate the charge for the duration of the INTG signal, time which can be select by the user from a minimum of 14µs. The channels are sampled when the SHS command is asserted then a new reset and STI start the following acquisition. The background noise acquired at the SHR command gets subtracted by the integrator from the value integrated during the SHS command, thus lowering the overall effect of the noise.

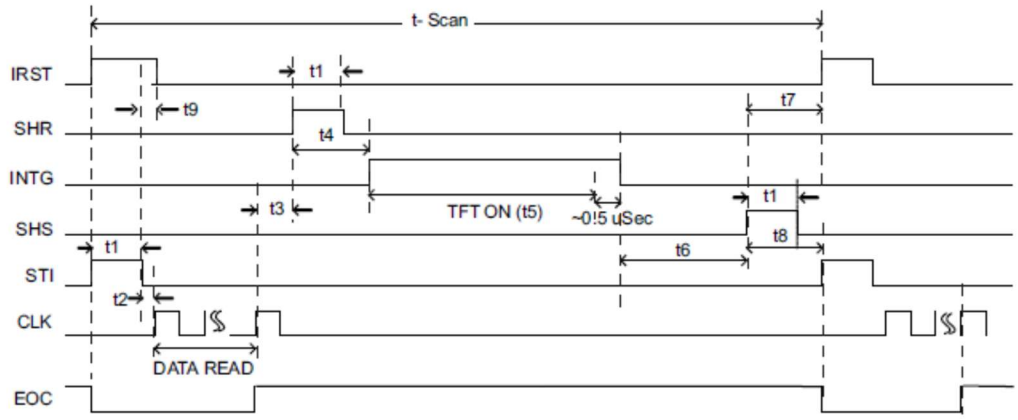

Figure 17: AFE0064 timing.

All the 64 channels are acquired in parallel and then become available to be read from two differential analog outputs with a dynamic of +1.4V in UP-mode and -1.4V in DOWN-mode. Unlike TERA06, AFE0064 outputs two analog signals which need to be coupled with an ADC, thus increasing the complexity of both the electronic and the digital design of the DAQ. The selection of the ADC predicated on the electrical characteristics of the chip and its application. Referring to the AFE0064 datasheet for the Equivalent Noise Charge and Feedback Capacitor values [32], noise level has a range about:VOUT-NOISE≈0.1mV @ C_{sensor}=20pF, Q_{range}=1.2pC and INTG=14us which determines a minimum of 14 bit of resolution for the ADC stage.

Principal requirements for the selection of the ADC are:

- Input signal: AFE0064 has a differential output → ADC interface must be differential
- Reference voltage: AFE0064 analog output V_{out}= ±1.4V → ADC reference greater than ±1.4V
- Sampling rate: AFE0064 output rate = 1 channel/ 2 clock cycles →1MSPS @ clock=2MHz
- Resolution: 14 bit is the minimum requested but a 16 bit output will be the most efficient way to interface the input of the FIFOs
- Interface: serial/SPI to avoid maximum usage of the FPGA I/O
- Number of channels: a 128 channels DAQ houses two AFE0064 two analog output each → a 4-channels ADC will minimize the number of components.

Table 3 presents a summary of the ADC short-listed against the required specifications.

Table 3: ADC selection short-list

	Resolution (bit)	n. of channels	Sample rate (MSPS)	Analog input	Reference (V)	Interface
Require-ments	14 to 16	1-2-4	~1	Differential	±1.4	Serial
ADS7263/ ADS8363	14/16	4	1	Differential	±4	SPI
ADS8413	16	1	2	Differential	4pp	Serial/ LVDS
AD7357	14	2	4.2	Differential	-0.5/2.6	SPI
LT1407	14	2	3	Differential	0-2.5	serial

From the best candidates, ADS8363 and ADS8413, the ADS8363 is the component which fits the application the best due to number of input channels available. This selection, in fact, allows using only one ADC for each 128-channels module, decreasing in that way the number of components required and potential synchronization problems of multiple devices (as using the ADS8413 would require four devices for any 128-ch module).

The internal architecture of the ADS8363 is configured to acquire 2x2 differential channels, meaning that 4 parallel channels are multiplexed to simultaneously convert two channels at 1MSPS [33]. This input configuration appears to be the best match for the AFE0064. The front end has in effect two different modalities to output the data: Simultaneous Mode and Sequential Mode. The first one is faster and outputs the channels at the same time; the second one is slower as the sequence to reset the integrators, integrate the charge and transfer the data requires 133 clock cycles against the 33 clock cycles needed in simultaneous mode. However, the Sequential Mode allows coupling both AFE0064 on the module to a single ADC maximizing the efficiency of the data transfer. Figure 18 shows a block diagram of the internal architecture of the ADC.

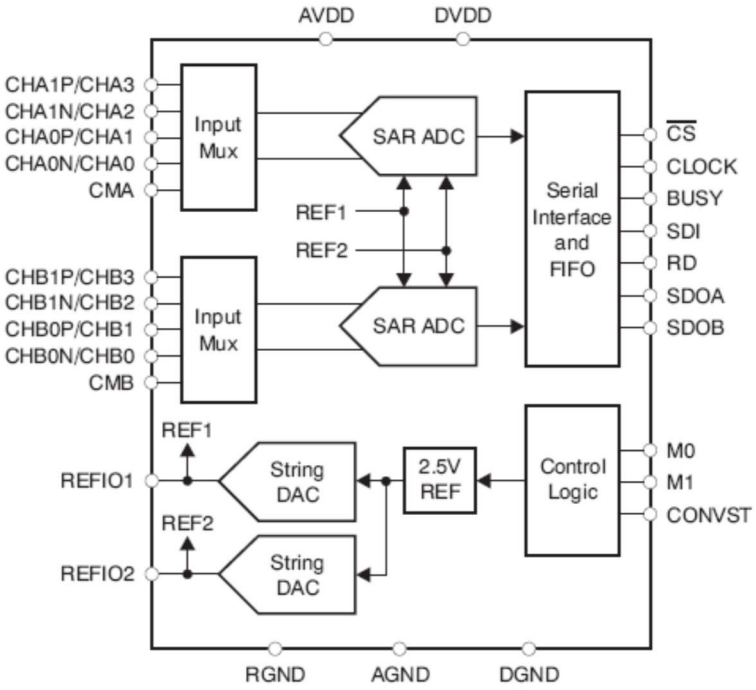

Figure 18: ADS8363 block diagram.

Four differential input channels CHA1, CHA0, CHB1, and CHB0 are directly connected to the two AFE labelled ID0 and ID1 (Figure 19).

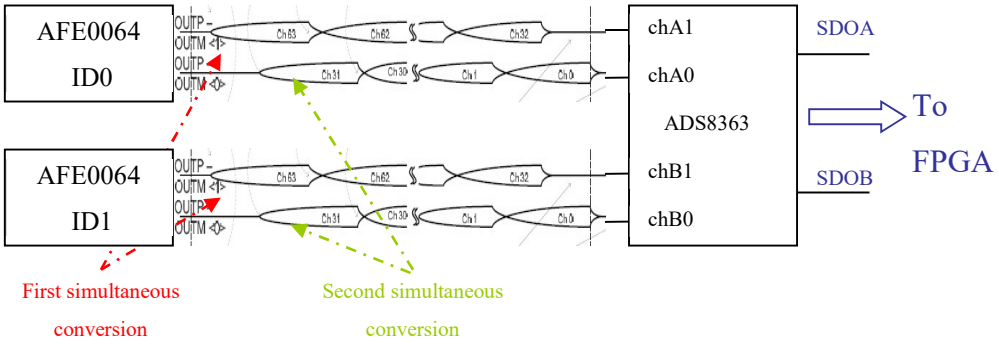

Figure 19: Acquisition block diagram.

Maximum clock frequency of the ADS8363 in Half-Clock Mode is 20 MHz. With this setup each AFE0064 runs at 500kSPS per channel with a total throughput of 1 MSPS. Based on all the previous considerations, one 128-channels module will achieve the following performances in terms of data rate and data handling (Figure 20):

- ✓ AFE0064 output rate per channel 500KHz

✓ 128 channel acquired in parallel and Ch63 of the ID0 simultaneously transferred with Ch63 of the ID1; Ch31 of the ID0 simultaneously transferred with Ch31 of the ID1

✓ ADC changeover frequency between Chx0 and Chx1 1 MHz

The AFE0064 timings given by design can be efficiently coupled, by the mean of a custom firmware, with the ADC to maximize the DAQ's data rate.

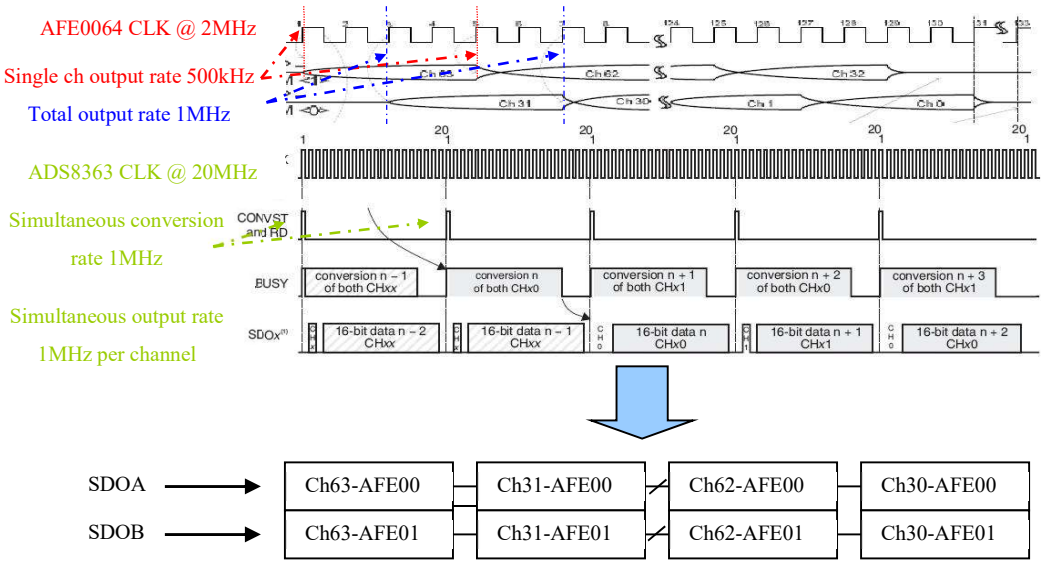

Figure 20: DAQ timing: AFE0064 coupled with ADS8363 using a custom firmware.

An additional advantage of the ADS8363 is the programmable reference level up to 4V. In fact, by setting the reference to 1.4V, which is the maximum output of the AFE0064, the DAQ operates at its optimum resolution.

5.1.2.1 Firmware description

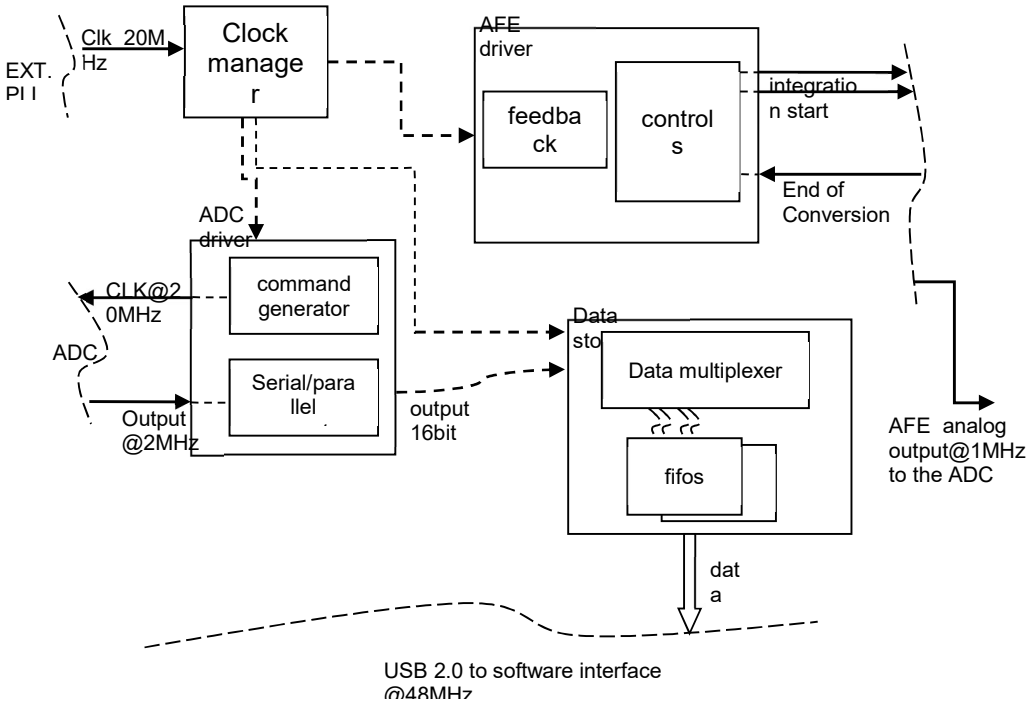

Figure 21: AFE0064 and ADS8363 firmware block diagram.

Figure 21 shows a block diagram of the firmware developed to control both AFE0064 chips and the ADS8363. Once again, DCM section is the same as for X-Tream project. The additional 2MHz clock is generated from the main 20MHz to multiplex the ADC outputs.

- The AFE Driver section is mostly a state machine. The commands generated follow the timing diagram shown in Figure 17, at the same time a strobe is sent to the ADC to start conversion of the data coming from the two AFE0064.
- The ADC driver allows the conversion to start. The interface with the ADS8363 resembles the one used on the X-Tream project as the ADC uses the same commands. Since the ADC output is a serial 16 bit, a serial-to-parallel converter has been implemented to get the data ready to be sent to the Data Storage section.
- The FIFOs on the Data Storage section are set up in the same way of the previous firmwares, but the multiplexer which organizes the data prior the FIFOs is designed differently. The header has two words: of these the first is fixed,

meaning a new set of data is coming; the second one ranges from 63 down to 0 and indicates the number of channel read. The header is followed by two values, 16 bits each, one from AFE ID0 and one from AFE ID1. Data rate of the DAQ is comparable to the one X-Tream, so that the number of words expected during the 3ms latency of the USB is about 6000, well contained into the memory stack allocated (chapter 4.2).

- The Timing section determines duration of the acquisition and integration time as per the TERA06 firmware, but it has an extra feature which allows setting up the frequency of the acquisition ranging from 30 Hz up to 5 KHz.

The DAQ has excellent performances in terms of signal to noise ratio, if fact it is able to perform accurate measures even when surrounded by water, using the smallest charge range. However, it has a major disadvantage when used for continuous dosimetry as brachytherapy requires: the timing diagram of the AFE0064 (Figure 17) shows that the integrators are not active for the whole duration of the DATA READ, which is 133 clock cycles for the Sequential Mode, as they are reset during the data transfer and then the noise is sampled. The 133 clock cycles translate into a dead time of about 70 μs at 2 MHz clock speed. Despite the dead time introduced, this DAQ has been successfully tested for real time dosimetry at its maximum speed, though generating a huge amount of data to handle for post processing analysis.

5.1.2.2 Preliminary characterization

The front end has been characterized by testing its linearity and noise. A constant current of 18.3±0.02 nA has been generated by applying a voltage across a set of 128 resistors of 10 MΩ and 0.1% tolerance connected to the input of the two AFE0064 chips. Figure 22 shows charge measured by the front-end and the expected measured versus integration time.

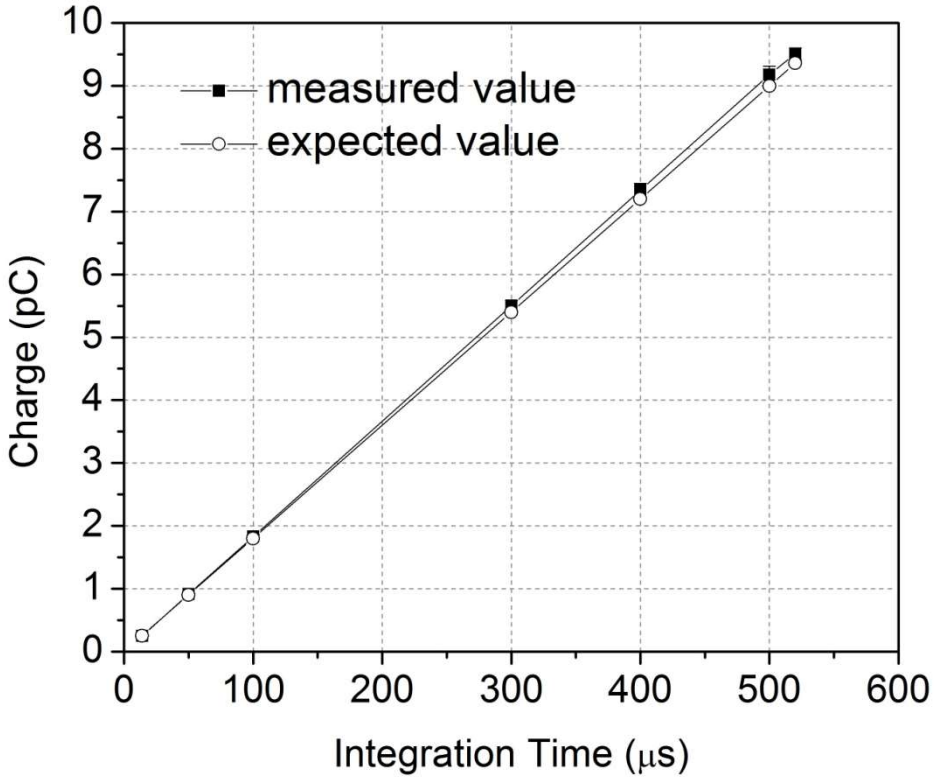

Figure 22: AFE front-end front end linearity.

The minimum value of the integration time is 14μs and it is fixed as per the specifications of the chip. A maximum value is not defined but, in this setup, integration times larger than 500μs cause a saturation of the chip; in fact the maximum measurable charge is 9.6pC at range 7. The response of the system is linear over all the full scale range; the experimental measurement overestimates the expected value by 2% with ±0.75% uncertainty caused by noise.

5.2 Experimental results

Three different front-ends have been used to develop a QA system for brachytherapy treatment: a single channel system, X-Tream, reading a single strip silicon diode and two multichannels, based on the TERA06 front end and on the AFE0064 front end, both reading MagicPlate 121. Each of them demonstrated certain advantages and disadvantages as summarized in Table 4.

Table 4: DAQ for Brachytherapy treatment

Front-end	n. of channels	Detector	Advantages	Disadvantages
X-Tream	1	Single strip	- Fast acquisition rate - High spatial resolution - Fast acquisition rate	A single detector is not sufficient for accurate speed evaluation and dose reconstruction
TERA06	128	MagicPlate 121	- Digital output - Simple ancillary electronics - No dead time - Multichannel - Daisy chainable for system's upgrades	- Limited acquisition rate - Limited sensitivity - Expensive
AFE0064	128	MagicPlate 121	- Multichannel - Flexible design - High sensitivity - High speed - Daisy chainable for system's upgrades	- Ancillary electronics more complex then TERA06 DAQ - Effect of the dead time needs to be evaluated in regard to the application

The three front ends have been tested in a clinical environment. Thanks to its fast sampling rate, X-Tream remains the best performing system in terms of timing resolution. However, due to its single channel architecture it is not suitable for the dwell position reconstruction and source tracking. The performances of the two multichannels have been tested and compared.

With the aim to realize a QA system for Brachytherapy applications, the DAQ has been used to reconstruct the position of the source during a treatment. This information is fundamental to apply the standard procedure called TG-43 to subsequent calculation of the total dose delivered [34]. The formalism, mainly based on Monte Carlo simulation, allows calculating the total dose in water, by knowing the characteristics of the source and its position. Tests have been performed using an Ir192 source. The detector has been placed in a solid water phantom. Measures were taken at various distances from the source, from 5 mm up to 60 mm. Both front ends were able to track the source giving information about its position during the treatment. Figure 23 show an example of source tracking using the TERA06 front end. The set of measurements displayed were taken at 11 mm depth with 2s dwell time. The sampling rate of the

system was set to 100ms, as it was the most reliable and standard setup, that will give 20 measurements per each step. As can be clearly seen, the DAQ is able to identify each and every dwell position and its duration.

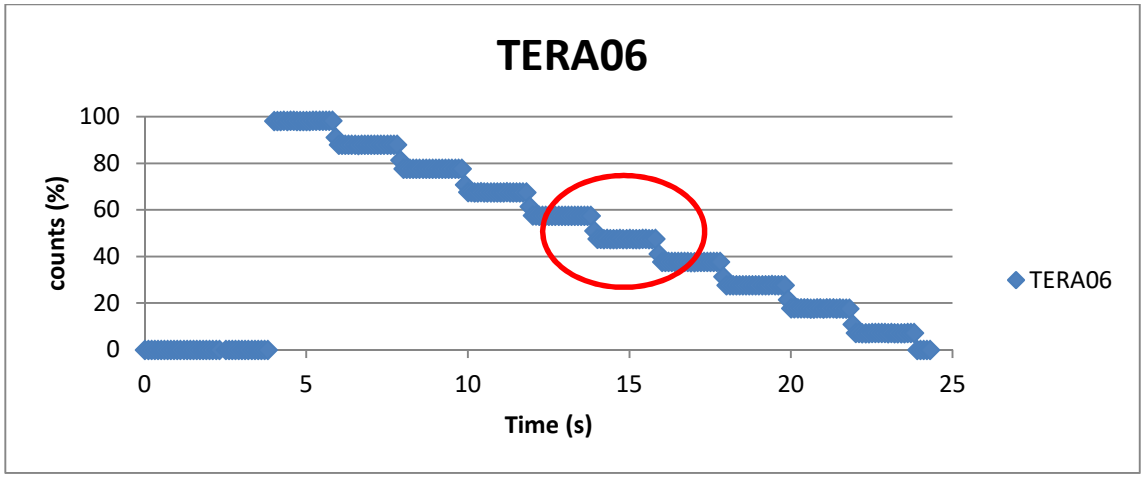

Figure 23: Source tracking using TERA06 front end

Figure 24 shows a magnified view of the area marked by a red oval. Due to the slow sampling rate, the measure look coarse and only one point can be picked up by the DAQ during the transition between two dwell positions while 19 points are collected for each dwell position as per calculation.

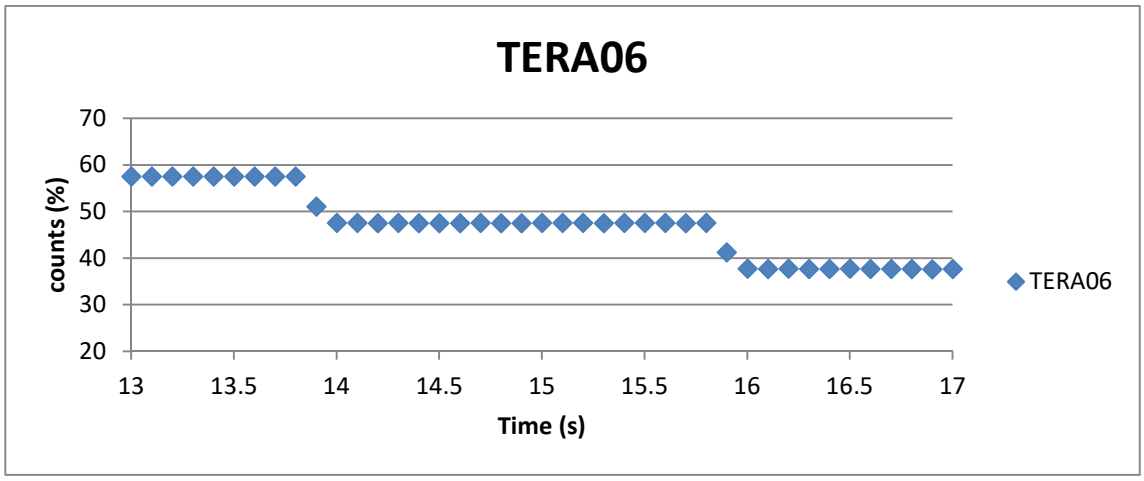

Figure 24: Source tracking magnified view.

Figure 25 shows a source tracking test done by using the same detector and the AFE0064 front end. The sampling rate of the DAQ has been set to 4 kHz and the sensitivity to 7.2pC per count. The system is clearly able to detect the position of the source every 250 µs and the transition between two dwell positions (magnified view

is shown in Figure 26) is not a single point anymore but it looks more like a continuous slope following the continuous movement of the source. If compared with the tracking profile obtained by using the X-Tream system (Figure 13), the timing resolution achieved by the single channel DAQ sampling at 1 MHz is much higher than the one obtained with the multichannel DAQs but the advantage of being able to reconstruct the position of the source speaks in favour of selection of the AFE0064 front end for such purpose. Dead time during the data transfer does not seem to have negative effects on the data collected; in fact the system is fast enough to give quantitative information for source tracking and dose reconstruction. Using the AFE0064 front end at high speed of 1 kHz to 10 kHz leads to the generation of a comparatively large amount of data per single acquisition. However, custom software designed to decode such amount of data shows the results in real time allowing the system to be used for QA purposes of the sources tracking.

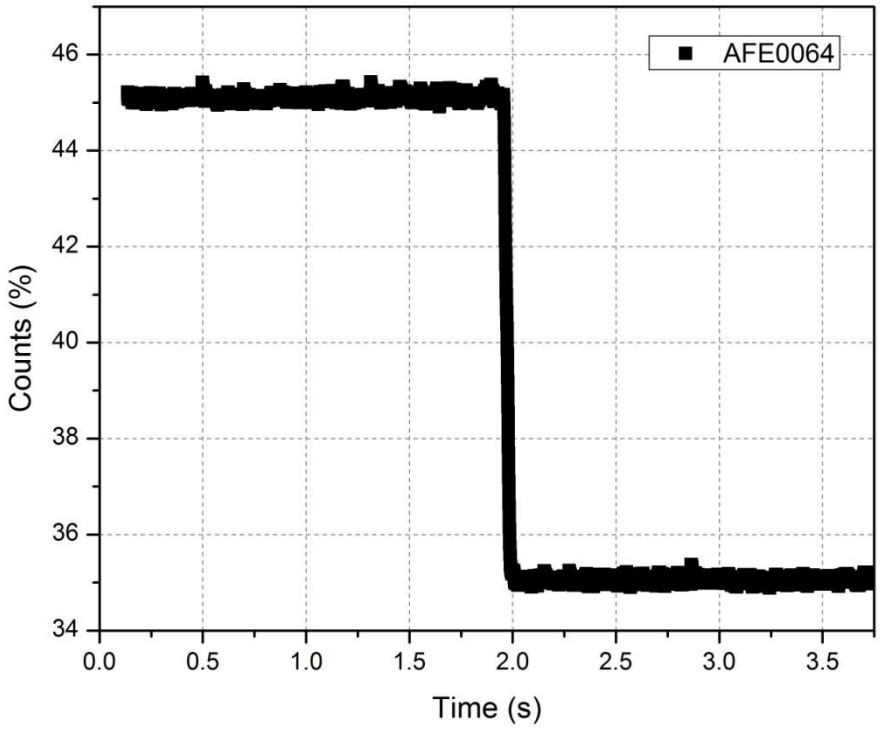

Figure 25: source tracking using AFE0064 front end.

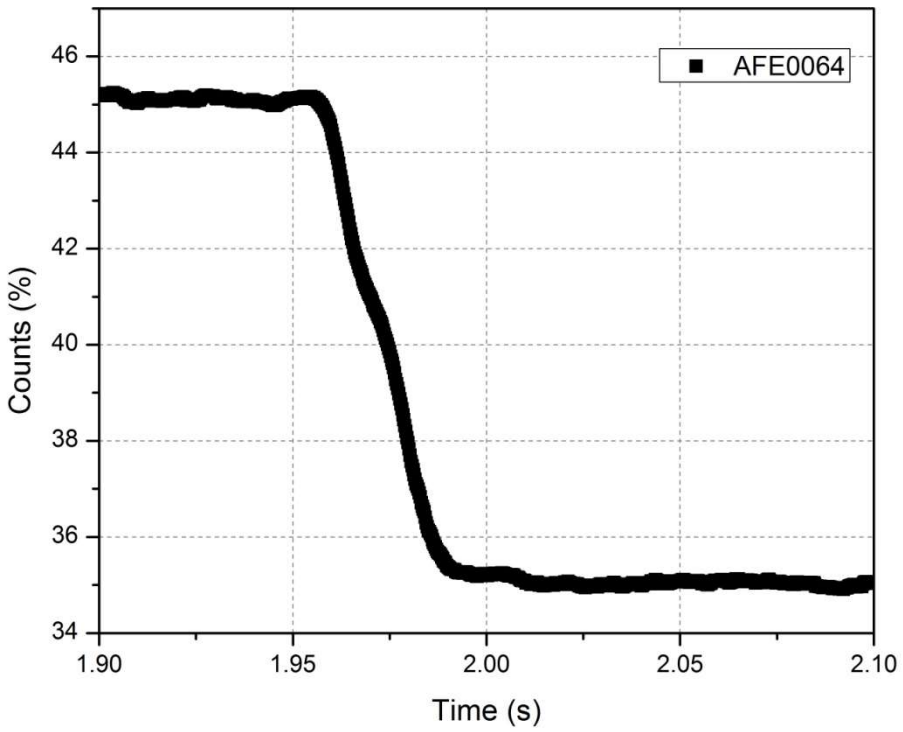

Figure 26: AFE0064 transition zoom-in.

Figure 27 shows a different representation of the data acquired which is a 3D charge map. Each point displayed is a single diode of the detector; the colour indicates the amount of charge collected. The information can be recorded as integral response over the entire acquisition, as shown in the picture, or can be visualized frame by frame, thus allowing watching the actual source moving along the Y axis. This 3D modality can be achieved with either of the two multichannel front ends.

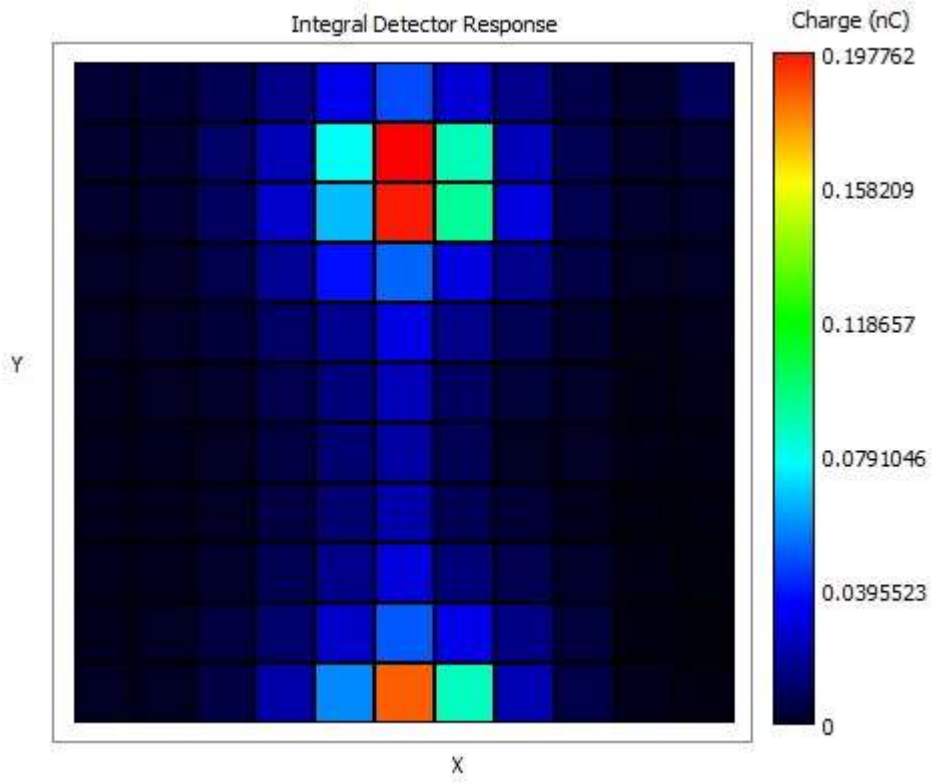

Figure 27: 3D map for dose reconstruction.

The second clinical experiment carried out in the brachytherapy environment is called "In-vivo Brachypix". The main difference, from the DAQ point of view, is the distance from the source to the detector which can be anywhere up to 15 cm. Radiation received by the diodes will be drastically attenuated, and the TERA06 front end is no longer able to detect any signal. In fact, its specifications in terms of sampling rate and sensitivity make the system usable for a maximum of 7 cm as distance from the source, which is not enough for the specific application. In comparison, AFE0064 system proves suitable to reach the goal.

Figure 28 shows an acquisition performed at 12cm source to detector distance. Gain of the AFE0064 has been set to 0.13pC per count, which is the lowest range available. As sampling rate and integration time are interdependent, a trade-off of between fast acquisition, to collect more sample, and long integration time, to detect low intensity signal, has been achieved by setting the sampling rate to 100 Hz and the integration time to 9920us. Figure 29 shows a magnified view of the transition between two dwell positions: the curve displayed is not fine and continuous as the one obtained using the

phantom in Figure 26 but the system is still able to track the movement of the source reasonably accurately.

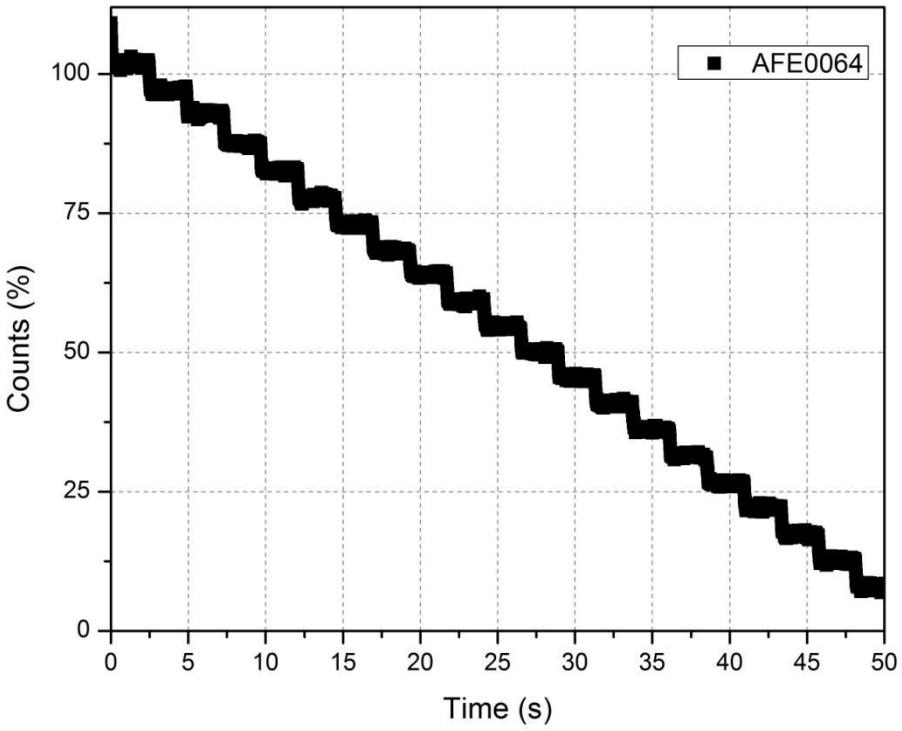

Figure 28: In-vivo “Brachypix” source tracking AFE0064 DAQ

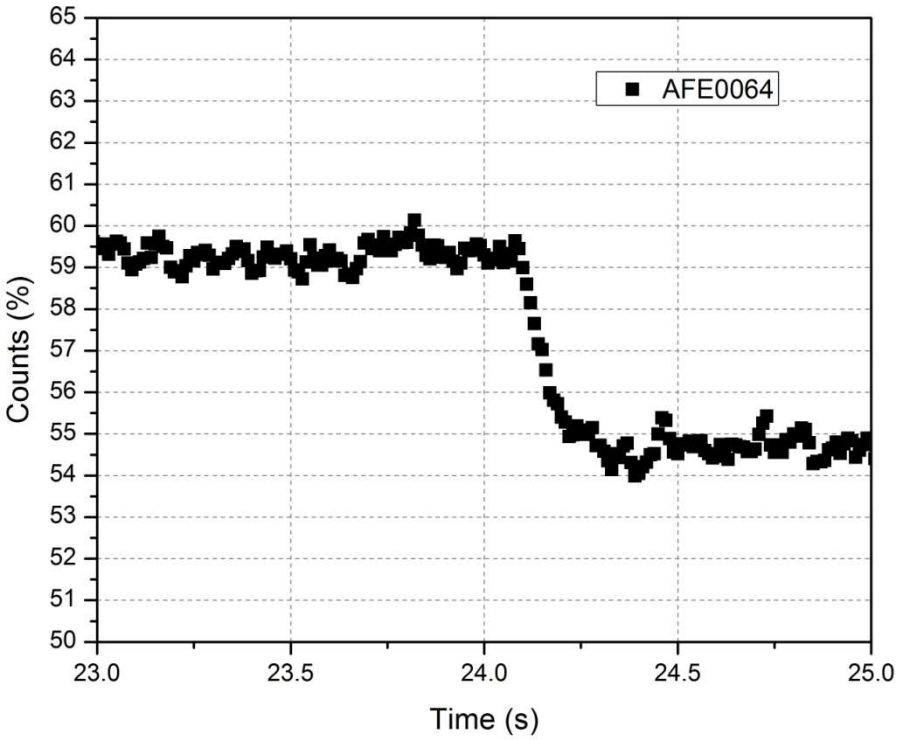

Figure 29: In-vivo “Brachypix” source tracking transition, magnified view.

Results of this research have been published by Espinoza et al. [25] and the value of the work has been internationally recognized.

Three different solutions have been evaluated with the aim of design a DAQ suitable for Brachytherapy applications. The X-tream system was the first approach s it was already available to be tested. Its excellent time resolution proves to be very useful but the limit of the single channel front end does not quite satisfy the requirements of the application. A new DAQ using the TERA06 front end as been promptly realized, as the front end easy to incorporate into a custom design. It allows to read a multichannel detector but its sensitivity and timing constraint are quite limited. The latest design of the DAQ, incorporating a new front end called AFE0064, although it required an extended development in terms of electronic and firmware, proved to be very performing. The DAQ proposed in fact is able to finely track the movement of the source; to identify positions and dwell times; and to measure the delivered dose. Nevertheless, a major improvement of the system can be made by introducing a different front end chip DDC264 (from Texas Instruments) able to perform continuous acquisition without introducing dead time. Like the two front ends previously described, the new chip allows acquiring 64 channels in parallel. An advantage compared to the AFE0064, is a double integration stages working alternating, thus to avoid any dead time during acquisition. The chip has been tested in its evaluation board giving promising results.

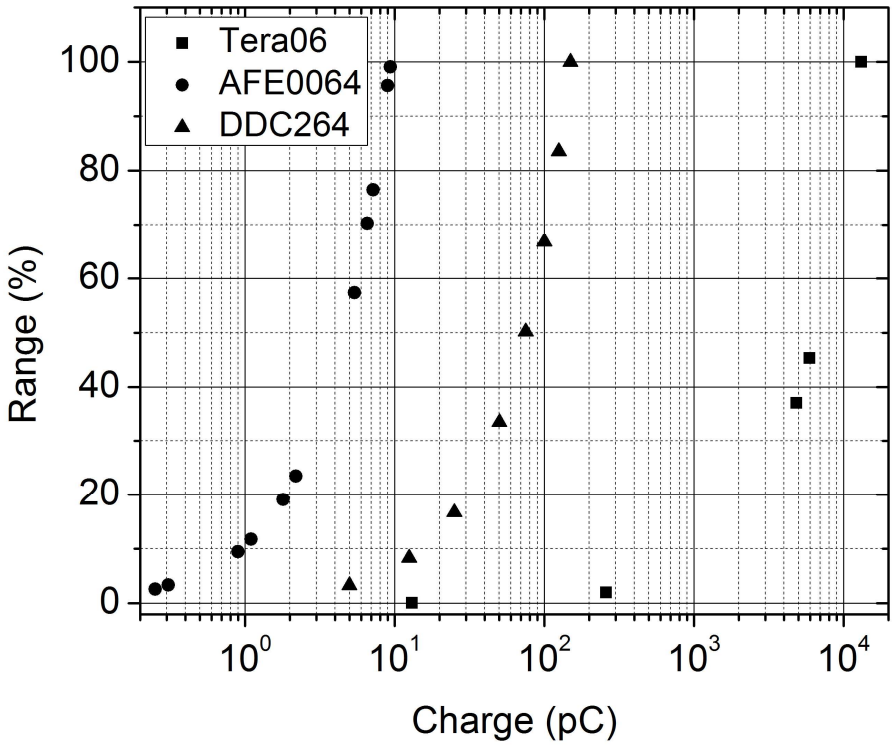

Figure 30: Tera06, AFE0064 and DDC264 sensitivity comparison expressed as percentage of the output range versus measured charge.

Figure 30 shows a comparison of the response of the three front ends to a constant input current. AFE0064 has the highest sensitivity, followed by DDC264 and then comes TERA06. The plot highlights the fact that the three systems are complimentary to each other, thus it seems reasonable to develop a new DAQ housing the DDC264 front end to be used as a complement to the two already described.

6 EXTERNAL BEAM RADIATION THERAPY: TRIGGERED DATA ACQUISITION SYSTEM

Methodologies and results discussed in this chapter have been published by *Aldossari et al.* [35] [36], *Fuduli et al* [37], *Petasecca et al.* [38], *Porumb et al.* [39]. The author has developed the firmware and tested the electronic hardware of all the DAQs involved on the listed publication.

The third range of applications requiring a DAQ for quality assurance is the External Beam Radiation Therapy (EBRT) on a LINAC. It comprises treatments like IMRT, VMAT, Tomotherapy. During this kind of treatments, the source of radiation is external to the patient and the beam is pointed to the area of the body that needs to be treated. The radiation is not continuous as in the Brachytherapy but pulsed and can be modulated over time. Pulse by pulse measurements are important for short and small field dosimetry and 2D, 3D and 4D dose reconstructions are necessary for QA during planning and delivery of the treatment. High spatial resolution, minimal angular dependence and low dose-rate dependence are some of the requirements for a DAQ along with the real time feedback and visualization of the beam.

6.1 Hardware description

The first approach to perform dosimetry on EBRT applications has been done by using TERA06 front end and the detector MagicPlate 121, as previously described on the Brachytherapy chapter. The aim was to build a system for quality assurance in both transmission mode and dose verification. In transmission mode the detector is placed close to the source and the beam flows through providing a measure of the energy fluence. This method is particularly important for QA procedures during treatment, as the real time feedback from the detector can be used to verify the treatment plan [40]. Dose verification is achieved by placing the detector on the couch to verify the effects of the treatment of the target area. A preliminary setup was realized by placing two Magic Plate detectors: one in a tray attached to the head of the LINAC and a second one in a water equivalent phantom on the couch under the beam. Upgrade of the DAQ from 128 channels to 256 channels was straightforward by simply adding a second TERA06 board to the system already designed. There is already a provision in TERA06 front end for daisy-chaining up to 16 boards by setting a board individual address by an internal 4-bit switch. No further changes in the ancillary electronics are

needed so that the second board can be connected directly to the FPGA. In the firmware, the counter generating the addresses on the Tera driver section must be expanded to 8 bit to count up to 256. Data multiplexer in the Data Store section has to handle 256 channels but, as the TERA06 boards output data sequentially the extra 128 channels are following the previous 128. Data format become a header followed by 256 values. Due to a relatively slow sampling rates normally used for the TERA06 front end, which is 100ms, the on board memory is enough to store all the 256 channels without data losses.

Figure 31 shows the synchronization diagram (left side) and the timings (right side) used by the Varian Linear Accelerator. As the treatment emits pulsed radiation, it would be useful having a triggered DAQ to perform measurements of the beam pulse by pulse. Unfortunately TERA06 has a quite long integration time, compared to the timings in Figure 31, and even if at its maximum tested reliable sampling rate of 1 kHz it could meet the specifications in terms of speed, it would not be sensitive enough to detect the signal. Furthermore, adding another board doubles the dead time of the DAQ, if used in SS mode, and almost doubles the cost of the DAQ, as the TERA board is the most expensive component of the system.

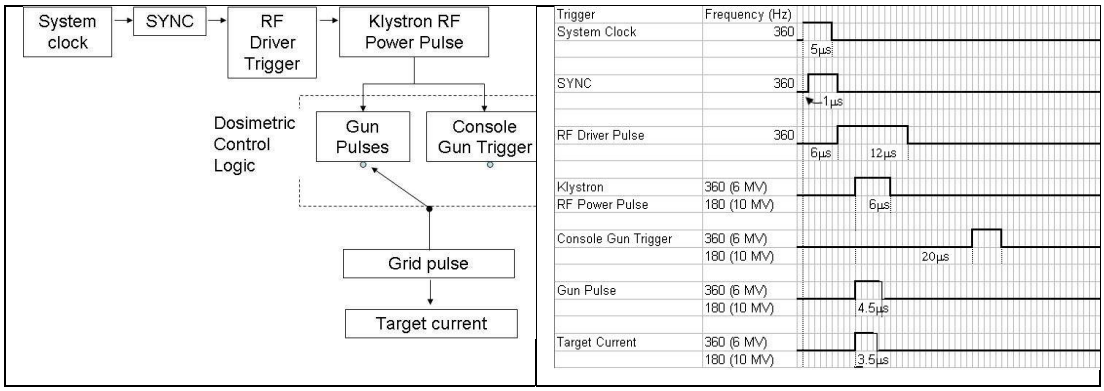

Figure 31: LINAC synchronization diagram (left) and timing (right).

Looking back at the timing diagram of the AFE0064 (Figure 17), it appears reasonable to adapt the DAQ with the AFE0064 front end to the EBRT project. As the data acquisition hardware for the AFE0064 has already been designed to be modular, the upgrade of the DAQ form 128 channel to 256 channels becomes almost straight forward by adding another module containing two AFE0064 and one ADC to the FPGA.

6.2 Firmware description

The firmware needs to undergo a few changes: the AFE driver remains the same, allowing four AFE0064 to receive commands in parallel and sample two detectors at the same time but an upgrade is necessary for ADC driver, Data Store and Timing sections. ADC driver has four input channels of serial to parallel converter, instead of two, and they have to be shifted at the same time and sent to the FIFOs. The multiplexer on the Data Store section has to handle double amount of data. The header in this case will be followed by four values, as shown in Table 5.

Table 5: Data format for the DAQ with the AFE0064 front end for 128 and 256 channels

128 channels	Header	Ch63 ID0	Ch63 ID1	Header	Ch31 ID0	Ch31 ID1	Header	Ch62 ID0	Ch62 ID1	
256 channels	Header	Ch63 ID0	Ch63 ID1	Ch63 ID2	Ch63 ID3	Header	Ch31 ID0	Ch31 ID1	Ch31 ID2	Ch31 ID3

Adding the external trigger feature has a major impact on the Timing section. There is already a counter to control the acquisition rate, set up from the GUI, and it could be used to synchronize the DAQ with the frequency of the LINAC pulse. However, once the state machine driving AFE0064 starts, the first 70μs are dedicated to reset the integrators and data transfer. Hence the SYNC of the LINAC cannot be used as trigger for the acquisition itself as there are only few microseconds of delay between the SYNC and the gun pulse, which are not enough to reset the AFE0064. Instead, it can be used to trigger the following acquisition. The triggering section has been designed as follow: assuming that LINAC pulse rate is 360Hz, once the trigger arrives, the Timing section will wait for about 2.6ms then the state machine starts the reset of the AFE0064 and the data transfer will take place. The SYNC signal is generated even if the beam is off. Using the SYNC to synchronize the system do not cause data losses in fact the DAQ starts acquiring few seconds before beam-on and the very first frame, which will be background noise anyway, is discarded by the decoding function. A pulse rate of 360Hz translates in a delay of 2.7ms. Allowing for 2.6ms delay from the SYNC to start of the next acquisition, ensures that the LINAC pulse falls fully within integration time, shortly after the reset and data transfer process. Trigger frequency can be selected through the GUI allowing using the DAQ with different LINACs, but still keeping the safety margin of 1ms for the reset and data transfer. This upgrade of

the Timing section does not replace the module designed for the brachytherapy application but it is optional so that the same firmware can run the DAQ with either the external trigger or asynchronously.

Since the AFE0064 based DAQ was designed to be modular, it can be easily expanded up to 512 channels with the advent of new larger detectors.

6.3 Preliminary characterization

Both systems have been tested using a LINAC Varian 2100iX at the Illawarra Cancer Care Centre of the Hospital of Wollongong. The results have been compared with the dose measured by a Markus ion chamber from PTW which is currently used for point dose measurement. Figure 33 shows the depth dose obtained using the setup on Figure 32. Each set of data is normalized independently by the response at D_{max} (1.5cm for a 6MV photon beam). Results agree within 1% for the TERA06 front end and the 0.8% for the AFE front end [26].

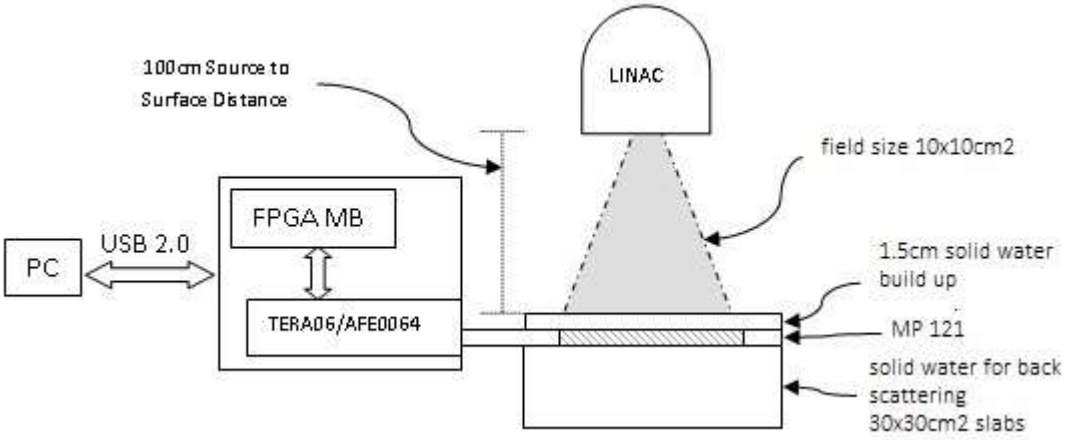

Figure 32: TERA06/AFE0064 test setup

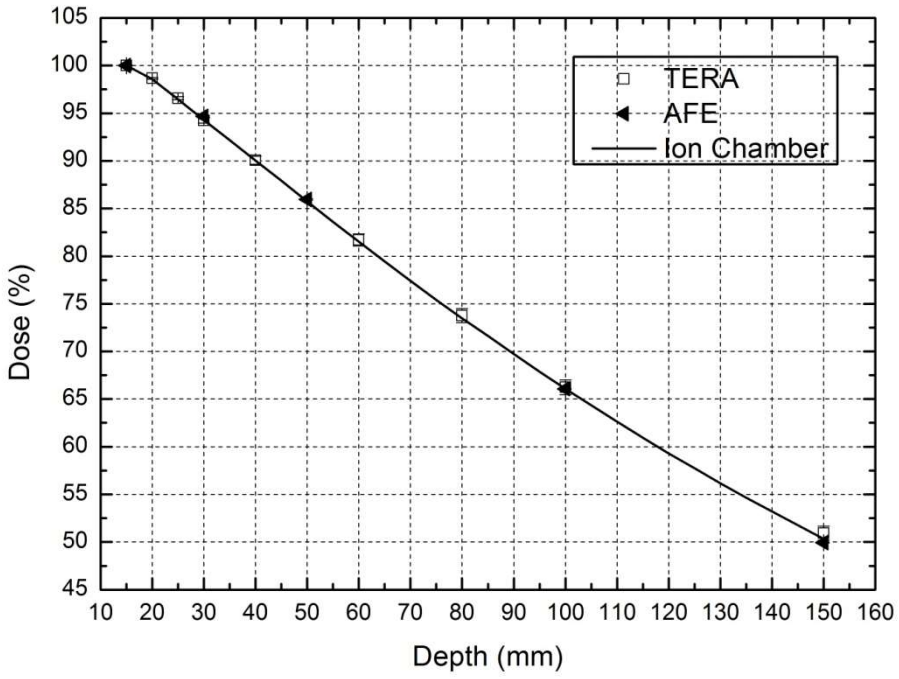

Figure 33: Depth dose measurements with TERA06 and AFE0064 front end.

An interesting application of the DAQ with the AFE0064 front end has been investigated to show possibility of pulse by pulse measurement of the instantaneous charge generated in the detector. As the system is synchronous with the LINAC's gun trigger, it samples and displays in real time each single pulse for different dose rates (Figure 34). The different amplitude of the pulses reflects the initial settling of the beam intensity. Figure 35 shows a time profile of a single channel of four different LINACs Varian 2100iX, during a delivery of 100MU. Although all the four machines use the same setup (trigger frequency 360 Hz, beam energy 6MV, dose-rate 600MU/min and the detector placed at 1.5 cm depth in a solid water phantom), the time profile shows evidence of different transient response of the beam intensity stabilisation. Fast response of the DAQ combined with the possibility to select and analyse each single channel of the detector array in real time, makes the system suitable for detecting malfunctioning such as overshoot of the beam or faulty start up and also makes possible to employ the system as a useful tool for fine tuning of the LINAC itself.

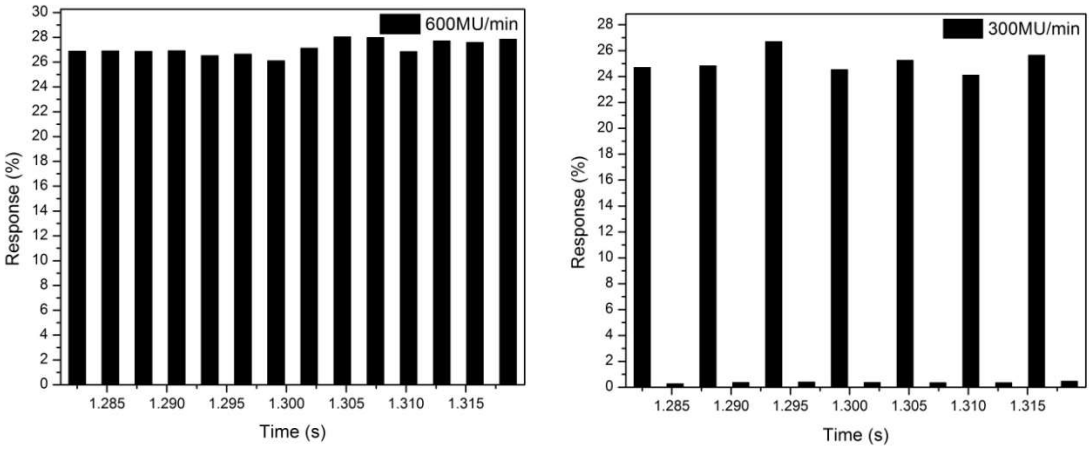

Figure 34: LINAC gun pulses at 600MU/min and 300MU/min at range 7 (9.6pC Full scale).

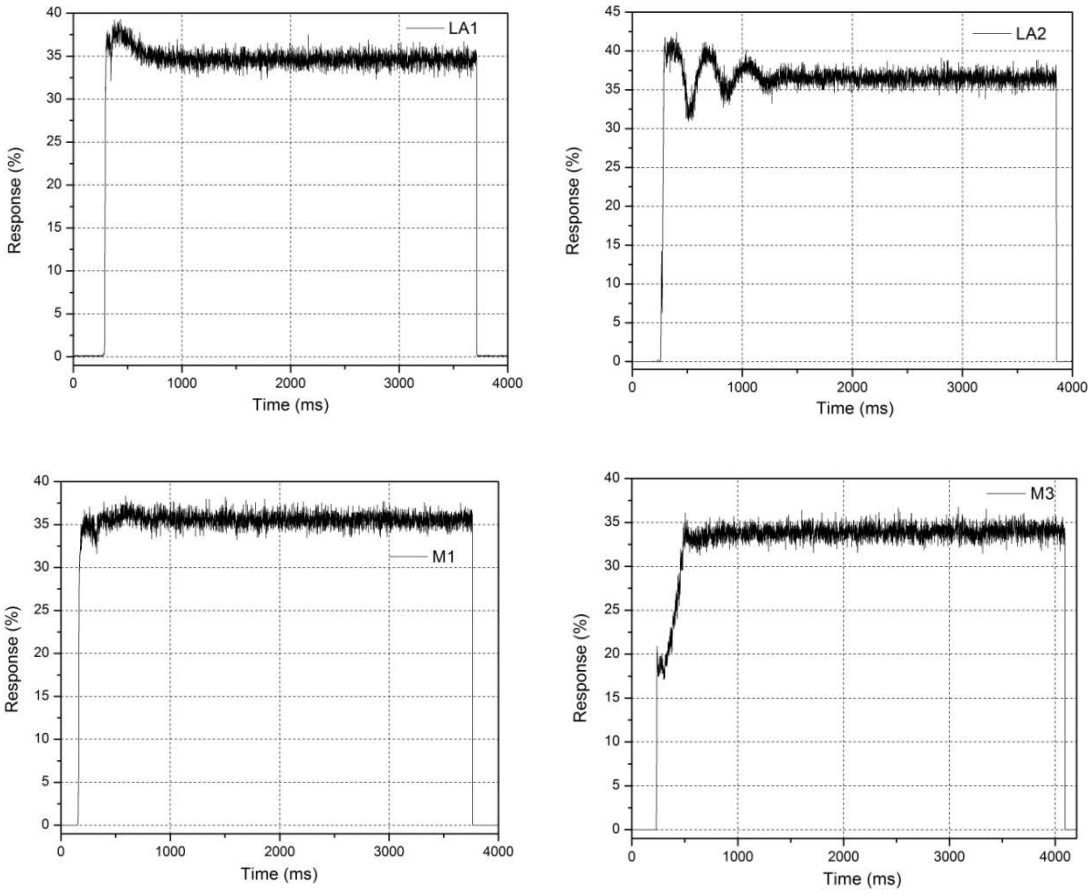

Figure 35: Four different beam output temporal profiles detected using DAQ B - LA1 and LA2 ICCC Wollongong Hospital, M1 and M3 Peter MacCallum Cancer Centre Melbourne at range 7 (9.6pC Full scale).

The same tests could not have been performed with TERA06 front end, because of its low sensitivity and long integration time. The performances of the system with the AFE0064 front end and its configuration ready to read 512 channels made possible to use detectors with different geometry in various applications which will be explained later in this chapter.

6.4 Rotatable phantom

The design of a custom DAQ has the aim to optimize the performances of the detector used. Therefore, the system must enhance the advantages by providing a suitable bias and power supply, fully resolve his dynamic, and minimize possible adverse effects. When "Magic Plate" (MP) was introduced for phantom measurements, the major challenge encountered in IMRT and VMAT therapy applications was the angular dependence of the diodes which should be taken into account in dose reconstruction in the case of arc delivery. As both treatments are delivered by rotating the head of the LINAC around the couch, a cylindrical phantom was designed to hold the detector and rotate it in accord to the treatment plan to always keep the beam perpendicular to the detector and avoid the angular dependence effect of the diodes. The cylindrical shape of the phantom was chosen to allow full rotation of ±180º and to simulate, from the material point of view, a human chest. The phantom has a diameter of 30 cm and 40 cm length and is entirely made from PMMA, which is tissue an equivalent material for 6 MV proton beam energy. It has an insert in the middle along the axis of rotation to house the detector and it is big enough that either MP-121 or MP-512 detector can be inserted into the phantom. In order to coordinate and synchronize rotation of the phantom with the position of the gantry, an inclinometer was placed on the head of the LINAC, and its feedback was used to detect the angle of the gantry and to tilt the phantom by the same angle. Figure 36 shows the setup of the whole system with the TERA06 front end and two MP, one in the phantom and one attached the gantry.

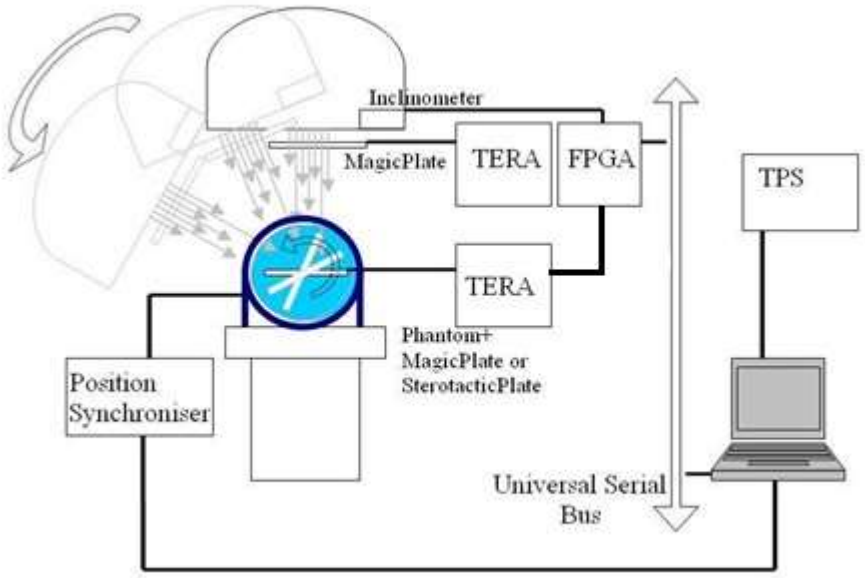

Figure 36: Rotatable phantom and TERA06 front-end DAQ setup.

The rotatable phantom and its movement control system is a separate project which was later merged with the existing DAQs. It comprises the inclinometer, to determine position of the gantry, a stepper motor to rotate the phantom and an encoder to provide phantom rotation angle feedback to the FGPA. It is a quite complex system in terms of hardware and digital interface which requires a detailed explanation of its design flow.

6.4.1 Mechanical and electronic components.

The first step for the development of the rotatable phantom and its moving system was the design of the cylindrical phantom. The model has been drawn using a 3D CAD, SolidWorks. A stepper motor rotates the phantom using a toothed belt drive. A driving 18-teeth gear is fitted to the shaft of a stepper motor, and a 64-teeth driven gear is attached to the phantom cylinder, providing a gear ratio Rg=3.555. This drive train was simulated in the software. Mechanical design and characterization of the phantom itself are no part of this work. Figure 37 shows a CT scan of the phantom which confirms the uniformity of the cylinder.

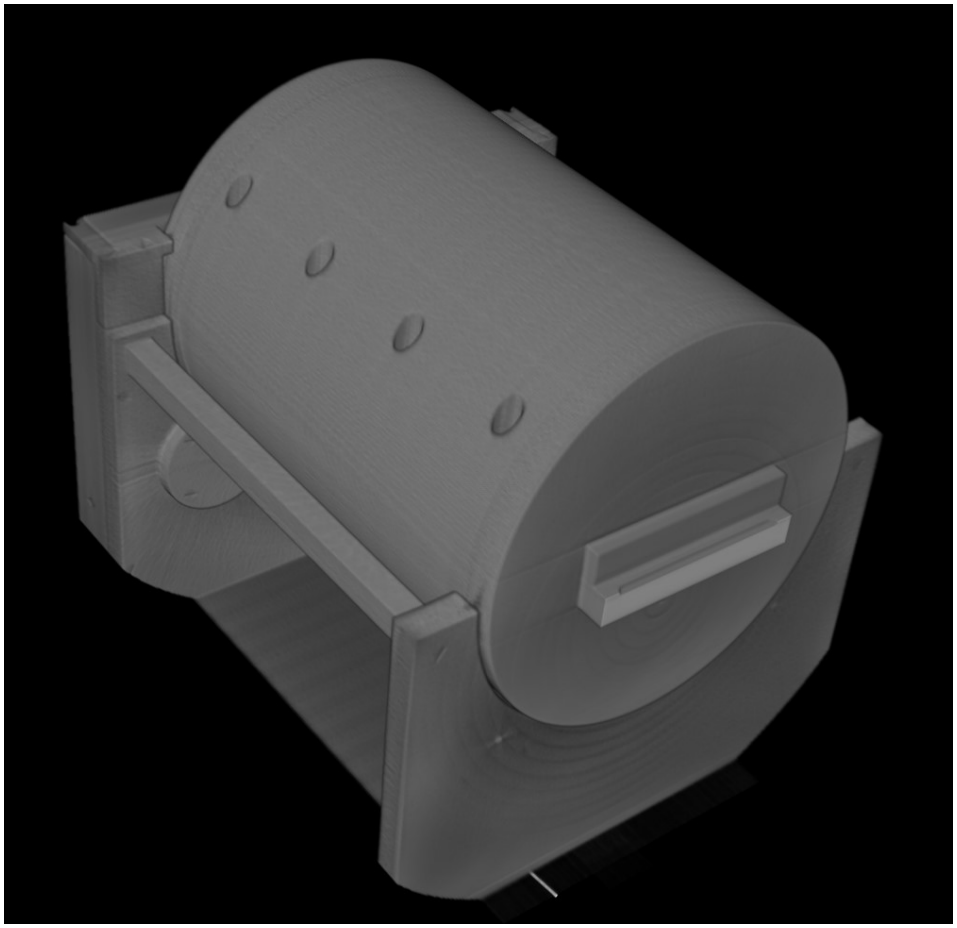

Figure 37: CT scan of the rotatable phantom.

Due to the dimensions of the phantom and its material, the total weight of the cylinder is about 35 kg. The motor chosen is a NEMA 24 which has a torque of 2.74 Nm and a step size of Rm=1.8º. The driver of the stepper motor is a commercial CPLD-based microstep drive G203V from GECKO [41] which increases the resolution of the motor steps by a factor Gf=10. The final resolution Rp of the phantom angular position reaches 0.05º per step Eq. 1.

$$\mathrm{Rp} = \frac{\mathrm{Rm}}{\mathrm{Rg}} * \mathrm{Gf} = \frac{1.8^\circ}{3.555} * 0.1 = 0.05^\circ \quad \text{Eq. 2}$$

G203V receives three signals from the FPGA: enable/disable of the motor, direction of the rotation and the step, all of which are opto-isolated to reduce interferences and noise between the motor and all the ancillary electronics.

The power supply has been designed to meet the requirements of the motor and to be at the same time a portable and not expensive solution. The motor needs input current of I=3.5A and it has an internal inductance of 2.8mH. Based on the recommendation

of the manufacturer, optimum power supply voltage is calculated according to the following equation [41]:

$$V = 32 * \sqrt{mH}\,\text{Inductance} = 32 * \sqrt{2.8mH} \approx 53.5V \qquad \text{Eq. 3}$$

The maximum rated voltage for the motor is stated as V_{max}=50V. The power supply unit has been equipped with a 160VA 36V, 4.4A, toroidal power transformer capable of supplying power to the motor and to all the other components of the system. As briefly anticipated, the phantom rotation control system, named Slow Control, also incorporates an optical encoder, which is connected to the shaft of the phantom and gives the feedback of the exact angle of rotation. The encoder is an ATM60-A4A12X12 from SICK STEGMANN, a multiturn absolute encoder with a 24-bits digital output. The "absolute" attribute allows setting a "home" position which is useful for alignment of the phantom with the LINAC beam. The most significant 12 bits (MSB) give the number of full revolutions and the least significant 12 bits (LSB) give the precise angle of rotation with the resolution of 1/4096 of 360 degrees that is 0.88º per step. The encoder requires a supply voltage between 10V and 32V and a current between 25mA and 80mA, which are well inside the range provided by the designed power supply. Digital output is expressed in Gray code and the transmission uses either a RS422 or a SSI protocol.

The last component of the Slow Control system is the inclinometer. The chip is a commercial device made by Analog Devices with a 16-bits digital output. It uses a Serial Peripheral Interface protocol (SPI) to receive commands and send information to the FPGA. Its resolution specified in the datasheet is 0.025º, over ±180º. The two MSB of the 16 bits output are control bits, which give a feedback about the status of the device and failures that can happened during communication and power up. In addition to the rotation angle, the chip can give information about power supply and SPI status, which is useful in debug mode, and allows setting a calibration factor in relation to the angle read. By using the calibration factor, the system can set any arbitrary position as angle 0º. This procedure has been optimized and together with the homing function of the encoder enables the alignment of all the component of the slow control system at any time during the acquisition.

6.4.2 Firmware

The main feature of the proposed system is the ability to detect the position of the gantry and activate the stepper motor to always keep the detector perpendicular to the beam, on the basis of the numerical information both from the inclinometer and the encoder.

The development of the firmware has to take into account few software and mechanical constraints which need to be addressed. First of all the resolution: the three main components, inclinometer, encoder and motor, have different resolution per LSB. Since the descriptive language used does not allow operations with real number, all the resolutions values were expressed in multiples of 1/1000º. Initially, acquisition of inclinometer and encoder were synchronised with the acquisition of the detectors. The angle read from the inclinometer is then compared to the angle read by the encoder. The absolute difference between the two, scaled by the respective conversion factor, gives the number of steps needed for the motor to reach the desired position. Additional controls are added to determine the direction of the rotation of the motor: if the encoder anticipates the inclinometer then the motor has to move backward, otherwise it has to move forward. Another constraint is related to the way the gantry moves: the LINAC spans the entire 360º from -180º to +180º but always coming back to the position 0º and never moving directly from -180º to +180º, and the phantom has to do the same in order to follow the gantry. Also, for safety reason, the phantom shall never make a full rotation otherwise the cables connecting the detector to the analog front end will be twisted. Damage can occur to either the connectors or the electronic. Moreover, the expression of the rotation angle as ±180º of the LINAC matches the output of the inclinometer, whilst the output of the encoder is expressed between 0º and 360º and needs to be scaled in order to be compared with the inclinometer and obtain the difference between the position of the phantom and the gantry. The difference in terms of angle, and so the number of steps, is not the only information needed by the motor to align the phantom. In fact, the frequency of the steps, which determines the speed of the motor, plays a key role on the capacity of the system to follow the gantry. Pulse frequency of the stepper motor in fact is where the control acts. Figure 38 shows a block diagram of the firmware coupled with the TERA front-end DAQ.

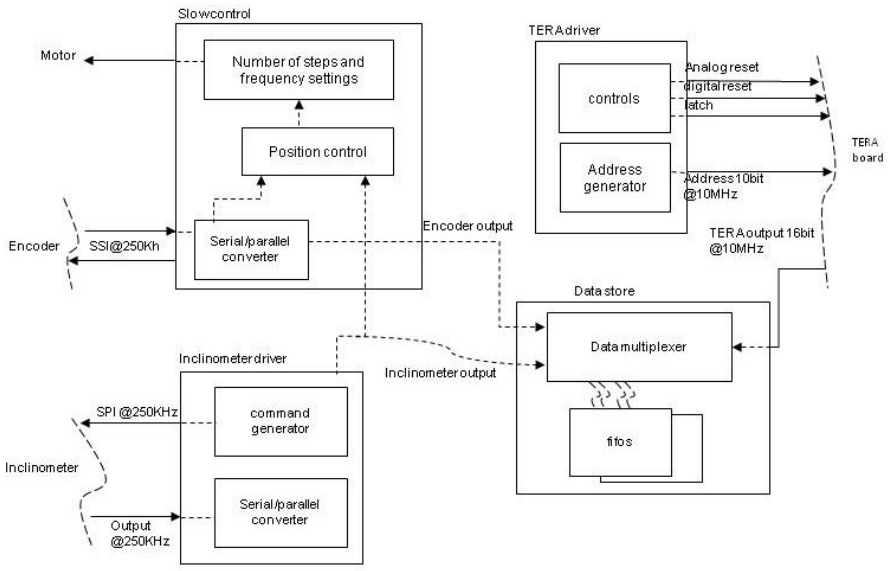

Figure 38: Slow Control firmware block diagram with the TERA06 front-end DAQ

- The TERA driver section is the same module previously described is chapter 5.1.1.1 and handles the clocks signals as well.
- The Inclinometer driver is the module which communicates with the inclinometer. The two main sections are: Command generator and Serial/parallel converter. On Command generator the FPGA takes as input the command sent form the GUI. As the device has multiple functionalities, software interface provides a look up table listing all the commands available. Preliminary tests of the chip showed that it was necessary to set up its sampling rate to the maximum speed in order to match the acquisition rate of the DAQ and provide a new angle reading for each frame. Each command sent to the inclinometer is made of two word of 16 bit each one, clocked by an external clock and synchronized as per SPI protocol. Once a command is received, the inclinometer outputs the requested values as a serial 16 bits word. The Serial/parallel converter section converts the word into a parallel format to be stored in the data store section. The GUI has been designed to only request the angle of rotation while running in acquisition mode. All the other parameters can be requested in debug mode by entering the desired commands on the software interface. As the inclinometer is mounted on the gantry, their position needs to be aligned. A zeroing procedure has been included in the GUI allowing to automatically setting the 0° point by adjusting the calibration

factor. This component has no non-volatile memory, so it needs to be calibrated every time following software or hardware reset or a power up (Appendix B Figure 66 and pg 120).

6.4.2.1 Slow-control section.

The Slow control section is the module responsible for rotation and alignment of the phantom. The FPGA queries the encoder, the gray code is converted in binary and then the value is multiplied by a conversion factor of 1000. The output from the inclinometer, multiplied by the same conversion factor, is fed into the position module. The two angles are compared and their difference is used to drive the motor. This process is called a closed loop control system.

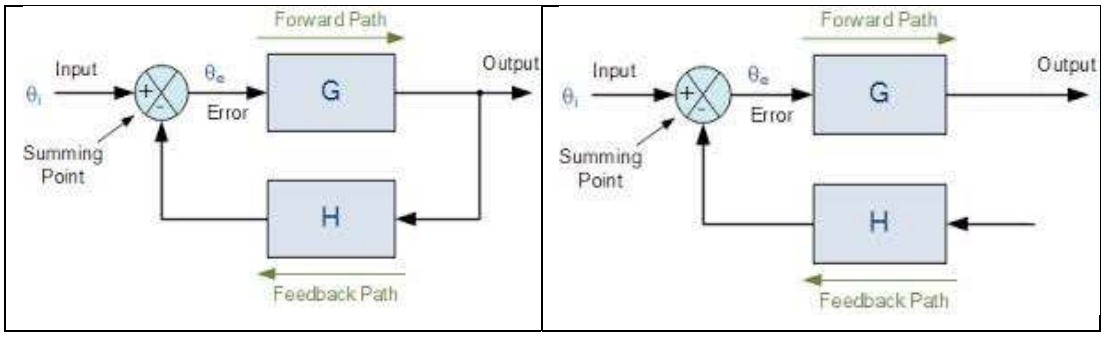

Figure 39: Closed loop system block diagrams.

Figure 39 shows two example of a closed loop system. In the left side, the feedback path is directly generated by the output of the transfer function G; in the right side instead it comes from an external source, which recalls the system implemented by using inclinometer and encoder. In the designed slow control module, the "input" is the position of the phantom read by the encoder; the "error" is the difference between the position of the phantom and the position of the gantry measured by the inclinometer; G is the transfer function which determines the actuation to be applied to the motor; the "output" is the number of step the motor has to do in order for the detector to reach the desired position.

$$\text{error} = \text{inclinometer output} - \text{encoder output} \qquad \text{Eq. 4}$$

The sign of the "error" of the error=inclinometer $\text{output} - \text{encoder output}$

Eq. 4 determines the direction of rotation of the phantom and its absolute value gives the number of steps to be sent to the motor. Once "error" has been calculated, the Slow Control has to set the frequency of the steps and so the speed of the motor.

The speed of the gantry ranges from 2º/s to 6º/s [42] and it can change during a treatment according to the treatment plan loaded and the distance the gantry has to travel. The motor has to rotate the phantom accelerating or decelerating to follow the movement of the gantry. Therefore, the control system has to modulate the frequency of the pulses, taking into account the inertia of the phantom/motor and load characteristics (torque versus speed) of the motor as well. A theory behind stepper motors highlight a relation among the torque provided by the motor, the drive current, the speed and the inertia of the system.

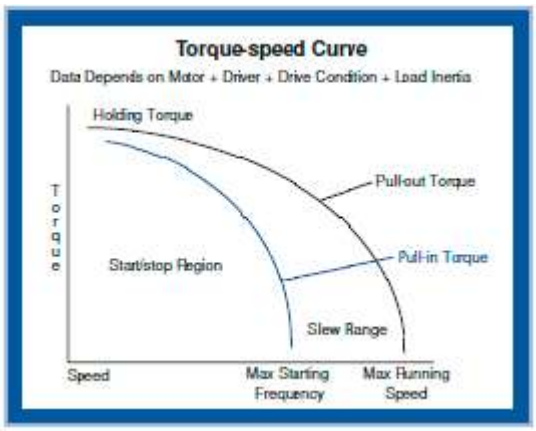

Figure 40: stepper motor torque versus speed chart.

There are different ways to design a control for the proposed system. Many theories suggest the use of a Proportional Integrative Derivative method (PID) as optimal method for a closed loop. The PID controller is a very well-known method which has been used for over 60 years. Although it is quite common, there is very little information in the literature about how to implement a digital PID in a FPGA [43]. The equation for the PID control is the following:

$$u(t) = kp * \left(e(t) + \frac{1}{Ti}\int e(t)dt + Td\frac{de(t)}{dt}\right) \quad \text{Eq. 5}$$

Where u(t) is the output; e(t) the error; kp the proportional gain; Ti and Td the integrative and derivative time constants respectively. A PID involves multiple calculations which keep memory of the past errors and generates an output which smoothly follows the behaviour of the input. In order to be implemented into the FPGA, the ut$= kp * \left(e(t) + \frac{1}{Ti}\int e(t)dt + Td\frac{de(t)}{dt}\right)$ Eq. 5 needs to be transformed into a discrete form which is obtained using the Z-transform. The equation of the discrete PID will be then:

$$u[k] = u[k-1] + K1 * e[k] + K2 * e[k-1] + K3 * e[k-2] \quad \text{Eq. 6}$$

Where k is the sampling time and K1, K2 and K3 are, according to [44]

$$K1 = Kp + Ti - Td \quad \text{Eq. 7}$$

$$K2 = -Kp - 2Td \quad \text{Eq. 8}$$

$$K3 = Td \quad \text{Eq. 9}$$

The PID module stores the error and the position at sampling time k, k-1 and k-2. Absolute difference between the position of the inclinometer and the one of the encoder determines by how many degrees the phantom has to rotate to reach the desired position. That angle has to be translated into the number of steps to be sent to the motor.

$$pulse\ rate = \frac{error^{\circ}}{dt} \quad \text{Eq. 9}$$

The value given by Eq. 9 is modulated using the coefficient given by the PID control uk=u[k − 1] + K1 ∗ e[k] + K2 ∗ e[k − 1] + K3 ∗ e[k − 2] Eq. 6). For optimum transient response, tracking accuracy and stability of the control loop, the PID control needs to be tuned. Figure 41 shows a simplified flow chart of the steps followed by the firmware to apply the PID control to the motor.

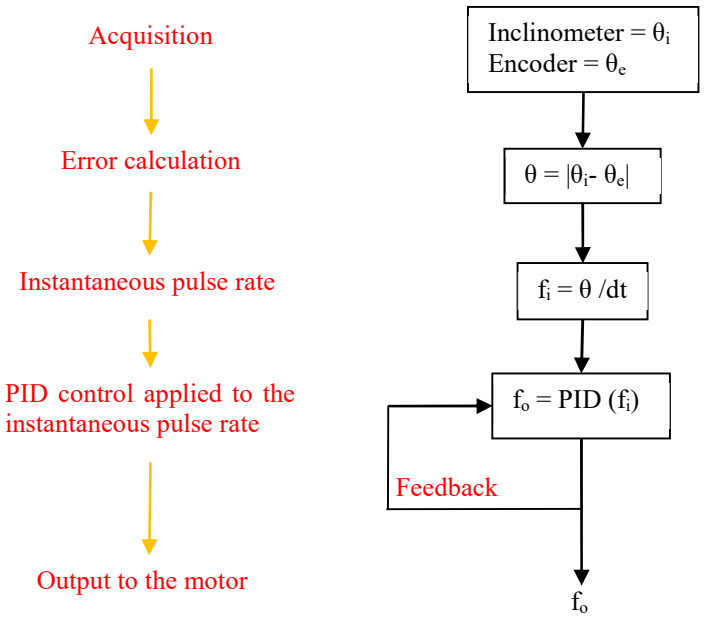

Figure 41: Flow chart of the PID algorithm

6.4.2.2 PID tuning and slow-control preliminary characterization

Tuning of the PID is the procedure to choose the best values for the coefficient Kp, Td and Ti of the $uk = u[k-1] + K1 * e[k] + K2 * e[k-1] + K3 * e[k-2]$

Eq. 6. For convenience, a digital stimulus generator was built into the firmware to simulate the inclinometer output. The PID has been tuned using the Ziegler-Nichols method [45]. The method consists on assuming Ti=0 and Td=0 and increasing Kp until the system become unstable. Once the instability is reached, the period of the oscillation is used to calculate the remaining parameters according to Kp=0.6Ku $Ti = 0.5Tu$ $Td = 0.125Tu$ Eq. 10, where Ku is the value of Kp which causes the oscillation and Tu is the period of the oscillation.

$$Kp = 0.6Ku \quad Ti = 0.5Tu \quad Td = 0.125Tu \qquad \text{Eq. 10}$$

Figure 42 shows how the response of the system changes at different gains. The test signal used simulates a continuous movement from 0º to 65º and backwards at the speed of 7º/s, which is the gantry maximum speed. At the minimum gain (Ku=1) the control is not fast enough to track the test signal; for gains higher than Ku=10 the system starts to follow the input. Various values of the gain have been tried before it reaches the point of instability at Ku=50. The period of the oscillation at Ku=50 has been calculated as Tu=0.6s. Then the three factors of the PID, Kp, Ti and Td, have

been calculated following the Ziegler-Nichols equations and the optimized PID has been tested, appearing to be fast enough to track the test signal and stable at the same time.

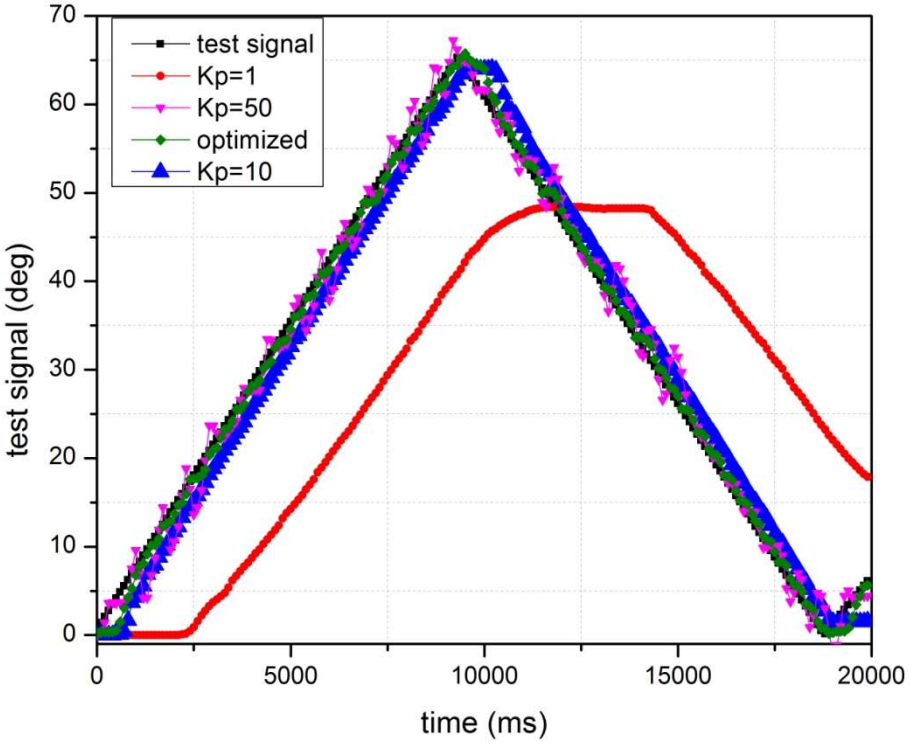

Figure 42: PID tuning tracking mode

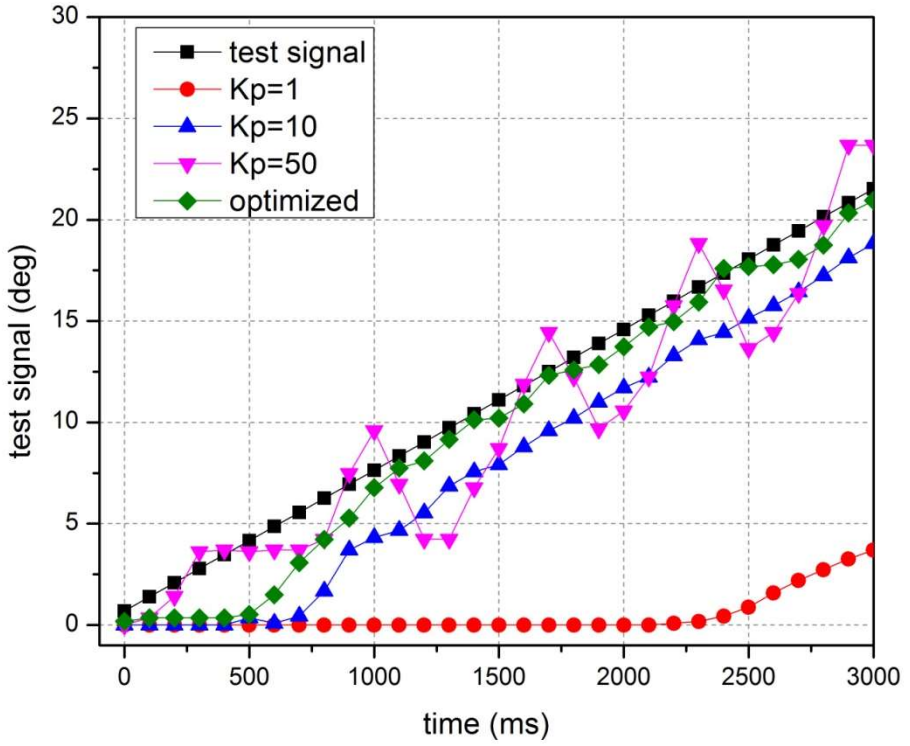

Figure 43: PID tracking magnified view

Once optimized, implementation of the PID control in the FPGA requires the use of lots of logical resources as many operations require division or fractional multiplication to calculate the frequency. It also slows down the overall timing performances as a division takes as many clock cycles as the number of bits of the dividend. Moreover, in the Slow Control proposed system the inclinometer and the encoder are sampled up to two times per acquisition, depending on the acquisition rate used. The motor step pulse frequency gets updated every 100ms, 50ms or even more frequently, depending on the settings. In the final design of the DAQ for the EBRT project, the same FPGA will be shared by both the front end and the Slow Control. The number of logical resources allocated for the PID control and its computation load might be excessive for the XEM3001, and a more powerful device shall be selected. Testing proved that such refined frequency update is not really needed in order to achieve adequate tracking system for a typical gantry rotation speed.

A solution alternative to PID regulator has been also developed with the purpose reducing the computation load of the tracking system. It is called Discrete Angle Control (DAC). The new method take advantage from the fact that the gantry speed range is known a priori. The "error" θ has been subdivided in five sub ranges and a fixed motor speed has been assigned to each sub range.

Table 6: Discrete Angle Control: pulse rate steps sub ranges division

Error = θ	Pulse rate output f_o
$\theta \leq 0.3^\circ$	$f_i=f_1\approx 2.5^\circ/s$
$0.3^\circ < \theta \leq 0.6^\circ$	$f_i=f_2\approx 5^\circ/s$
$0.6^\circ < \theta \leq 1^\circ$	$f_i=f_3\approx 7^\circ/s$
$1^\circ < \theta \leq 5^\circ$	$f_i=f_4\approx 10^\circ/s$
$\theta > 5^\circ$	$f_i=f_5\approx 20^\circ/s$

Table 1 lists the sub range division of the position displacement θ and the related pulse rate of the output f_o. By selecting a sub range, the motor will rotate faster than the maximum gantry speed, if the phantom is far apart and the motor has to quickly catch up with the gantry, whilst it will rotate at a speed of 2º/s to 6º/s as the angular error progressively diminishes. Having a more refined discrete value of the error when the difference falls below 1˚, allows the motor to gently decrease its speed and stop the phantom without incurring in overshoot due to the inertia of the system. The selection

of the sub ranges and their output frequency did undergo multiple tests and values in Table 1 have been chosen best match to give the system good tracking performances. The implementation of the new control system becomes a combinatorial circuit which does not involve any mathematical calculation (flow chart shown in Figure 43. The DAC control appears to be very simple to implement but it can be slow to catch up with the gantry if it accelerates as the algorithm has no memory of the previous position and only relies on the absolute error.

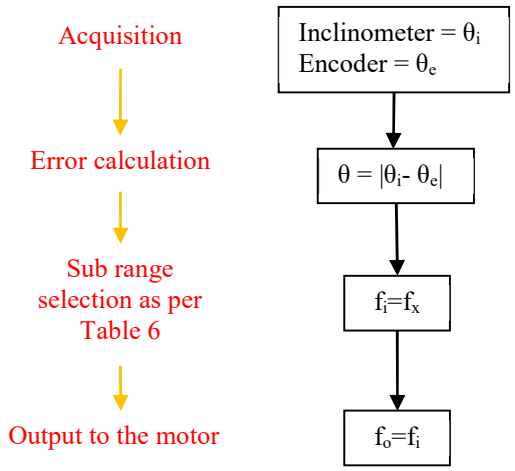

Figure 44: Discrete Angle Control algorithm flow chart.

A third solution, called Adaptive Discrete Angle Control (ADAC), has been developed in order to add more flexibility to the DAC mode. The ADAC checks the position error and set the initial speed of the motor using the same sub ranges of Table 1, but the information about the last error is kept in the memory (θ_o). At the next acquisition, the algorithm compares the new error θ with the previous θ_o. At that stage, even if the value falls in the same frequency sub range, the ADAC control accelerates the motor if the error increases, or decelerates its speed if the error decreases of a fixed offset (f_{offset}) which is about 1°/s. Thus, even though the algorithm does not require multiplications or divisions, the system appears to be able to quickly and accurately track the gantry speed variation (flow chart shown in Figure 43).

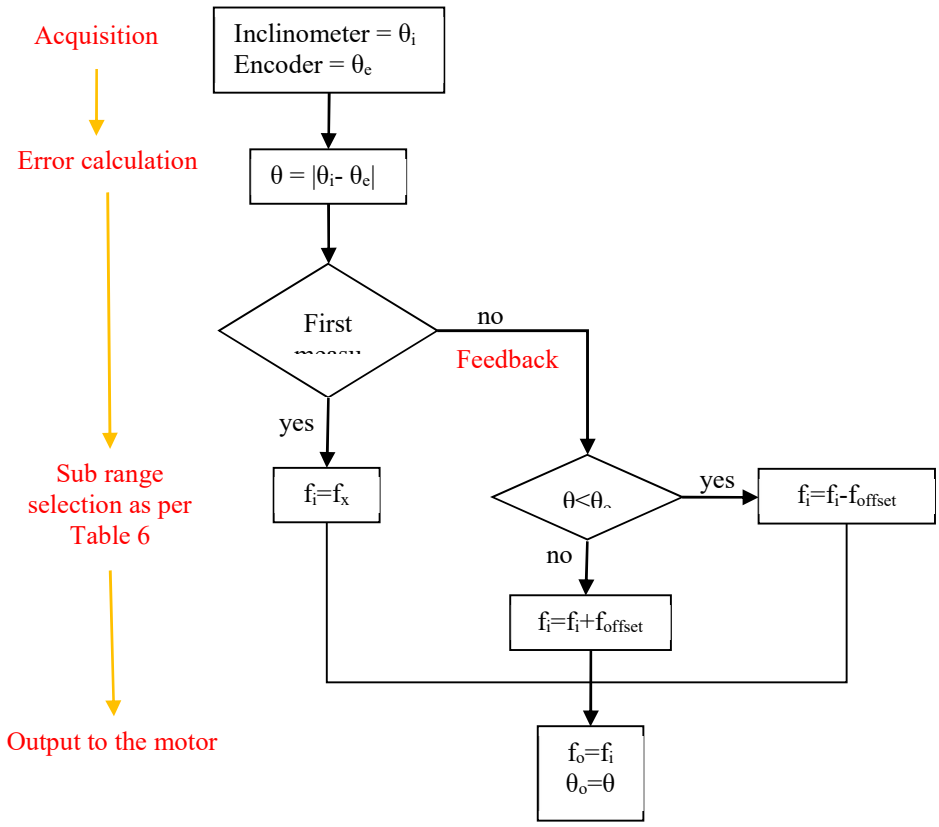

Figure 45: Adaptive Discrete Angle Control algorithm flow chart.

Table 7 summarizes the usage of the internal resources into the FPGA: the DAC algorithm is the design which uses a minor number of resources, closely followed by the ADAC; the PID instead nearly saturates the number of slices available. This parameter become important as the control system needs to be integrated with the reading and data handling of the detector, plus with the new detectors coming and the number of channels will increase up to 512, the resources available need to be taken into account.

Table 7: resource FPGA

Resources	DAC	ADAC	PID
Flip Flop	21%	22%	64%
LUT	19%	20%	33%
Slices	38%	40%	93%

The three control methods have been tested in the lab applying the same test signal used for the tuning of the PID and displayed in Figure 42 Figure 43 to verify the

response of the systems to a controlled step signal. Figure 46 compares the output of the three algorithms. As highlighted on the zoom on the right side, the ADAC method has the fastest response and it is the quickest which catches up the movement of the gantry. Once the phantom reaches the gantry position and the motor keeps tracking the gantry, all the three control methods show close tracking the test signal and the ADAC method remains best having a standard deviation against the test signal of 0.175º whilst the PID has 0.411º and the DAC has 0.541º.

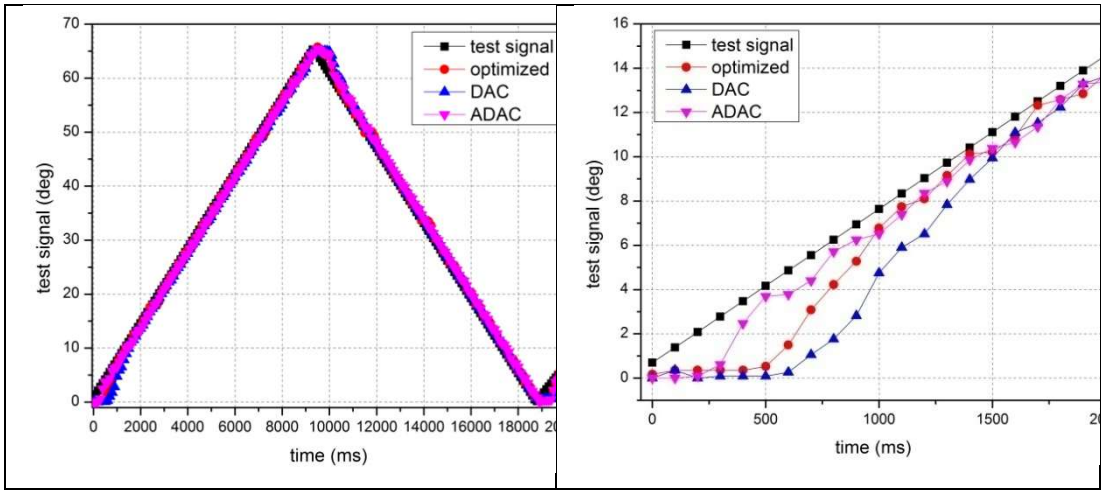

Figure 46: PID, DAC and ADAC tracking comparison.

In order to compare performance of the three methods against a step signal, we define Rising Time, Overshoot and Settling Time as per Figure 47.

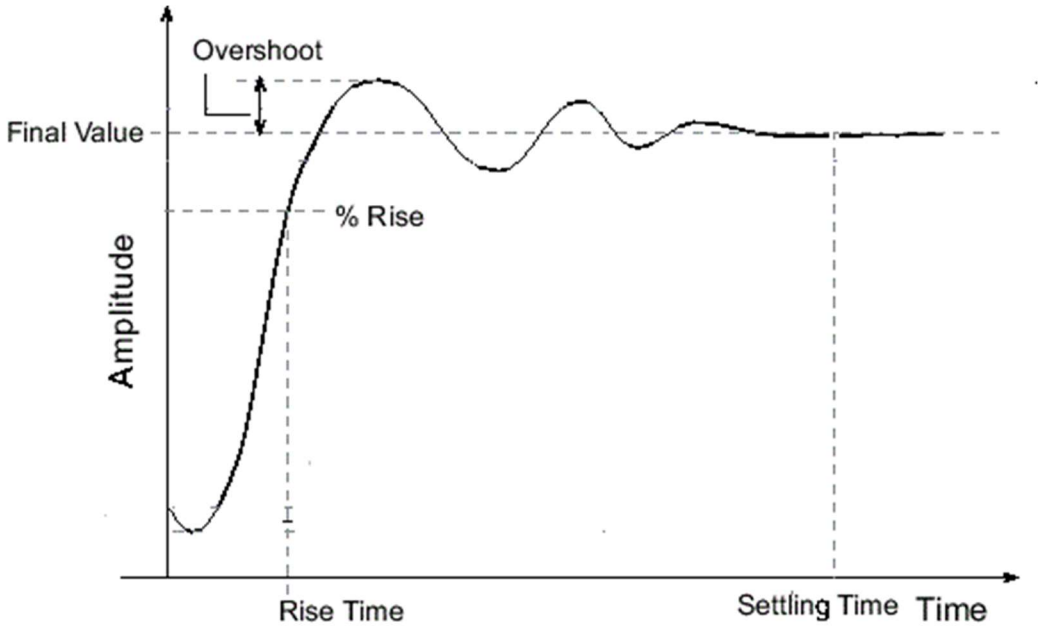

Figure 47: Timing parameters.

Figure 48 shows the response of the three control systems to a step of 90º step stimulus. Once again the ADAC method appears to perform the best. The timing results summarized in Table 8, confirms the ADAC as the one which better controls the motor. In particular, the step response has no overshoot, characteristic which is particularly relevant for the designed system due to the inertia of the phantom.

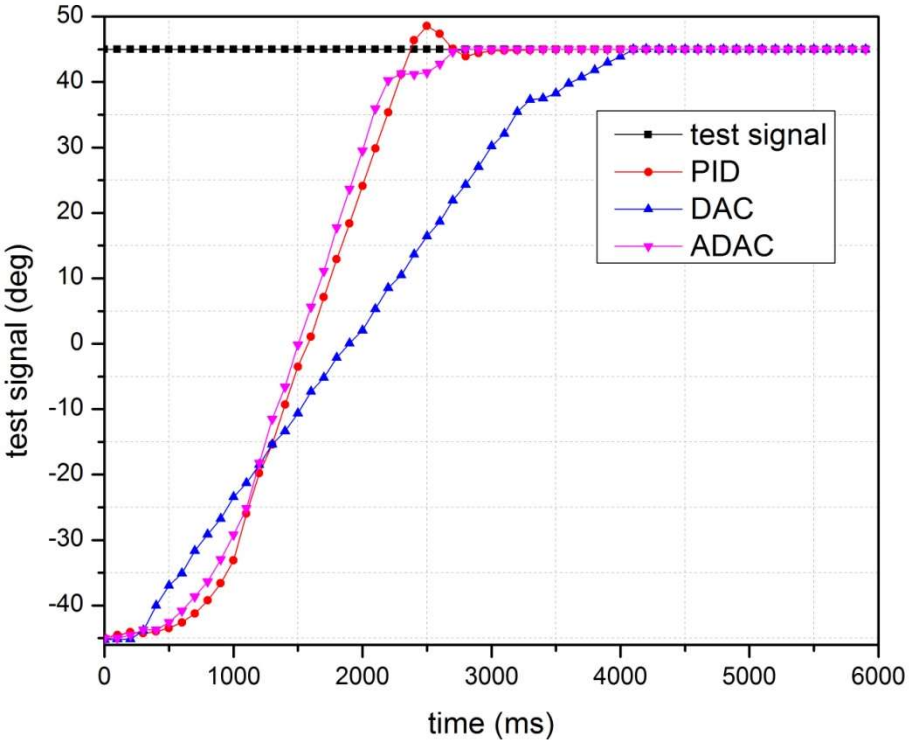

Figure 48: step response.

Table 8: Timing performances

Method/parameter	DAC	ADAC	Optimized PID
Rise time @ 90% (s)	3.4	2.3	2.4
Overshoot (deg)	0.056	0	4.664
Settling time (s)	1	0.6	1.1
Std. deviation of tracking error (deg)	0.21	0.19	0.39

The three controls methods have been tested in a real clinical environment. Figure 49 is a picture of a test setup taken at the Illawarra Cancer Care Centre of the Wollongong

Hospital which replicates the setup described in Figure 36. The DAQ uses two MP-121 for a total read out of 256 channels. One detector is attached to the gantry and read the dose in fluence mode. The inclinometer measuring the position of the gantry is mounted inside the same enclosure. The second detector is inserted into the rotatable phantom. The picture clearly shows how the rotation of the phantom matches the tilt of the LINAC gantry. The insert made on the phantom to house the detector has been designed to be modular as well, thus giving the opportunity to use the same setup with different detectors.

The control methods have been tested on the real gantry using a random pattern. The results confirm that the ADAC is the most suitable control method for the designed slow control system.

Figure 49: Test setup with the rotatable phantom and 256 channels DAQ.

6.5 Clinical experimental results

The DAQ has been used in several clinical experiments. The flexibility of the design allows selecting the configuration which is the best match for the selected clinical environment. Two major research outcomes will be discussed in connection with the application of the DAQ in the EBRT field: small field dosimetry quality assurance and movable target quality assurance. All the system characterization results and the Slow

Control design and characterization are part of this work; however the test ran for the small field dosimetry QA and movable target QA have been carried out by Aldosari et al. [35] and Petasecca et al. [38]. Although the proposed results do not include the use of the Slow Control at this stage, they have been selected to highlight the performances of the DAQ for EBRT applications as they have already been published in international peer reviewed journals.

Small field dosimetry is a technique used for the Stereotactic Body Radiation Therapy (SBRT). In principal, a SBRT treatment delivers high controlled doses in a small number of fractions aiming at ablating the tumour while minimizing the toxicity of the treatment [46]. A particular characteristic of this technique is the dimension of the field which is generally a square between 0.3 cm^2 and 4 cm^2. The beam is shaped by the jaw or the multileaf collimator of the LINAC setup which causes an electronic disequilibrium at the edge of the beam. This condition, generated by the scattering of secondary electrons, although it is still affecting the edges of the beam, do not exist in the centre of large size beams. It becomes relevant when the treatment involves small field radiation beams as the perturbations, which are related to the energy and the density of the material, effects the whole field [35]. The detector plays a major role in verifying that the beam conforms to the treatment requirements. In fact, it has to be as small as possible to avoid perturbation of the beam; the pitch between pixels must be minimal to be able to resolve the penumbra; and a small sensitive volume to avoid averaging effects of the measures of steep dose gradients. The detector designed for this application is called MagicPlate-512 (MP-512). It is a silicon monolithic detector containing an array of 512 pixels. Each pixel has 0.5x0.5mm^2 size and the pitch between them is 2mm (Figure 50).

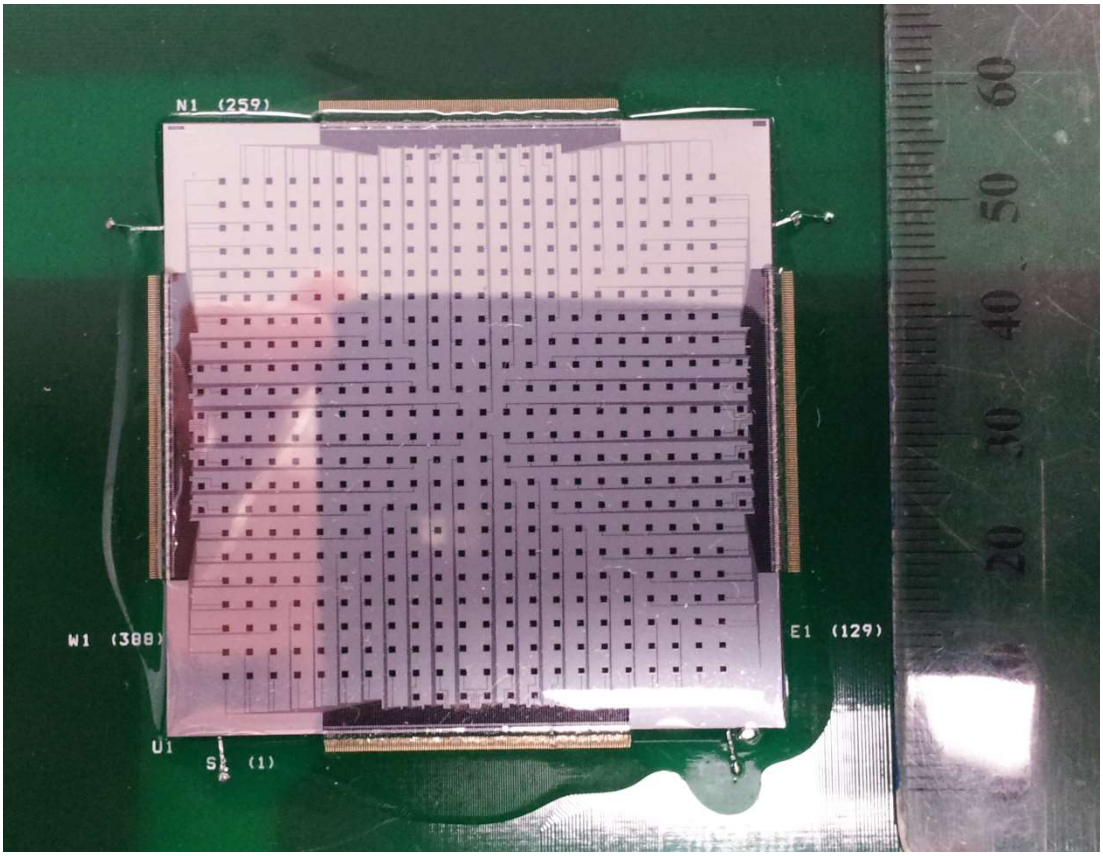

Figure 50: Magnified vision of MagicPlate 512.

Due to the large number of channels of the detector, the DAQ with the AFE0064 front end was chosen. Since the DAQ is upgradable and modular, stacking four AFE0064 based modules of 128 channels and expanding the FPGA data multiplexer was all to migrate from 128 to 512 channels. The system is normally running at 360Hz, triggered by the SYNC signal of the LINAC, and the on board memory is still large enough to assure no data losses during the acquisition. The GUI was modified to allow for mapping of all 512 pixels of the detector. Figure 51 illustrates performances of the system in terms of uniformity (left side) and linearity (right side). Tests were done using the AFE0064 front end connected with the MP-512. Both parameters have been calculated after the equalization factor has been applied to the measures. The procedure described by Wong et al. [10] for characterization and equalization of MP121 has been applied to MP-512 as well. As result of the equalization, the uniformity reports a standard deviation from the mean value of 0.25% and the linearly has a regression coefficient of R^2=0.9988.

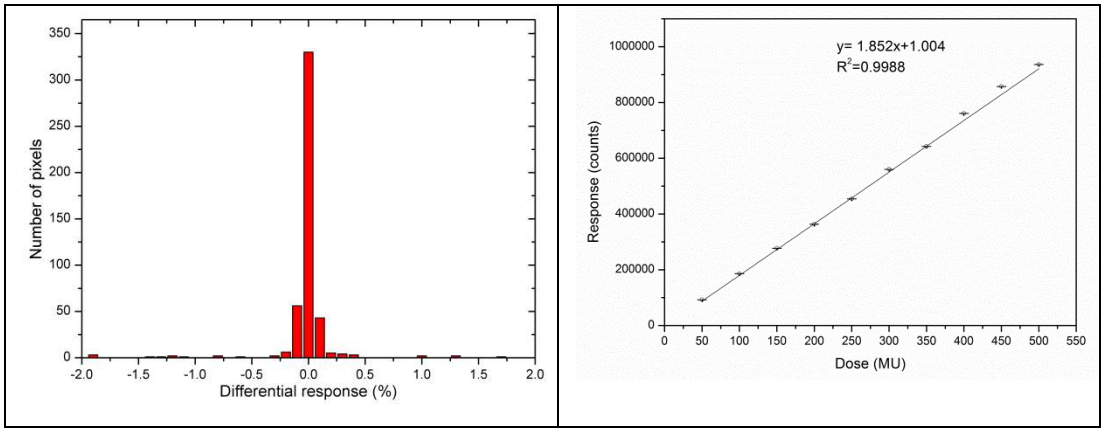

Figure 51: Uniformity (left) and linearity (right) of the DAQ: AFE0064 plus MP-512.

Tests have been performed to compare beam profiles; penumbra and output factor measured both with the AFE front-end and MagicPlate-512 versus the EBT3 films. Figure 52 shows some of the beam profiles at different field sizes compared to the one obtained using the EBT3 film.

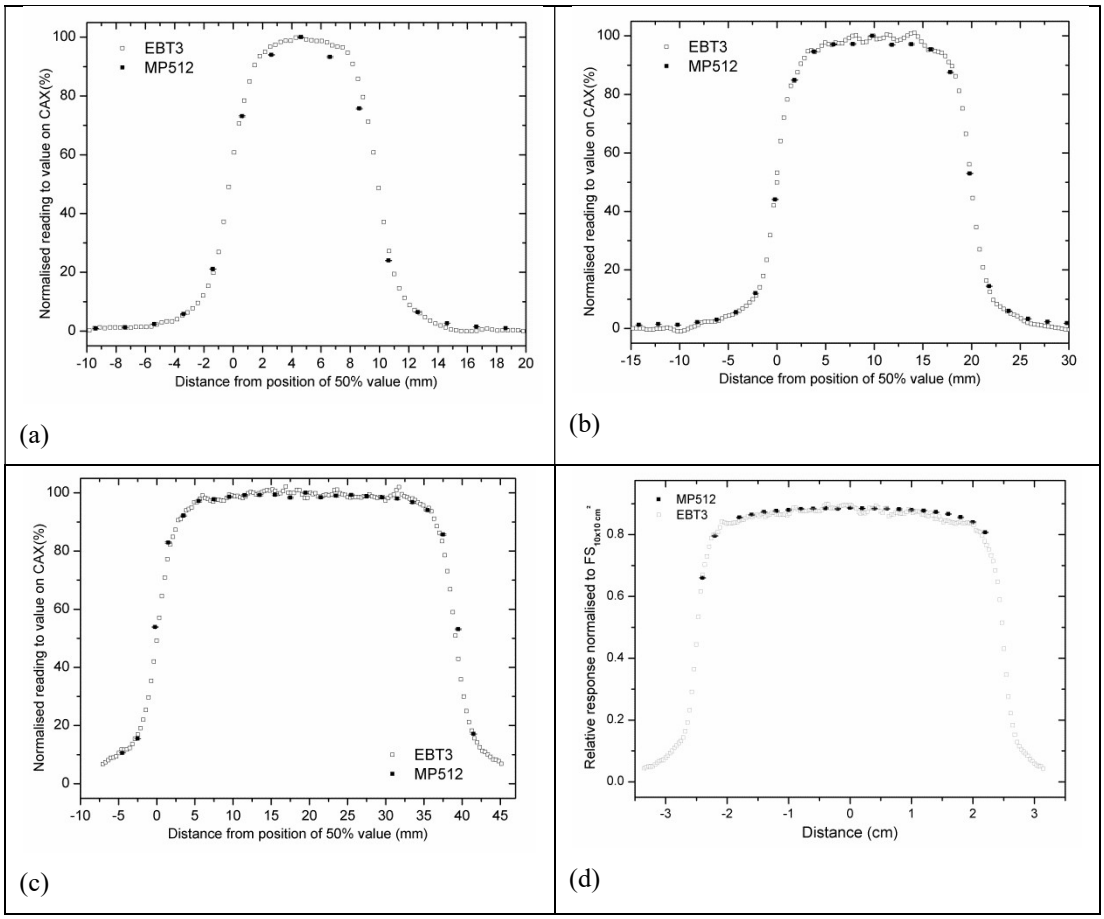

Figure 52: Beam profiles comparison EBT3 film and AFE0064 front-end with MP-512 at different field sizes (1x1cm^2 (a), 2x2 cm^2 (b), 3x3cm^2 (c), 5x5 cm^2 (d)).

MP512 and EBT3 films demonstrate good agreement on the evaluation of the full with half maximum of the field size. The largest discrepancy measured is the 1.36% for the 5x5 mm^2 field size, suggesting that the system can be suitable for beam profile reconstruction. The dataset was analysed using Curve Fitting Toolbox of MATLAB to generate a fit. Data points of FWHM and penumbra measurements have been interpolated using the interpolation-shape-preserving fit with a resolution step of 0.01mm [35].

The second application chosen to highlight the performances of the DAQ is the stereotactic motion adaptive radiotherapy. Once again, the aim is to show how the very same system can be used in a substantially different clinical environment and, without applying any hardware or software modification, it is still suitable and accurate.

The setup under test is used for the treatment of the lung cancer. As during the treatment the patient is breathing, the target moves for up to 25-30mm, meaning that the volume to be irradiated needs to be increased to be sure the treatment covers the whole affected area. Alternatively, a chest movement tracking system can be used to get the beam following the movement of the target (tumour) thus making possible to minimize healthy tissue over radiation. In this test, the DAQ previously used for the small field project has been combined with a movable platform called HexaMotion (simulating chest movement) and a radiofrequency tracking system called Calypso (Figure 53).

Figure 53: Setup for the moving target test with the detector placed on a movable tray.

The aim of the test is to measure dose distribution of a small field square beam in three different conditions: first in static condition, were all the components of the setup are stationary; second with the platform moving according to breathing pattern, mimicking the motion of the tumour in the lung; third with both the platform “breathing” and the tracking system activated. A preliminary test has been performed to check the effect of the tracking system, which uses RF range. Figure 54 shows the effect of the radiated RF on the DAQ noise distribution; the baseline measurements were taken in a dark condition. The first set (in green) is without either the RF or the shielding showing rather small noise confined within 1%. When the RF was switched on (black) the noise increased up to 10%. Once the detector was placed on a shielding aluminium enclosure with 2mm thick walls, the noise reduced to about 2% (red histogram) which was acceptable. The thickness of the aluminium slab has been calculated in order to attenuate up to 99.9% of the electromagnetic wave generate by Calypso at a frequency of 300 kHz [38].

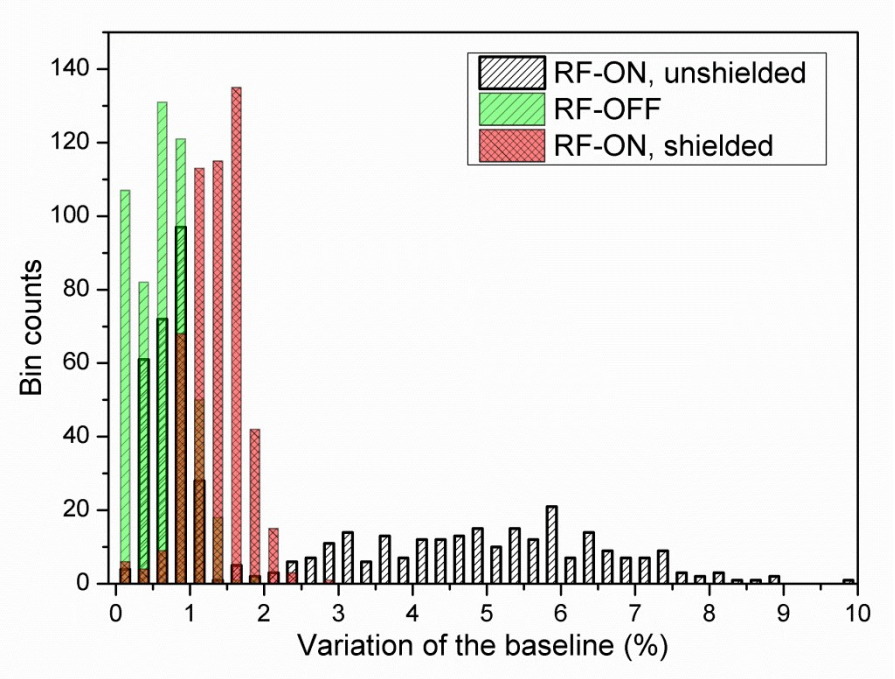

Figure 54: Noise distribution without RF, with RF and no shielding and with RF and shielding

Figure 55 shows an integral dose profile calculated along the central Y axis on the MP-512. The plot compares the no-motion response with motion and motion plus tracking system. On the lower panel of the plot, a difference (in %) relative to the stationary condition results was +15% maximum; while with motion and no-tracking the response was -18% along the wedge and up to +75% on the penumbra. Same results have been obtained using the EBT3 film (Figure 56).

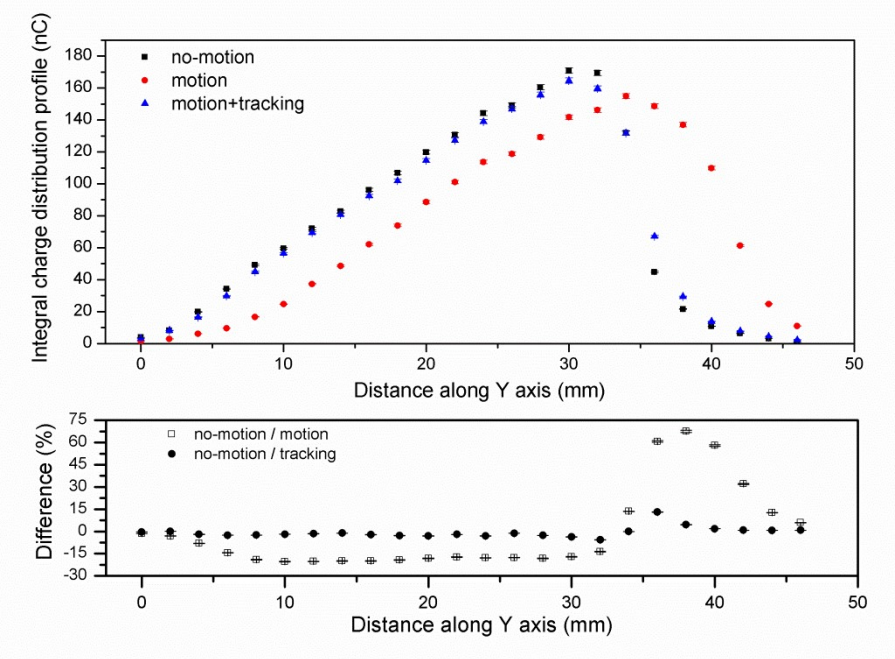

Figure 55: Integral dose profile along the central Y axis and percentage difference normalized to the no-motion response.

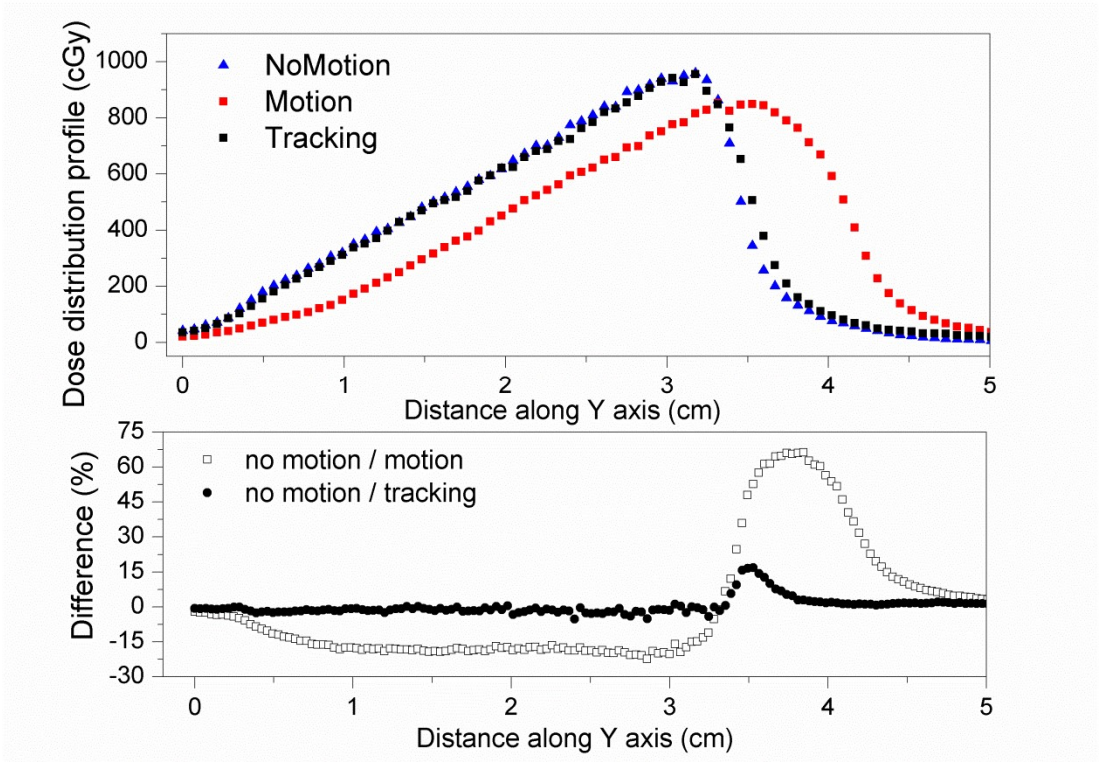

Figure 56: Integral dose profile and percentage difference with EBT3film.

Overall, the developed DAQ shows excellent match with the standard dosimetric systems normally used. The DAQ can show the acquisition is the real time, allows frame-by-frame readout and has high time resolution. This makes a detailed analysis

on pixel-by-pixel basis possible in order to characterize and/or improve the tracking system. A possible future upgrade can be done by inserting MP-512 in the rotatable phantom to allow the angular dependence correction by rotating the detector.

The DAQ designed for brachytherapy application described in chapter 5 has proved to produce interesting data even in a different clinical scenario like the EBRT. The addition of the rotatable phantom, although is still under test, showed to be a feasible and useful upgrade. The modularity of the system gives the opportunity to activate the module, if needed, or simply disable the feature for standard measurements, complying with the requirements of a unified modular DAQ. More than an analysis of the data acquired against the existing dosimeter devices, the aim of the results presented is to demonstrate how the very same system can satisfy different setups and applications. An extensive and detailed literature review and discussion of the results can be found on the published references [36] and [38].

CONCLUSIONS AND RECOMMENDATIONS

The presented work/project explores feasibility of developing and designing a unified Data Acquisition System for Quality Assurance purposes of radiation therapy. The project evaluates different treatments which require a custom DAQ. Three major radiation oncology modalities were considered: Micro Beam Radiation Therapy; Brachytherapy and External Beam Radiation therapy. Each of them presents different characteristics in the way how patients are radiated; different intensity of radiation; multiple shapes of the beam and various timing of the beam. Combination of these parameters determines the requirements for the design of a custom DAQ. A part from the application specific requirement, the aim of the project was the design of a DAQ which could be a universal platform to be used in different scenarios only applying minimal changes. The design of a new DAQ involves multiple steps and skills: there is the detector whose shape, sensitivity and electrical characteristics have to suite the proposed application; then there is the ancillary electronics and digital hardware which have to provide all the necessary power supplies and signals the allows the system working, this section houses the analog front end as well, one of the key components of the DAQ; then there is the firmware which is the logic core of the system, and the software both extremely important to enable the communication between the user and the hardware. The main focuses of this project were ancillary electronics, digital hardware and firmware, sections covering a large part of the DAQ.

Several versions of the DAQ were developed. The pilot project was the MRT application. The detector used in this application was a single strip silicon diode, requiring a single channel DAQ. The main challenges from the electronic point of view were: high gain, about 10^5 as order of magnitude; high spatial resolution on the range of 10-15 μm; real-time feedback from the acquisition. The DAQ designed, called X-Tream, meets all the specifications: it is able to detect the dose irradiated at all time during the treatment (i.e. peak and valley detection); it is capable of distinguish each single peak; its fast sampling rate of 1 MSPS give a very high time and spatial resolution; and Rad-Plot, the software interface custom designed for this application, provides an excellent real-time feedback from the acquisition with the ability of run a post-process analysis of the data. The effort put on the design of X-Tream, did open

the opportunity to upgrade and modify the DAQ for different applications. Although the single channel DAQ was not a valid option anymore for Brachytherapy and EBRT treatments, and the detectors have changed, the basic components of the ancillary electronic, firmware and software have been maintained as fundaments of the new data acquisition systems.

The upgrade of the X-Tream project leads to the design of a DAQ for Brachytherapy treatments. This new treatment mainly involves the spatial reconstruction in 2D or 3D of a moving source. As the detector used for the MRT project was no longer the best solution, a multichannel detector has been introduced; in fact, the DAQ for the Brachytherapy application is not using anymore a single strip diode but a matrix of 121 diodes, called MagicPlate 121(MP-121). This radical upgrade needed a rework of the digital hardware with the introduction of a multichannel analog front end. Two different solutions have been evaluated, one based on a research grade component, TERA06, and on based on a commercial component AFE0064. The digital hardware and the logic core designed for the MRT project have not been replaced but just modified by adding the electrical connections needed to feed and read the new front ends. The firmware itself went through few modifications: the main functional blocks handling clock section, memory stage and communications with the Host PC remained the same but additional function have been added to drive the front ends and collect and organize the data from the multichannel detector. The software interface instead has been custom designed for the specific application. This project led to the design of two new DAQ one using the TERA06 as analog front end, and another one using the AFE0064. The first one was straighter forward as the front end is a self-contained board which generates all the polarization needed by the chip and outputs directly a digital signal. The design of the digital hardware and firmware was relatively simple but the performances of the DAQ were poor, in terms of time resolution and sensitivity, for the Brachytherapy experiment.

The AFE0064 front end has been developed, following TERA06. It required a quite complex buffering stage of the input signals and the addition of an ADC stage to digitalize the output. The firmware itself had to generate a state machine to control both chip and ADC and particular care has been taken on the synchronization of this

two key components. The result is a DAQ system with a fine sensitivity, able to detect the dose irradiated even far from the source for in-vivo application. Its variable acquisition rate, from 30Hz up to 10 kHz gives the system the flexibility to be successfully used for the Brachytherapy application. Moreover, the design of the new DAQs opened the possibility to increase the number of channels to be read by the DAQ and allowed the introduction of new detectors. TERA06 in fact is ready to be daisy-chained and the system housing the AFE front end has been designed with a modular approach, thinking already to the opportunity of stacking modules to increase the total number of channels to be acquired.

The last challenge of this research project was the DAQ for the External Beam Radiation Therapy. Providing that the two systems designed for the Brachytherapy experiment were both performing and reliable, they have been adapted to be used in the EBT environment too. In particular, the fast sampling rate of the DAQ housing the AFE0064 front end has been modified into a triggered DAQ which takes the synchronization signal from the LINAC to start its measurements. Thus enhance the performance of the DAQ making possible the sampling of each beam pulse. The total number of channel has been doubled allowing the reading of two MP-121 at once. A new feature has been added with the introduction of a rotatable phantom to compensate the angular dependence of the diodes in therapies such VMAT and IMRT. The rotatable phantom has brought a whole new section both into the hardware and firmware. The slow control, which enables the movement of the phantom, needed a very detailed design of its power supply, moving and control system. Few techniques for the control of the phantom have been tested at firmware level: the traditional PID and two newly introduced control method called Discrete Angle Control (DAC) and Adaptive Discrete Angle Control (ADAC). All of them have been compared with the ADAC showing the best performances in terms of rise time, ripple and overshoot of the output. At the same time, new detectors have been introduced housing a range of channels form 256 up to 512. The high sensitivity, low cost, modularity and flexibility of the DAQ with the AFE0064 front end have led to promote that system has first choice to be used with the new devices. In particular, a monolithic array of 512 channels, called MagicPlate-512 (MP-512), has been used for different applications: two of them are small field dosimetry and movable target dosimetry. The results

obtained with the DAQ were very promising: if compared with the data calculated using the standard dosimetric device EBT3 film, the confidence of the results is normally within the 1%. Plus, the DAQ adds the features of displaying the output in real-time; allowing data analysis and post-processing; giving the flexibility to adapt the system to each particular set of measures.

Overall, the result of the research project has been very satisfying: a unified platform for data acquisition in radiotherapy treatment has been developed. The system designed is at the same time customized to each application but based on a common core which has been update and upgraded as required.

Table 9: List of detectors, front end and projects currently developed

Detector	n. of channels	Front end	Applications
Single strip epitaxial diode	1	- X-tream	- MRT - Brachytherapy
MP 121	121	- TERA06 - AFE0064	- Brachytherapy - IMRT
DMG	128	- TERA06 - AFE0064	- SRS
SDMG	256	- TERA06 - AFE0064	- SRS - SBRT - Hadron therapy
Double MP	242	- TERA06 - AFE0064	- IMRT - VMAT
MP-512	512	- AFE0064	- SBRT
Duo	512	- AFE0064	- SRS
Octa	512	- AFE0064	- SRS

Table 9 lists the detectors currently used by the CMRP, the front ends and the combination of them most suitable for each application. This ultimately highlights the aim of the research project which hit the goal of designing a high performing unified platform DAQ. The most modular DAQ, obtained using the AFE006 front end and it's electronic, has been built step by step over existing designs with a particular attention on keeping each piece of the system compatible as much as possible with his previous version. From here, the achievement of having one system which can read any multichannel detector in use at the moment by the CMRP.

Modifications and upgrades are always under development: on the system for the MRT treatment a new communication protocol will improve the versatility of the DAQ. In fact, the DAQ is actually connected to the host PC through a USB link; the introduction of an Ethernet communication protocol will enable the upload of the settings of the

acquisition and data sets into the beam control system. The system used for the Brachytherapy dosimetry instead, will benefit from the introduction of a new front end. As deeply explained in chapter five, the nature of the application uses a continuous source, the DAQ adopted for the dosimetry is the one with the AFE0064 front end, which has a significant dead time. Although there are no commercially available DAQ which can be compared with the proposed system highlighting the effect of the dead time on the measures, a new front end has already been selected called DDC264. It has already been characterized in its evaluation board and it features high sensitivity; fast sampling rate and no dead time during the acquisition. A new design is already at its preliminary stage developing a new DAQ housing the DDC264 front end in the same modular way adopted for the AFE0064 front end. The DDC264 has a more compact design, if compared to the AFE0064, as it has already a digital output and does not require the ADC stage. This characteristic will be an advantage as the CMRP is planning to introduce new detector with even higher number of channels. The new system will be tested in the EBRT environment using both old and new detectors. The same DAQ will be coupled with the rotatable phantom system to enhance the performance of the detectors and the quality of the results if required. As for the previous design, the new front end will have the same fundamentals as the AFE0064 system to keep electronic and firmware compatible and interchangeable as much as possible .

REFERENCES

[1] W. H. Organization, "Fact sheets by cancer," 2016. [Online]. Available: http://globocan.iarc.fr/Pages/fact_sheets_cancer.aspx. [Accessed 01 06 2016].

[2] A. C. Begg, F. A. Stewart and C. Vens, "Strategies to improve radiotheraphy with targeted drugs," *Nature Reviews Cancer,* vol. 11, pp. 239-253, 2011.

[3] The American Heritage Science Dictionary, Houghton Mifflin, 2002.

[4] J. Park and S. Mackay, Practical data acquisition for instrumentation and control systems, Elsevier, 2003.

[5] B. Thomadsen, M. J. Rivard and W. M. Butler, Brachytherapy Physics, Madison WI: Medical Physics Publishing, 2005.

[6] M. Petasecca, A. Cullen, I. Fuduli, A. A. Espinoza, C. Porumb, C. Stanton, A. H. Aldosari, E. Brauer-Krisch, H. Requardt, A. Bravin, V. Perevertaylo, A. B. Rosenfeld and M. L. Lerch, "X-Tream: a novel dosimetry system for Synchrotron Microbeam Radiation Therapy," *JINST,* vol. 7, no. P07022, 2012.

[7] N. Hardcastle, W. A. Tome', K. Foo, A. Miller, M. Carolan and P. Metcalfe, "Comparison of prostate IMRT and VMAT biologically optimized treatment plans," *Medical Dosimetry,* vol. 36, no. 3, pp. 292-298, 2011.

[8] V. Feygelman and B. Nelms, "Dosimetric quality assurance of highly conformal external beam treatments: from 2D phantom comparisons to 4D patient dose reconstruction," in *7th IC3DDose*, Journal of Physics: Conference Series 444 doi:10.1088/1742-6596/444/1/012012, 2013.

[9] G. A. Ezzel, J. W. Burmeister, N. Dogan, T. J. LoSasso, J. G. Mechalakos, D. Mihailidis, A. Molineu, J. R. Palta, C. R. Ramsey, B. J. Salter, J. Shi, P. Xia, N. J. Yue and Y. Xiao, "IMRT commissioning: multiple institution planning and dosimetry comparison, a report from AAPM Task Group 119," *Medical Physics,* vol. 36, p. 5359, 2009.

[10] J. H. Wong, "Characterization of a novel two dimensional diode array the "magic plate" as a radiation detector for radiation therapy treatment," vol. 39, no. 5, 2012.

[11] M. R. Weaver, J. A. Green, M. Petasecca, M. L. Lerch, D. L. Cutajar, D. R. Franklin, J. Jakubek, M. G. Carolan, M. Conway, S. Pospisil, T. Kron, P. E. Metcalfe, M. Zaider and A. Rozenfeld, “Three-dimensional dosimetry imaging of I-125 plaque for eye cancer treatment,” *Nuclear Instruments and Methods in Physics Research Section A: Accelerators, Spectrometers, Detectors and associated equipment,* vol. 633, pp. 276-278, 2011.

[12] J. Kozelka, J. Robinson, B. Nelms, G. Zhang, D. Savitskij and V. Feygelman, “Optimizing the accuracy of a helical diode array dosimeter: a comprehensive calibration methodology coupled with a novel virtual inclinometer,” *Medical Physics,* vol. 38, no. 9, 2011.

[13] “http://www.sunnuclear.com/documents/1220B05102010.pdf,” [Online]. [Accessed 19 05 2014].

[14] “http://www.ptw.de/2403.html?&cId=13151,” PTW Freiburg GmbH 2012, 13 09 2013. [Online]. [Accessed 15 01 2014].

[15] C. K. McGarry, B. F. O'Connell, M. W. Grattan, C. E. Agnew, D. M. Irvine and A. R. Hounsell, “Ocatvius 4D characterization for flattened and flattening filter free rotational deliveries,” *Medical Physics,* vol. 40, no. 9, p. http://dx.doi.org/10.1118/1.4817482, 2013.

[16] R. Sadagopan, J. A. Bencomo, R. L. Martin, G. Nilsson, T. Matzen and P. A. Balter, “Characterization and clinical evaluation of a nvel IMRT quality assurance system,” vol. 10, no. 2, 2009.

[17] “XEM3001 opal Kelly,” Opal Kelly, [Online]. Available: http://www.opalkelly.com/products/xem3001/. [Accessed 05 05 2014].

[18] E. Brauer-Krisch, A. Bravin, M. Lerch, A. Rosenfeld, J. Stepanek, M. Di Michiel and J. A. Laissue, “MOSFET dosimetry for microbeam radiation therapy at the European Synchrotron Radiation Facility,” *Mediacl Physics,* vol. 30, no. 4, p. 583, 2003.

[19] “http://www.ti.com/lit/ds/symlink/ads8405.pdf,” december 2004. [Online]. [Accessed 13 february 2015].

[20] R. N. Williams, "A painless guide to CRC error detection algorithms," Rocksoft TM Pty Ltd, 19 August 1993. [Online]. Available: http://www.ross.net/crc/download/crc_v3.txt. [Accessed 2 March 2016].

[21] S. Gupta, "Simple Error Detection Method," vol. 4, no. 4, 2013.

[22] "Universal Serial Bus Specification," 27 April 2000. [Online]. Available: http://sdphca.ucsd.edu/lab_equip_manuals/usb_20.pdf. [Accessed 3 March 2016].

[23] ESRF, "Beamline Control Unit," ESRF, [Online]. Available: http://www.esrf.eu/Instrumentation/software/beamline-control/BLISS. [Accessed 15 March 2016].

[24] A. Espinoza, B. Beeksma, I. Fuduli, C. Porumb, M. Petasecca, D. Cutajar, S. Corde', M. Jackson, M. L. Lerch and A. B. Rosenfeld, "The feasibility study and characterization of MagicPlate for High Dose Rate brechytherapy quality assurance," *Medical Physics,* vol. 40, no. 11, 2013.

[25] A. Espinoza, M. Petasecca, I. Fuduli, A. Howie, J. Bucci, S. Corde, M. Jackson, M. Lerch and A. Rosenfeld, "The evaluation of a 2D diode array in "magic phantom" for use in high dose rate brachytherapy pretreatment quality assurance," *Medical Physics,* vol. 4, no. 2, pp. 663-673, 2015.

[26] I. Fuduli, C. Porumb, A. Espinoza, A. Aldosari, M. Carolan, M. Lerch, P. Metcalfe, A. Rosenfeld and M. Petasecca, "A comparative analysis of multichannel data acquisition system for quality assurance in external beam radiation therpy," *Journal of Instrumentation,* vol. 9, no. 6, pp. 1-12, 2014.

[27] J. H. e. a. Wong, "Characterization of a novel two dimensional diode array the "magic plate" as a radiation detector for radiation therapy treatment," *Medical Physics,* vol. 39, no. 5, pp. 2544-2558, 2012.

[28] "Brachytherapy," wikipedia, 16 February 2015. [Online]. Available: http://en.wikipedia.org/wiki/Brachytherapy#Treatment_delivery. [Accessed 18 February 2015].

[29] R. A. Minamisawa, R. A. Rubo, R. M. Seraide, J. R. Rocha and A. Almeida, "Direct measurement of instantaneous source speed for a HDR brachytherapy unit using an optical fiber based detector," vol. 10, no. 37, 2010.

[30] I. A. Pecka Valencia, Test and characterization of the beam monitor systemfor the Centro Nazionale di Androterapia Oncologica, Univerity of Torino: PhD thesys, 2008.

[31] A. La Rosa, M. Donetti, M. Borri, F. RIvero, A. Attili, F. Bourhaleb, R. Cirio, M. A. Garella, S. Giordanengo, N. Givehchi, G. Mazza, F. Marchetto, J. Pardo, A. Pecka and C. Peroni, “Characterization of a front-end electronics for the monitoring and control of handrotherapy beams,” *Nuclear Intruments and Methods in Physics Research A,* no. doi: 10.1016/j.nima2007.12.012, pp. 270-275, 2008.

[32] “64 Channel Analog Front End for Digital X-Ray Detector,” Texas Instruments, 09 2009. [Online]. Available: http://www.ti.com/lit/ds/symlink/afe0064.pdf. [Accessed 30 10 2013].

[33] “Dual, 1MSPS, 16-/14-/12-Bit, 4×2 or 2×2 Channel, Simultaneous Sampling Analog-to-Digital Converter,” January 2011. [Online]. Available: http://www.ti.com/lit/ds/symlink/ads8363.pdf. [Accessed 25 02 2015].

[34] M. J. Rivard, B. M. Coursey, L. A. DeWerd, W. F. Hanson, M. S. Huq, M. G. Ibbott, M. G. Mitch, R. Nath and J. F. Williamson, “"Update of AAPM Task GroupNo. 43 Report: A revised AAPM protocol for brachytherapy dose calculation,” *Medical Physics,* vol. 31, no. 3, pp. 633-674, 2004.

[35] A. H. Aldosari, M. Petasecca, A. Espinoza, M. Newall, I. Fuduli, C. Porumb, S. Alshaikh, Z. A. Alrowaili, M. R. Weaver, P. Metcalfe, M. Carolan, M. L. Lerch, V. Perevertaylo and A. B. Rosenfeld, “A two dimensional silicon detectors array for quality assurance in stereotactic radiotherapy: MagicPlate-512,” *Medical Physics,* vol. 41, no. 9, pp. 0917071-10, 9 2014.

[36] A. H. Aldosari, A. Espinoza, D. Robinson, I. Fuduli, C. Porumb, S. Alshikh, M. Carolan, M. Lerch, V. Perevertaylo, A. Rosenfeld and M. Petasecca, "Characterization of an innovative p-type epitaxial diode for dosimetry in modern external beam radiation therapy," *IEEE Transactions on Nuclear Sciences,* vol. 60, no. 6, pp. 4705-4712, 2013.

[37] I. Fuduli, M. K. Newall, A. Espinoza, C. S. Porumb, M. Carolan, M. L. F. Lerch, P. Metcalfe, A. B. Rosenfeld and M. Petasecca, "Multichannel Data Acquisition System comparison for Quality Assurance in External Beam Radiation Therapy," *Radiation Measurements,* vol. 71, pp. 338-341, 2014.

[38] M. Petasecca, M. K. Newall, J. T. Booth, M. Duncan, A. H. Aldosari, I. Fuduli, A. A. Espinoza, C. S. Porumb, S. Guatelli, P. Metcalfe, E. Colvill, D.

Cammarano, M. Carolan, B. Oborn, M. L. Lerch, V. Perevertaylo, P. J. Keall and A. B. Rosenfeld, “MagicPlate-512: a 2D silicon detector array for quality assurance of stereotactic motion adaptive radiotherapy,” *Medical Physics,* vol. 42, no. 6, pp. 2992-3004, June 2015.

[39] C. Porumb, A. H. Aldosari, I. Fuduli, D. L. Cutajar, M. Newall, P. Metcalfe, M. Carolan, M. Lerch, V. Perevertaylo, A. Rosenfeld and M. Petasecca, "Characterisation of silicon arrays for dosimetry in external beam radiation therapy," *IEEE Transactions on Nuclear Science,* vol. 63, no. 3, pp. 1808-1817, 2016.

[40] P. Metcalfe, A. Quinn, K. Loo, M. Lerch, M. Petasecca, J. Wong, N. Hardcastle, M. Carolan, J. McNamara, D. Cutajar, I. Fuduli, A. Espinoza, C. Porumb and A. Rosenfeld, “Review of four novel dosimeters developed for use in radiotherapy,” *Journal of Physics,* pp. doi: 10.1088/1742-6596/444/1/012088, Conference Series 444 2013.

[41] “geckodrive.com,” 07 01 2010. [Online]. Available: http://www.geckodrive.com/gecko/images/cms_files/G203V-REV-7-MANUAL.pdf. [Accessed 24 04 2015].

[42] P. Rowshnfarzad, M. Sabet, D. J. O'Connor, P. M. McCowan, B. M. McCurdy and P. B. Greer, “Gantry angle determonation during arc IMRT: evaluation of a simple EPID_based technique and two commercial inclinometers,” vol. 13, no. 6, 2012.

[43] A. Trimeche, S. A., A. Mtibaa and M. Benrejeb, “PID Controller using FPGA technology,” in *Advances in PID control*, InTech ISBN: 978-953-307-267-8, 2011, pp. 260-274.

[44] “Discrete-time PID Controller Implementation,” 08 08 2014. [Online]. Available: http://controlsystemslab.com/discrete-time-pid-controller-implementation/. [Accessed 29 04 2015].

[45] J. G. Ziegel and N. B. Nichols, “Optimum settings for automatic controllers,” *Transactions of the ASME,* no. 64, pp. 759-768, 1942.

[46] A. Martin and A. Gaya, “Stereotactic body radiotherapy: A review,” *Clinical Oncology,* vol. 22, no. 3, pp. 157-172, 2010.

[47] G. e. a. Mazza, "A large dynamic range charge measurement ASIC family for beam monitoring in radiotherapy applications," 19-25 Oct 2008.

[48] D. G. Kaurin, L. E. Sweeney, E. I. Marshall and S. Mahendra, "VMAT testing for an Elekta accelerator," *Journal of Applied Clinical Medical Physics,* vol. 13, no. 2, 2012.

[49] P. Rowshnfarzad, M. Sabet, D. J. O'Connor, P. M. McCowan, B. M. McCurdy and P. B. Greer, "Gantry angle determonation during arc IMRT: evaluation of a simple EPID_based technique and two commercial inclinometers," *Journal of Applied Clinical Medical Physics,* vol. 13, no. 6, pp. 203-212, 2012.

[50] "http://www.opalkelly.com/products/," Opal Kelly. [Online]. [Accessed 11 04 2014].

[51] "http://www.xilinx.com/support/download/index.html/content/xilinx/en/downloadNav/design-tools.html," Xilinx. [Online]. [Accessed 11 04 2014].

[52] D. N. Slatkin et al., "Microbeam radiation therapy," *Medical Physics,* vol. 19, pp. 1395-1400, 1992.

[53] E. Brauer Krisch, A. B. Rosenfeld, M. Lerch, M. Petasecca, M. Akselrod, J. Sykora, J. Bartz, M. Ptaszkiewicz, P. Olko, A. Berg, M. Wieland, S. Doran, T. Brochard, A. Kamlowski, G. Cellere, A. Paccagnella, E. A. Siegbahn, Y. Prezado, I. Martinez Rovira, A. Bravin, L. Dusseau and P. Berkvens, "Potential high resolution dosimeters for MRT," in *AIP Conference Proceedings*, http://dx.doi.org/10.1063/1.3478205, 2010.

[54] R. M. Hernandez and A. COLLABORATION, "A portable readout systemfor microstrip silicon sensor (ALIBAVA)," *IEEE Transactions on Nuclear Science,* vol. 56, no. 3, pp. 1642-1650, 2009.

[55] "http://en.wikipedia.org/wiki/Ziegler%E2%80%93Nichols_method," 28 02 2014. [Online]. [Accessed 31 03 2014].

APPENDIX A ACRONISMS

ADAC Adaptive Discrete Angle Control
ADC Analog Digital Converter
CMRP Centre for Medical Radiation Physics
CSD Correlated Double Sampling
DAC Discrete Angle Control
DAQ Data Acquisition System
DCM Digital Clock Manager
DI Digital Interface
DLL Dynamic Langiage Libraries
DS Double Sampling
EBRT External Beam Radiation Therapy
EPID Electronic Portable Imaging Devices
FIFO First In First Out
FPGA Field Programmable Gate Array
FWHM Full Width Half Maximum
GUI Graphical User Interface
HDR High Dose Rate
IMAT Intensity Modulated Arc Therapy
IMRT Intensity Modulated Radiation Therapy
IO input/output
IT Integration Time
LDR Low Dose Rate
LINAC Linear Accelerator
MP-121 Magic Plate 121 channels
MRT Microbeam Radiation Therapy
PC Personal Computer
PID Proportional Integrative Derivative
PLL Phase Lock Loop
QA Quality Assurance
RAM Random Access Memory
RF Radio Frequency
SPI Serial Peripheral Interface
SRS Stereotactic Radio Surgery
SS Single Sampling
TFT Thin Film Transistor
TTL Transistor Transistor Logic
UCF User Constrain File
USB Universal Serial Bus
VCO Voltage Controlled Oscillator
VHDL Very High Descriptive Language
VMAT Volumetric Modulated Arc Therapy

APPENDIX B FIRMWARE AND CODE

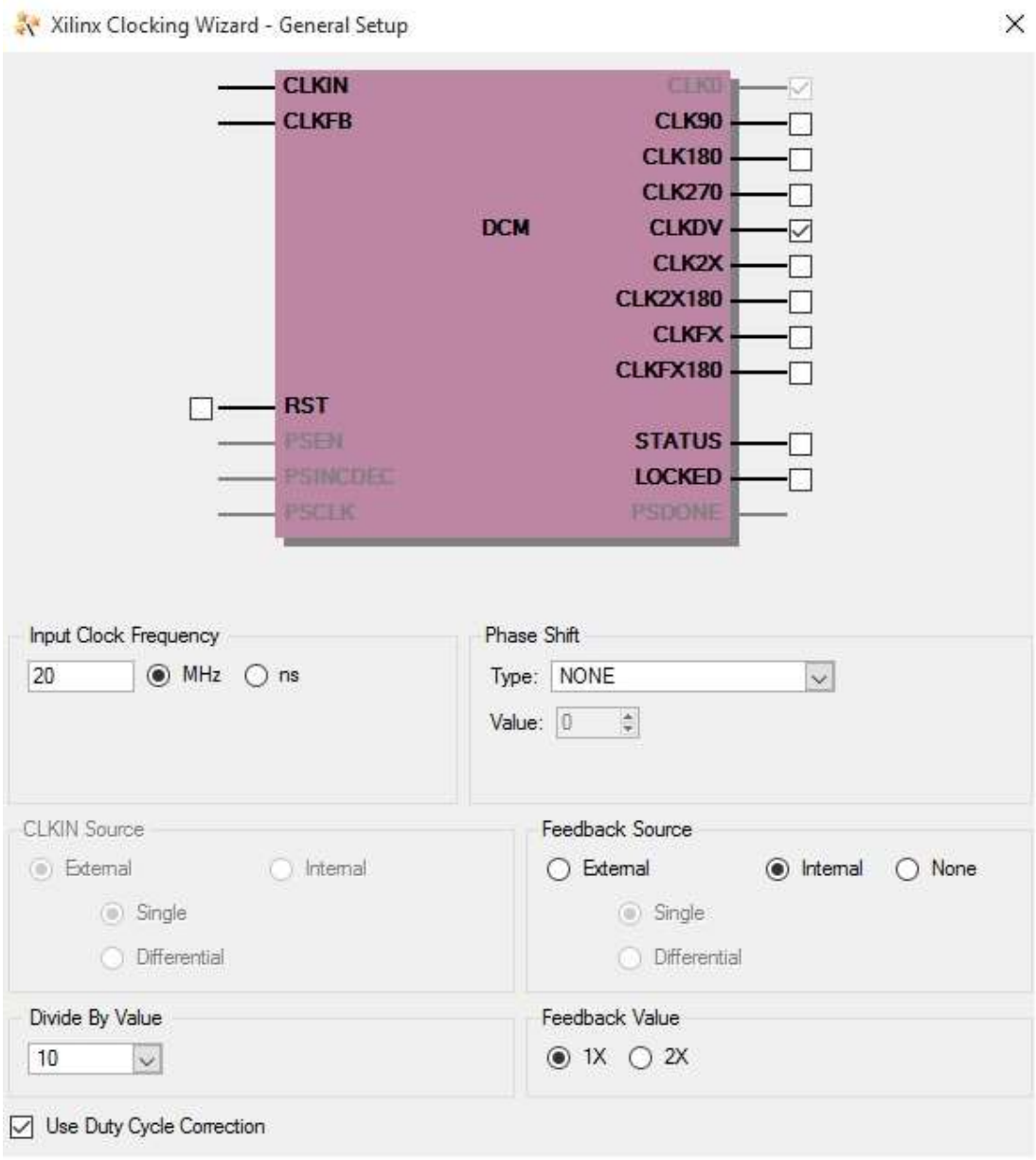

Figure 57: DCM clock wizard

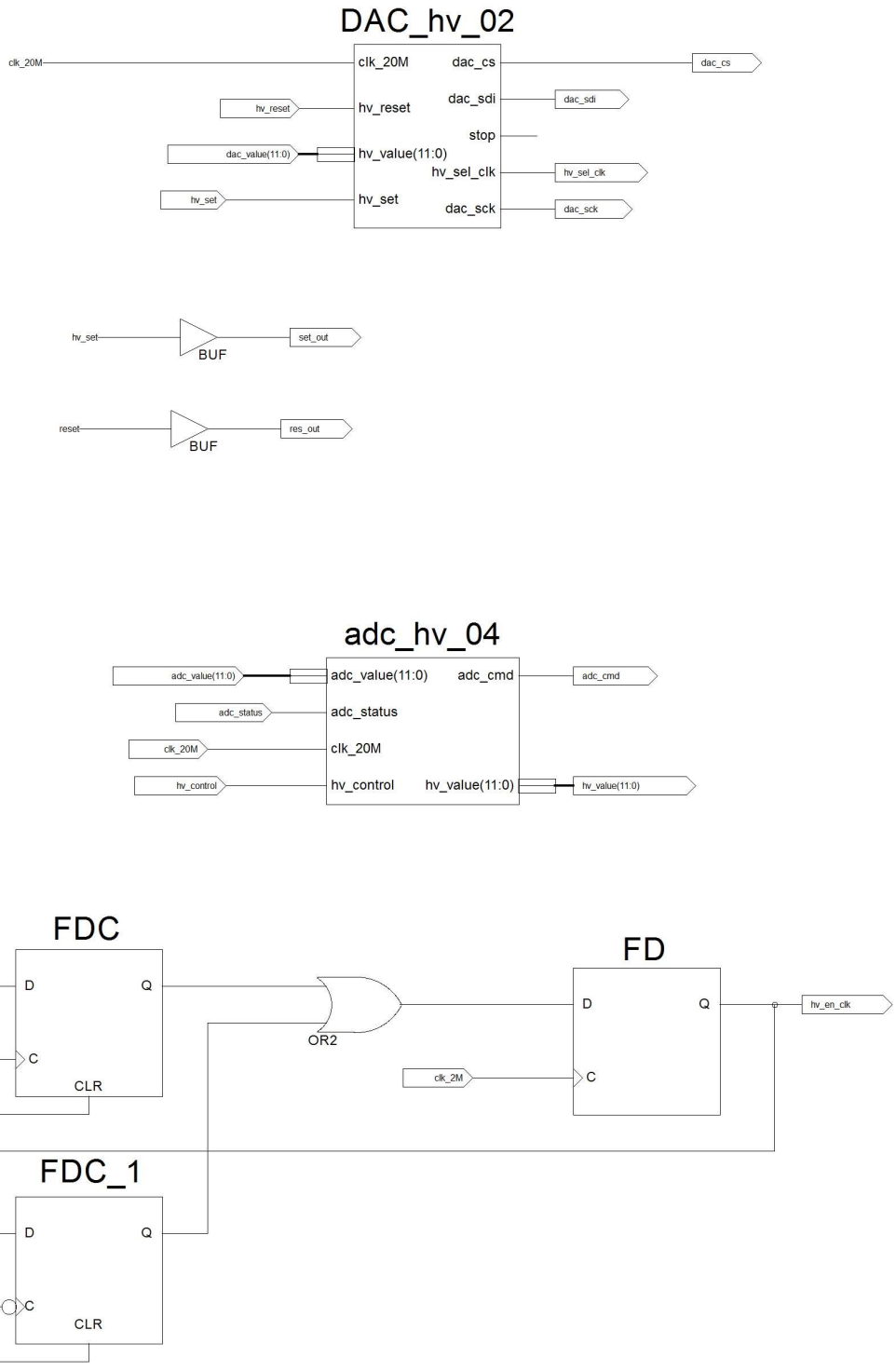

Figure 58: HV setting and monitoring MRT

ADC state machine MRT

```
//  C:\USERS\IOLANDA\DOCUMENTS\...\ADC_DRIVER.v
//  Verilog created by Xilinx's StateCAD 9.2i
//  Thu Mar 25 04:28:58 2010


//  This Verilog code (for use with Xilinx XST) was generated using:
//  one-hot state assignment with boolean code format.
//  Minimization is enabled,  implied else is enabled,
//  and outputs are speed optimized.

`timescale 1s/1s

module adc_driver(CLK,busy,RESET,start,convst);

        input CLK;
        input busy,RESET,start;
        output convst;
        reg convst,next_convst;
        reg acquisition,next_acquisition,conversion,next_conversion,idle,next_idle;

        always @(posedge CLK)
        begin
                acquisition = next_acquisition;
                conversion = next_conversion;
                idle = next_idle;
                convst = next_convst;
        end

        always @ (acquisition or busy or conversion or idle or RESET or start)
        begin

                if ( busy & ~RESET & acquisition | ~RESET & busy & conversion )
                        next_acquisition=1;
                else next_acquisition=0;

                if ( ~RESET & ~busy & acquisition | ~busy & ~RESET & conversion |
~RESET &
                        start & ~busy & idle ) next_conversion=1;
                else next_conversion=0;

                if ( ~start & idle | busy & idle | RESET ) next_idle=1;
                else next_idle=0;


                if ( busy & acquisition | busy & conversion | ~start & idle | busy & idle |
                        RESET ) next_convst=1;
                else next_convst=0;
        end
endmodule
```

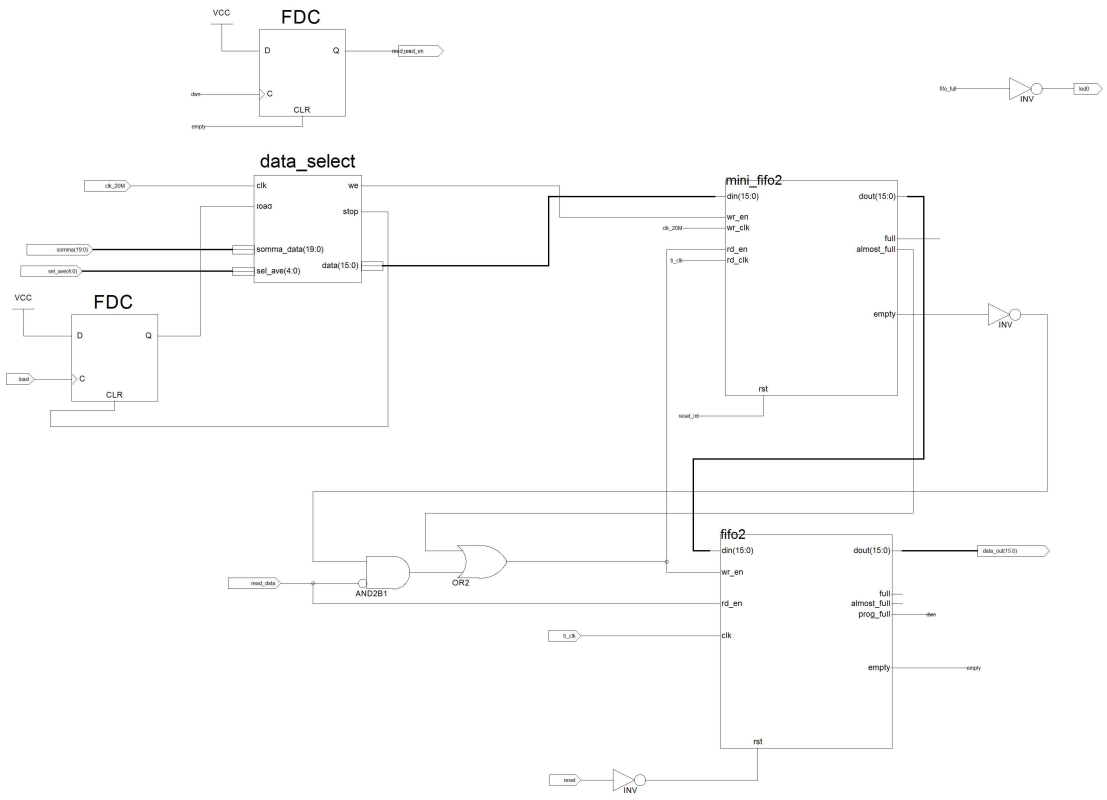

Figure 59: Data Store MRT

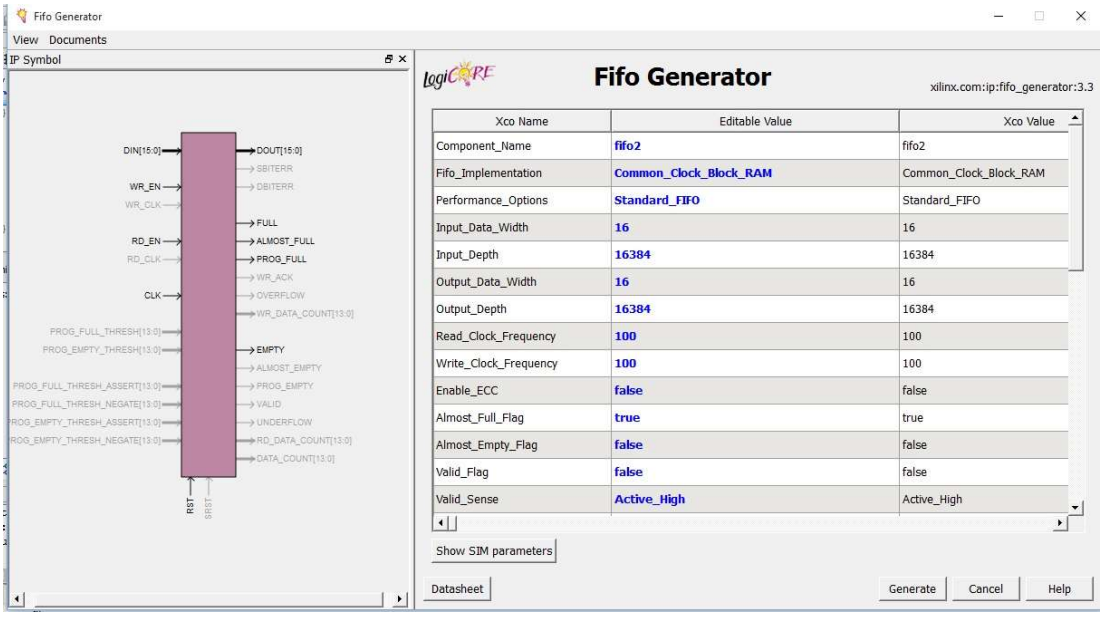

Figure 60: FIFO settings

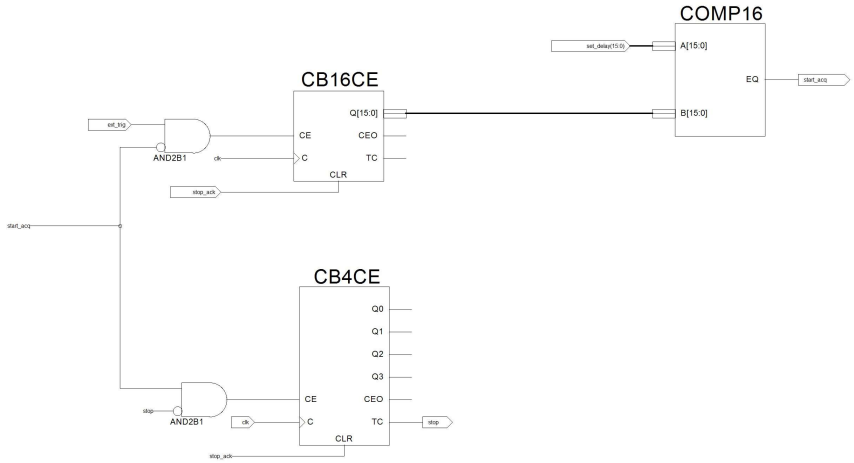

Figure 61: multi trigger MRT

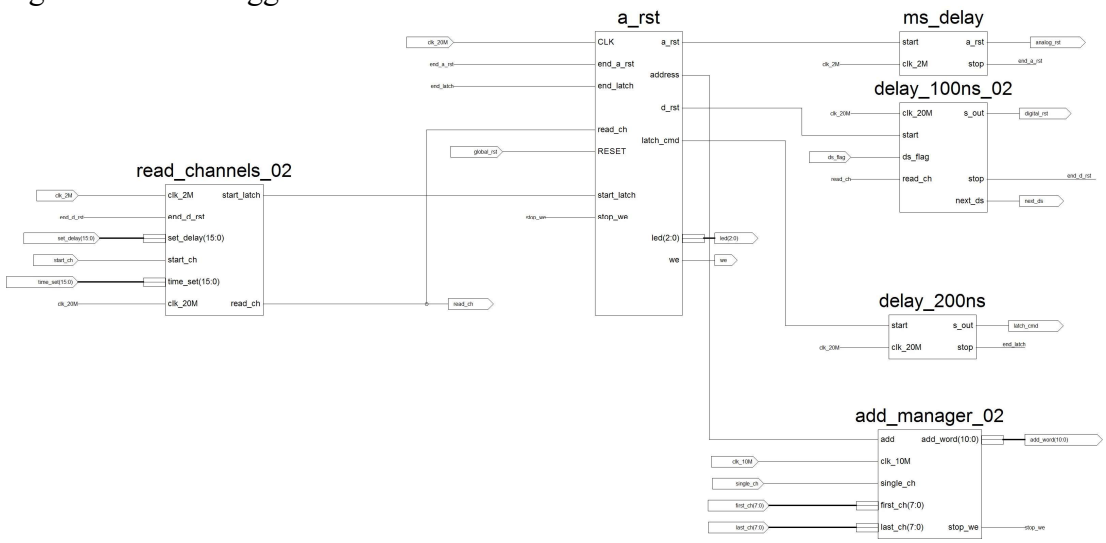

Figure 62: Tera driver

Data Store multiplexing – TERA

```
`timescale 1ns / 1ps
//////////////////////////////////////////////////////////////////////////////////
// Company:
// Engineer: Iolanda Fuduli
//
// Create Date:    05:45:59 22/03/2012
// Design Name: Tera_inc_rev10
// Module Name:    data_select
// Project Name: tera plus inclinometro
// Target Devices:
// Tool versions:
// Description: multipleing dei dati del tera e dell'inclinometro
//
// Dependencies:
//
// Revision: 07 - header 32-bit
// Revision: 06 - aggiunto inclinometro
// Revision: 05 - rimosso inclinometro
// Revision: 04 - handling dei dati dall'inclinometro e dalla tera06
// Revision: 03 - rimossa la prima word con il delay ed inserito l'header
// Revision: 02 - delay bus a 16 bits
// Revision: 01 - File Created
// Additional Comments:
//
//////////////////////////////////////////////////////////////////////////////////
module data_select_02(clk,data,tera_out,we,tera_data,incli_out,incli,incli_clr,
          reset);//,count
    input clk,tera_data,incli,reset;
    input [15:0] tera_out;
           input [15:0] incli_out;
           output reg [15:0] data;
           output reg we,incli_clr;

reg [2:0]count;
reg [15:0]temp;
reg next_state;
initial we=0;
initial count=0;
initial next_state=0;

always @(posedge clk) begin
          if ((reset==1)||(tera_data==0 & count==0 & incli==0)) begin
                    data<={16'hzzzz};
                    we<=0;
                    next_state<=0;
                    incli_clr<=0;
          end
          else if (tera_data==1 & count==0) begin
                    we<=1;
                    data<={16'hffff};
```

```
                count<=1;
        end
        else if (tera_data==1 & count==1) begin
                we<=1;
                data<={16'haaff};
                count<=2;
        end
        else if (tera_data==1 & count==2) begin
                we<=1;
                data<={tera_out};
                next_state<=1;
        end
        else if (tera_data==0 & count==2 & next_state==1) begin
                we<=1;
                data<={tera_out};
                count<=0;
        end
        else if (incli==1 && tera_data==0) begin
                if (count==0) begin
                        we<=1;
                        data<={16'hffff};
                        temp<={incli_out};
                        count<=1;
                end
                else if (count==1) begin
                        we<=1;
                        data<={16'hbbff};
                        temp<={incli_out};
                        count<=2;
                end
                else if (count==2) begin
                        we<=1;
                        data<={temp};
                        count<=count+1;
                end
                else if (count==3) begin
                        we<=1;
                        data<={16'hzzzz};
                        count<=0;
                        incli_clr<=1;
                end
        end
end

endmodule
```

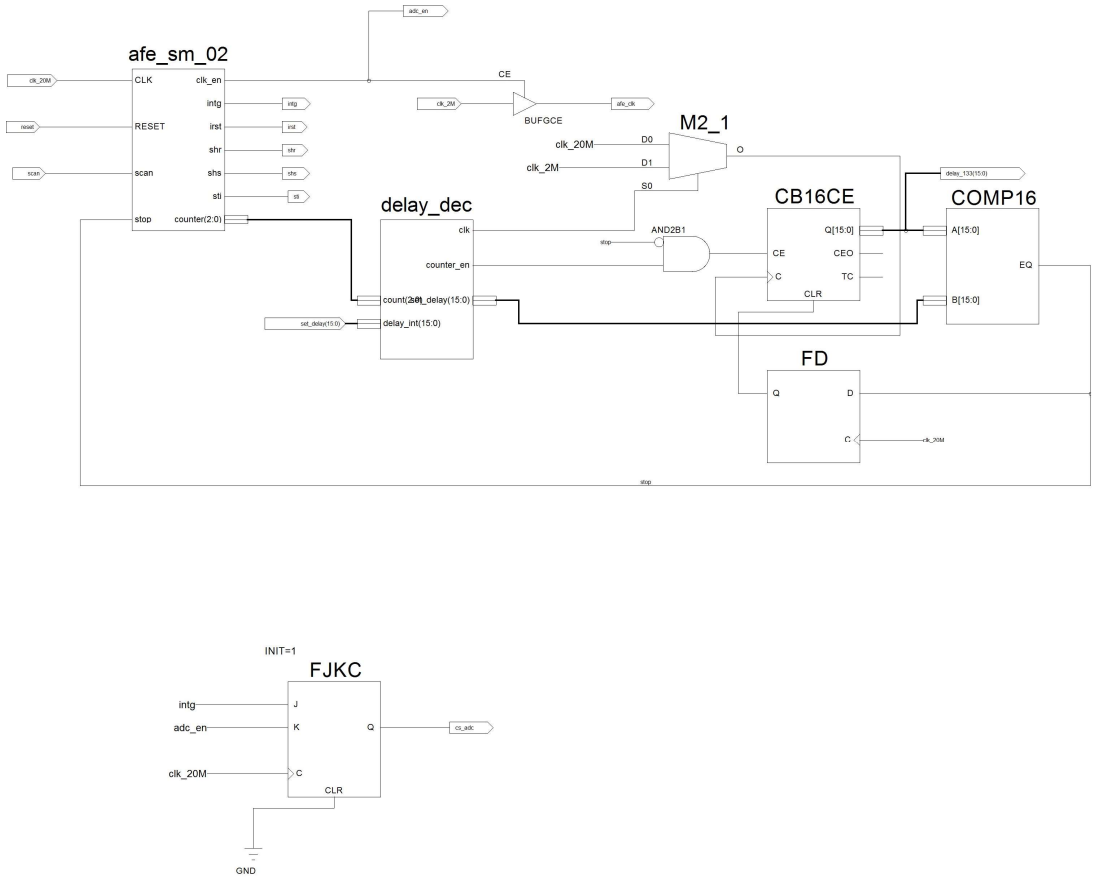

Figure 63: AFE driver

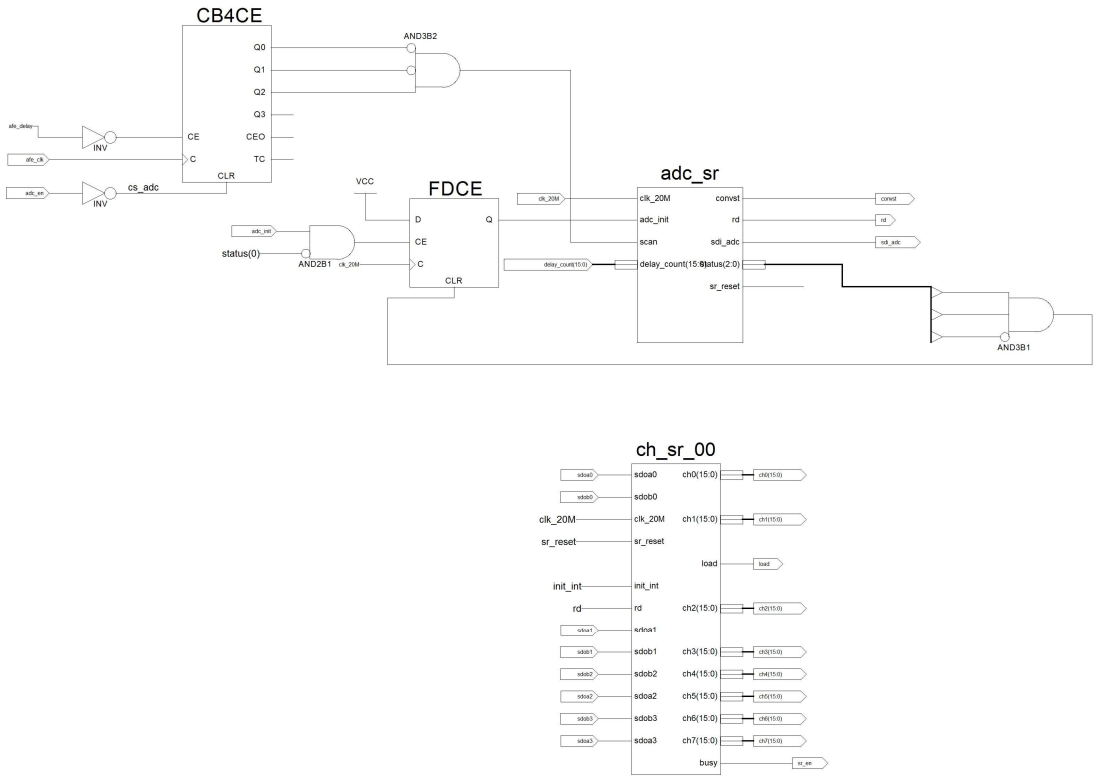

Figure 64: ADC driver

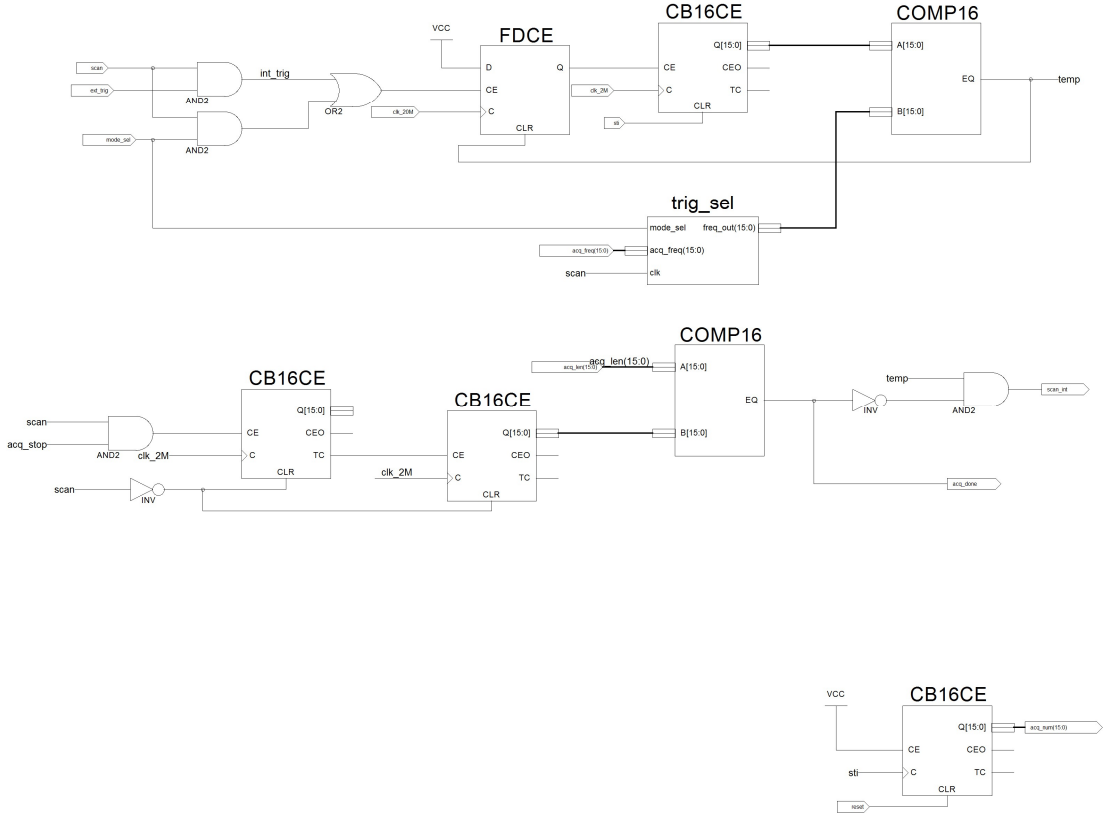

Figure 65: Timing

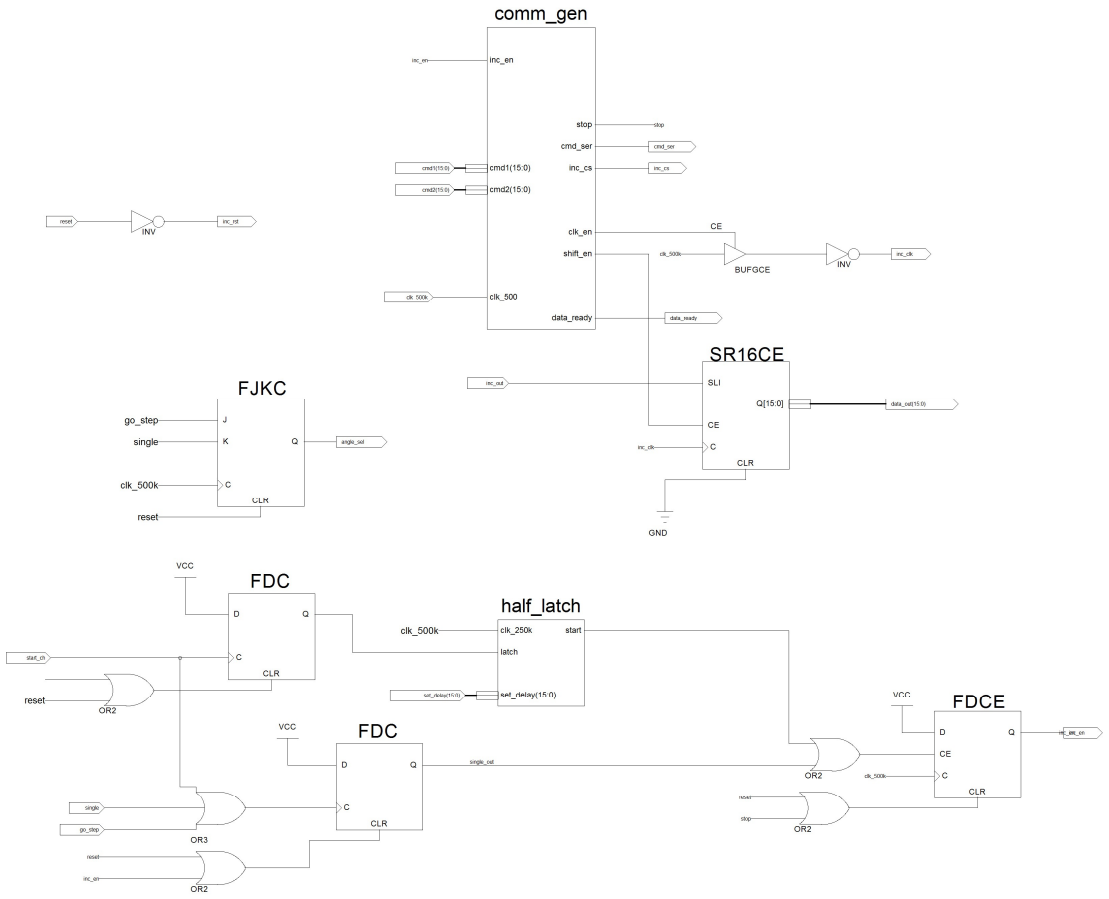

Figure 66: Inclinometer module

```
`timescale 1ns / 1ps
//////////////////////////////////////////////////////////////////////////////////
// Company:
// Engineer: Iolanda Fuduli
//
// Create Date:    05:06:13 03/31/2010
// Design Name: tera_incli_rev05
// Module Name:    comm_gen
// Project Name: Tera06 plus inclinometer
// Target Devices:
// Tool versions:
// Description: genera il comando da mandare all'inclinometro
// Revision: 02 - inserito data_ready per inviare dati alla fifo
// Revision: 01 - File Created
// Additional Comments:
```

```
//
//////////////////////////////////////////////////////////////////////////////////
module comm_gen(clk_500,cmd1,cmd2,cmd_ser,inc_en,stop,inc_cs,clk_en,shift_en,
        data_ready);
   input [15:0] cmd1;
         input [15:0] cmd2;
   input clk_500,inc_en;
   output reg cmd_ser,inc_cs,stop,clk_en,shift_en,data_ready;

reg [15:0]cmd_temp;
reg read_out;
reg [5:0]counter;
initial stop<=0;
initial counter<=0;

always @(posedge clk_500) begin
        if (inc_en==0) begin
                counter=0;
                stop=0;
                inc_cs=1;
                cmd_ser=0;
                clk_en=0;
                shift_en=0;
                data_ready=0;
        end
        else begin
                counter=counter+1;
                if (counter==1) begin
                        inc_cs = 0;
                        cmd_ser = 0;
                        stop = 0;
                        clk_en=0;
                        shift_en=0;
```

```
                data_ready=0;
        end
        if (counter==2) begin
                inc_cs = 0;
                cmd_temp = cmd1;//carico primo comando
                cmd_ser = cmd1[15];
                stop = 0;
                clk_en=1;
                shift_en=0;
                data_ready=0;
                if (cmd1[15]==1)
                        read_out = 0;//erano invertiti credo 11mar2011
                else read_out = 1;
        end
        else if(counter>2 && counter<18) begin//conta 16clk per il primo
comando
                cmd_ser = cmd_temp[18-counter];
                inc_cs = 0;
                stop = 0;
                clk_en=1;
                shift_en=0;
                data_ready=0;
        end
        else if (counter==18) begin
                inc_cs = 0;
                cmd_ser = cmd_temp[18-counter];
                stop = 0;
                clk_en=0;
                shift_en=0;
                data_ready=0;
        end
        else if (counter>=19 && counter<28) begin//stall
                inc_cs = 1;
```

```
            cmd_ser = 0;
            stop = 0;
            clk_en=0;
            shift_en=0;
            data_ready=0;
end
else if (counter==28) begin
            inc_cs = 0;
            cmd_ser = 0;
            clk_en = 0;
            shift_en = read_out;
            data_ready=0;
end
else if (counter==29) begin
            inc_cs = 0;
            cmd_temp = cmd2;//carico secondo comando
            cmd_ser = cmd2[15];
            clk_en=1;
            shift_en= read_out;
            data_ready=0;
end
else if (counter>29 && counter<45) begin
            cmd_ser = cmd_temp[45-counter];//16clk
            inc_cs = 0;
            stop = 0;
            clk_en=1;
            shift_en= read_out;
            data_ready=0;
end
else if (counter==45) begin
            inc_cs = 0;
            cmd_ser = cmd_temp[45-counter];//16clk
            clk_en=0;
```

```
                stop = 0;
                shift_en= read_out;
                data_ready=0;
        end
        else if (counter==46) begin
                inc_cs = 0;
                clk_en=0;
                counter = 0;
                stop = 1;
                shift_en= read_out;
                if (shift_en==1)
                        data_ready=1;
        end
    end
end
endmodule
```

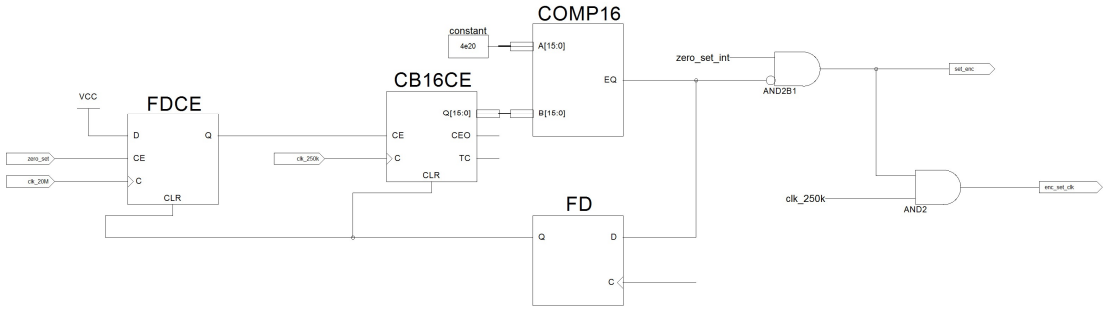

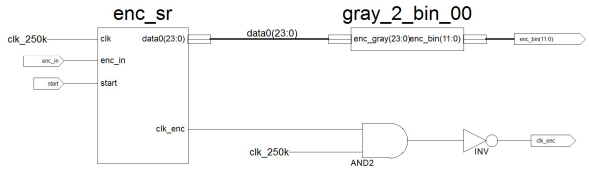

Figure 67: Encoder

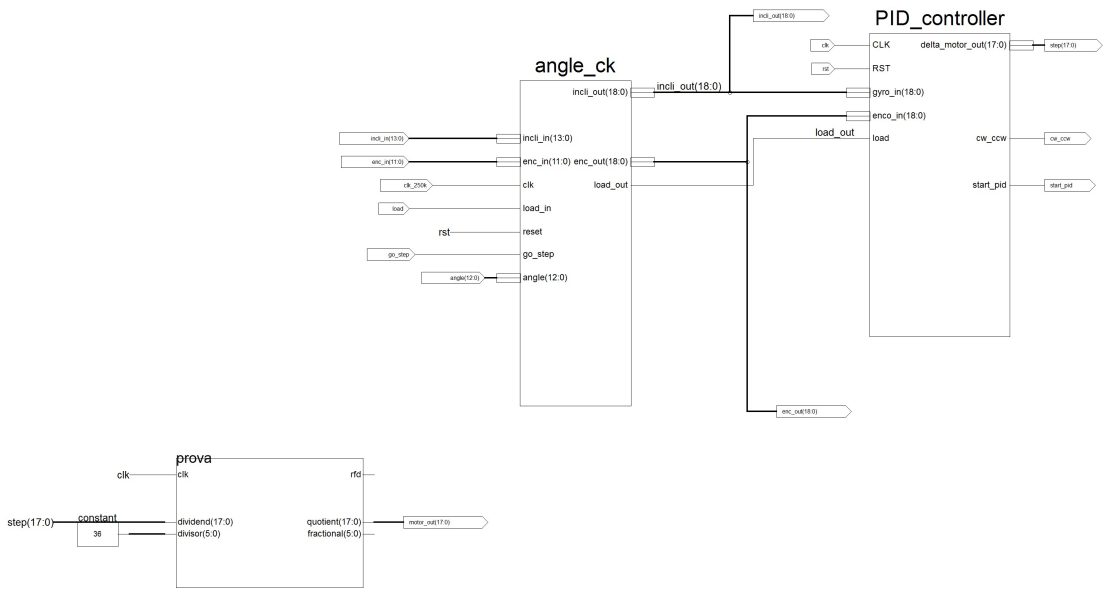

Figure 68: Slow control